1996

Nd:YAG laser-assisted turning of difficult-to-machine silicon nitride

Bruce Clyde Janvrin
Iowa State University

INFORMATION TO USERS

This manuscript has been reproduced from the microfilm master. UMI films the text directly from the original or copy submitted. Thus, some thesis and dissertation copies are in typewriter face, while others may be from any type of computer printer.

The quality of this reproduction is dependent upon the quality of the copy submitted. Broken or indistinct print, colored or poor quality illustrations and photographs, print bleedthrough, substandard margins, and improper alignment can adversely affect reproduction.

In the unlikely event that the author did not send UMI a complete manuscript and there are missing pages, these will be noted. Also, if unauthorized copyright material had to be removed, a note will indicate the deletion.

Oversize materials (e.g., maps, drawings, charts) are reproduced by sectioning the original, beginning at the upper left-hand corner and continuing from left to right in equal sections with small overlaps. Each original is also photographed in one exposure and is included in reduced form at the back of the book.

Photographs included in the original manuscript have been reproduced xerographically in this copy. Higher quality 6" x 9" black and white photographic prints are available for any photographs or illustrations appearing in this copy for an additional charge. Contact UMI directly to order.

UMI

A Bell & Howell Information Company
300 North Zeeb Road, Ann Arbor MI 48106-1346 USA
313/761-4700 800/521-0600

Nd:YAG laser-assisted turning of difficult-to-machine silicon nitride

by

Bruce Clyde Janvrin

A dissertation submitted to the graduate faculty

in partial fulfillment of the requirements for the degree of

DOCTOR OF PHILOSOPHY

Major: Mechanical Engineering

Major Professor: Palaniappa A Molian

Iowa State University

Ames, Iowa

1996

Graduate College
Iowa State University

This is to certify that the Doctoral dissertation of

Bruce Clyde Janvrin

has met the dissertation requirements of Iowa State University

Signature was redacted for privacy.

Committee Member

Signature was redacted for privacy.

Committee Member

Signature was redacted for privacy.

Committee Member

Signature was redacted for privacy.

Committee Member

Signature was redacted for privacy.

Major Professor

Signature was redacted for privacy.

For the Major Program

Signature was redacted for privacy.

For the Graduate College

TABLE OF CONTENTS

LIST OF TABLES

LIST OF FIGURES

ABSTRACT

Hot machining has been applied to the turning of extremely hard metals. Ceramics materials have been traditionally formed to near net shape and fired. If finer tolerances are required, then the fired part is ground. The cost of the grinding operation is expensive, up to 90 % of a parts total costs are grinding costs. Previous attempts to use lasers for hot machining of ceramics by carbon dioxide lasers have resulted in severe degradation of material properties. Carbon dioxide and Nd:YAG laser assisted machining of ceramics were evaluated based on the physics, materials, and mechanics of the process to determine the feasibility of the process. These factors were also evaluated to determine the limitations of carbon dioxide and Nd:YAG laser assisted machining and candidate materials. Nd:YAG laser assisted machining of silicon nitride experimentally produces a surface finish of .3 micrometers. The structure of hot isostatic pressed silicon nitride is grains of beta silicon nitride separated by intergranualar silica SiO_2, TiO_2 and other rare earth oxides. These oxides are transparent to Nd:YAG laser wavelength of 1064 nanometer but the beta structure is highly absorbing. The beta structure is thermal shock resistant where the oxides are not thermal shock resistant. Consequently, Nd:YAG laser assistance of the turning results in softening of the tougher grain by irradiation with softening of the intergranular oxides only by conduction of heat from the grain. Carbon dioxide laser wavelength of 10600 nanometer is absorbed readily by the oxide glasses but not as readily as the beta Si_3N_4 and would result in the fracture of the intergranular oxides without softening of the grains.

ACKNOWLEDGEMENTS

I am sincerely indebted to my major professor, Dr P. A. Molian for his guidance, support, encouragement, and patience throughout this work. I would also like to thank Dr. R. F. Scrutton for his advice and analysis in discussions of the field and thank the other members of my committee Drs. Gemmill, Hall, and Verhoeven for their analysis and questions of my research. I express my sincere appreciation to the Iowa Center for Emerging Manufacturing Technology for the generous support of this research.

I am greatly indebted to my wife Diane and my son Brice for the sacrifices of our time during my studies. I am thankful to my fellow graduate students including Alok Kapoor, Srikanth Padmanabhan, and Shou-Heng Huang for the many discussions and camradirie. Many thanks to the support staff at Iowa State University; Mr. Gaylord Scandrett, Mr. Brian Espeland, and Ms. Rosalie Enfield of the Mechanical Engineering Department, and lastly, special thanks to the Thesis Office for their support and patience.

1 INTRODUCTION

Hot machining has been characteristically applied to metals, specifically to those metals with a definite brittle-to-ductile transition temperature. For the purpose of this research, hot machining will be defined as the addition of thermal energy to a part by any non-mechanical means to aid in the material removal process. Ceramic materials also exhibit this brittle-to-ductile transition. The transition temperature for ceramic materials tends to be much higher and hence it is difficult to apply hot machining to ceramics.

Ceramic materials are usually either molded and fired to final dimension or fired and ground to final dimension. Molding to final dimension results in a large finish tolerance. Grinding to final dimension results in a tight finish tolerance on the final part. The cost of the grinding operation is expensive, up to 90% of the parts costs are grinding costs.

An additional significant non-monetary cost of grinding is the loss in material properties. The grinding operation is a brittle operation and leaves tensile residual stresses on the surface. The tensile residual stresses can cause minute surface imperfections to open and grow. The growth of these microcracks to macrocracks can result in catastrophic failure of the finished part [1].

If, instead of machining the material in the brittle region, the process were carried out in the ductile region, the final part would have compressive residual stresses. These stresses would tend to close surface imperfections and stop the growth of microcracks into cracks. In addition, these stresses would retard catastrophic failure rather than encourage it.

Hot machining ceramic materials requires finding a suitable ceramic with properties that justify the expense of the operation. The first required property of the ceramic material involves finding the brittle-to-ductile transition temperature which fall below the materials liquidus or

sublimation temperature. It also requires a heat source capable of raising the cutting zone temperature to the brittle-to-ductile transition temperature rapidly without raising the bulk body temperature which otherwise generates thermal cracking, differential thermal expansion, excessive melting, or chemical reactions.

The material selected for this research is silicon nitride. The heat source used was a continuous wave Neodymium Yttrium Alumina Garnet (Nd:YAG) laser. The basics of the Nd:YAG laser assisted turning process and justifications for material, heat source and processing decisions will be presented in the following chapters.

The focus of this thesis is to determine what makes laser assisted hot machining of silicon nitride possible. Determination of the parameters that control laser assisted hot machining requires a broad look at the areas of materials, optics, laser-material interactions, heat transfer, material absorption of light, and cutting tool material interactions. Silicon nitride as a material has properties which are desirable, but the process of shaping the silicon nitride to final form is exceedingly expensive. The first question to be resolved is the possibility of laser assisted machining of silicon nitride to produce a part without excessive surface damage. After Nd:YAG laser hot machining was determined feasible, questions examined in this thesis include: What parameters controlled the operations? Why was laser assisted machining possible for Nd:YAG but not advisable for carbon dioxide lasers? What alternate processes exist? Finally, what are the capabilities of these alternate processes? In short, if given a piece of silicon nitride bar stock and asked to manufacture a precise part, why would the laser assisted machining process be recommended, what limitations does this machining process possess, and what limitations of alternate processes would support the use of laser assisted turning.

2 BACKGROUND OF GENERAL MACHINING

2.1 Machining

The machining process is usually classified into three different groups. Group I has fracture as the primary means of chip formation. These chips are usually formed when a ductile material is machined at low speeds or when a brittle material is machined. Group II has plastic deformation as the rate controlling mechanism for chip formation. These chips are formed when a ductile material is machined and stringy, highly curled chips develop. Group III is a hybrid of group I and group II in which plastic deformation and fracture determine the chip formation [2]. The preferred method of machining is to be in the group III region for purposes of chip handling and disposal [2, 3, 4].

2.2 Brittle machining

Brittle machining usually involves the formation of discontinuous, inhomogeneous, or serrated chips. Some factors influencing the formation of discontinuous chips are inhomogeneous materials, local hard particles, impurities, slow cutting speed, or large depth of cut. When a brittle material is machined, the shear stresses rise on the shear plane until the stresses are above a critical value for crack growth. The crack then grows rapidly from the tool tip to the work piece surface minimizing the energy of crack growth by using any existing flaws, in effect, following the path of least resistance. The resulting surface finish is rough. The chips will be irregularly shaped with little curl [3, 4, 5].

2.3 Ductile machining

Ductile machining produces a generally superior surface finish. Compressive residual stresses are left at the workpiece surface, which tend to impede the formation of surface cracks. By contrast, brittle machining methods leave residual tensile stress at the surface which tend to promote the growth of cracks [6]. Investigations carried out with high hardness cutting tools at ambient temperature suggest that wear of the tool was by tribomechanical wear, plastic deformation, and brittle fracture. The ratio of critical crack lengths of silicon nitride is quite similar to that of 4340 steels [7, 8].

2.4 Conventional turning of brittle ceramics

In conventional turning, the workpiece is rotated and deformed against the rigid tool. The machining can be ductile, brittle, or a combination of the two. If the chip formation follows group I machining, there is an initiation and propagation of cracks in the material. The propagation of cracks produces a somewhat irregular surface which contains surface defects. The surface defects serve as ideal locations for crack initiation sites. If the machining is brittle, the surface may be under tensile residual stresses. Under tensile residual stresses, there is a tendency for the cracks to grow. If the cracks achieve critical size, then they can grow catastrophically [1, 4, 2, 9, 10].

2.5 Grinding

Grinding is a process involving random single point cutting operations on a workpiece. The randomness of the grinding operation is due to random cutting points and random abrasive grain orientation. The grinding point abrasive grains also tend to fracture periodically during the grinding process. The fractured abrasive grain material is then removed periodically from the bond material. The bond material is designed to allow the removal of grinding abrasive grain.

In an ideal situation, the downfeed rates of the wheel would allow the material removal from

the workpiece in the plastic machining mode. The randomness of the grinding grain prevents optimization of the machining process. The grinding grains vary in rake, side rake, relief angle, nose radius, etc. The fracturing of grains and the removal of grains from the grinding wheel make it difficult to control the cutting depth from one cycle to the next cycle. In the case of a single grain cutting a surface, a small amount of material is removed from the workpiece with each passage of the single grain of the grinding wheel. The maximum material removed is determined by a combination of the arc swept by the grain on the wheel periphery and the forward travel of the workpiece relative to the wheel.

Grinding can be carried out in the ductile region for hard materials such as silicon carbide and silicon nitride. Grinding silicon nitride in the ductile region requires low feeds, high speeds, small abrasive grains, hard grains such as diamond, high abrasive grain density, large nose radius, and high cutting forces [11, 12, 13, 14].

The ductile grinding method suffers from the inability to perform rough grinding due to the fine abrasive grain size. The wheel suffers from dressing difficulty with high density diamond tools. The small size of the abrasive grains makes the removal of the grain from the bond easier due to overstressing. Diamond also graphitizes at temperatures greater than 850 ^{o} C. For higher temperature applications, cubic boron nitride is necessary.

2.6 Grinding of brittle ceramics

The final grinding operation is a brittle machining process that results in surface cracking, rough surfaces, and discontinuous brittle chips [15]. A tensile residual stress is left on the material surface. The residual stresses are relieved by small cracks opening up on the surface. For normal grinding machines, the ratio of normal to tangential forces is 5 to 1. In the case of ceramic material grinding, the ratio of normal to tangential forces is 20 to 1. In the case of grinding high performance ceramic materials, reliability and integrity may be compromised. Additionally on a finished ceramic part, grinding costs may compose up to 90 % of the total finished part costs [11, 16]. If fine grained abrasives are used, the grinding time increases. If coarse grained abrasives are used, then surface finish suffers and grinding time decreases.

When the surface finish is poor, the strength of the material is reduced appreciably [17, 4, 11, 18, 19, 16].

Grinding is a process involving a random orientation single point cutting operations on a workpiece. The randomness of the grinding operation is due to random orientation of cutting points and the random cutting grain orientation. The grinding point grains also tend to fracture periodically during the grinding process and are removed periodically from the bond material. The bond material is designed to allow the periodic removal of grinding grain.

In an ideal situation, the downfeed rates of the wheel would allow the material removal from the workpiece in the plastic machining mode. The randomness of the grinding grain prevents optimization of the machining process. The grinding grains vary in rake, side rake, relief angle, nose radius, etc. The fracturing of grains and the removal of grains from the grinding wheel make it difficult to control the cutting depth from one cycle to the next cycle. In the case of a single grain cutting a surface, a small amount of material is removed from the workpiece with each passage of the grain of the grinding wheel. The maximum material removed is determined by a combination of the arc swept by the grain on the wheel periphery and the forward travel of the workpiece relative to the wheel.

Grinding can be carried out ductile region for hard materials such as silicon carbide and silicon nitride [20]. Ductile region grinding of ceramics such as silicon nitride requires low feeds, high speeds, small abrasive grains, hard grains such as diamond, high abrasive grain density, large nose radius, and high cutting forces [11].

The ductile grinding method suffers from the inability to perform rough grinding due to the fine abrasive grain size. The wheel suffers from dressing difficulty with high density diamond tools. The small size of the abrasive grains makes the removal of the grain from the bond easier due to overstressing. Diamond also graphitizes at temperatures greater than 850 ^{o} C. Grinding temperatures for silicon nitride excede 1400 K [21]. For higher temperature applications, cubic boron nitride is necessary.

In grinding of silicon nitride under the conditions above, the bulk material is damaged during the material removal process due to fracturing out clumps or grains of silicon nitride.

Using small diamonds at a density of over 6 grains per millimeter (150 grains per inch) in a high speed grinding wheel, a surface finish of 0.05 microns was obtained with over 2 % of the surface area damaged. The size of flaws monitored were 5-20 microns [22].

Grinding of hot pressed silicon nitride requires a specific energy of up to 800 J/mm ^{3} for finish with required specific energies for rough grinding to 13 J/mm^3. These energies are approximate to the levels for high strength metallic materials [23]. The characteristic of glass and metal where specific energy decreases as material removal rate increases is present in hot presses Si_3N_4. Surface finishes of hot pressed silicon nitride is 0.6 μm are required [24].

2.7 Electric discharge machining

Electric discharge machining can be used to machine some hard ceramics such as Sylon 501 but the electrical properties of silicon nitride do not lend them to this machining process. Electric discharge machining also causes micro-cracking at the sparking surface [15]. In order to electric discharge machine a silicon nitride part, different binders must be used. The binders raise the electrical conductivity. The binders also reduce the strength by about one half and the hardness considerably [17, 25, 26, 27].

2.8 Thermal removal of ceramic material

Thermal removal of material by use of a pure thermal source such as lasers or electron guns. Removal of material has been proposed by Bass, Chryssolouris, Copley and others and has been extensively researched. Silicon nitride parts have been produced but suffer from rough surface finishes and loss of 1/3 to 2/3 of the flexural strength using carbon dioxide lasers[15, 28, 29, 30, 31, 32, 33, 34, 35, 36, 37]. Silicon nitride has been removed by pulsed Nd:YAG lasers for the removal of material abalation [38, 39, 40, 41, 42]. Zirconia has been machined by Nd:YAG laser [43].

2.9 Machining of ceramics

Ceramic materials have historically been ground to the final shape. At elevated temperatures, ceramic materials are stronger and harder than most metals. In high temperature structural systems applications, ceramic materials made to precise dimensions are required. To this end, an improved method of manufacturing ceramic materials to tight tolerances without degrading the properties is necessary. Grinding of ceramic materials to tight tolerances is expensive, time consuming, and can produce residual tensile stress at the surface. Low fracture toughness materials generally respond to applied forces by crack generation and crack propagation [44].

Machining of ceramic material is usually carried out under brittle machining conditions. The brittle machining mode can leave unfavorable residual stresses at the surface. The chip formation is discontinuous and microcracks may extend down into the part surface [1]. Discontinuous or brittle chips are formed in the machining of brittle materials due to the material's inability to undergo the shear stresses involved in cutting. Shear localization also results in discontinuous chips. These discontinuous chips are also called serrated or inhomogeneous chips. Low thermal conductivity, high localized strains, and high strain rates are associated with the formation of discontinuous chips. Ductile machining would improve the surface finish and eliminate crack initiation sites. In order to ductile turn the ceramic, the material must be heated above the glass transition temperature [45]. The heating of the material above the glass transition temperature must be done in a manner that does not introduce thermal cracking or bulk expansions which could lead to inaccuracy in the finished part [44, 5, 46].

3 BACKGROUND OF HOT MACHINING

The general theory of hot machining, as applied to the lathe, is to reduce the energy required at the cutting tool to turn the part. The reduction in turning energy is accomplished by decreasing the strength and hardness of the workpiece material without overly reducing the strength and hardness of the cutting tool. The increased temperature of the workpiece results in reduced workpiece material strength and hardness.

3.1 Introduction to hot machining involving experimentation

The technique of hot machining involves heating the material being machined immediately before the cutting tool (see Figure 3.1). The general purpose of this heating is to reduce the amount of energy needed to shear the chips from the bulk workpiece. The heat source for the hot machining may take the form of an electrical current, a radio frequency induction heater, a flame ring, a flame torch, a gas plasma torch, or a laser beam. The general arrangement of laser assisted hot machining is shown in Figure 3.2. Hot machining is investigated for the purpose of turning ceramic materials. Ceramic materials as a general class are ground and not turned. In the grinding operation, the ceramic is subject to brittle failure at the surface which leaves a tensile residual stress at the surface. The purpose of hot machining of the ceramic is to produce a machined part without producing surface damage.

3.2 Hot machining

Research in thermal-assisted machining first began during the World War II at Krupp in Germany where a machine for hot slabbing molybdenum case hardening steel at temperatures up to 1273 K (1000 ^{o} C) was built and used. Tungsten carbide with 4 % titanium carbide and

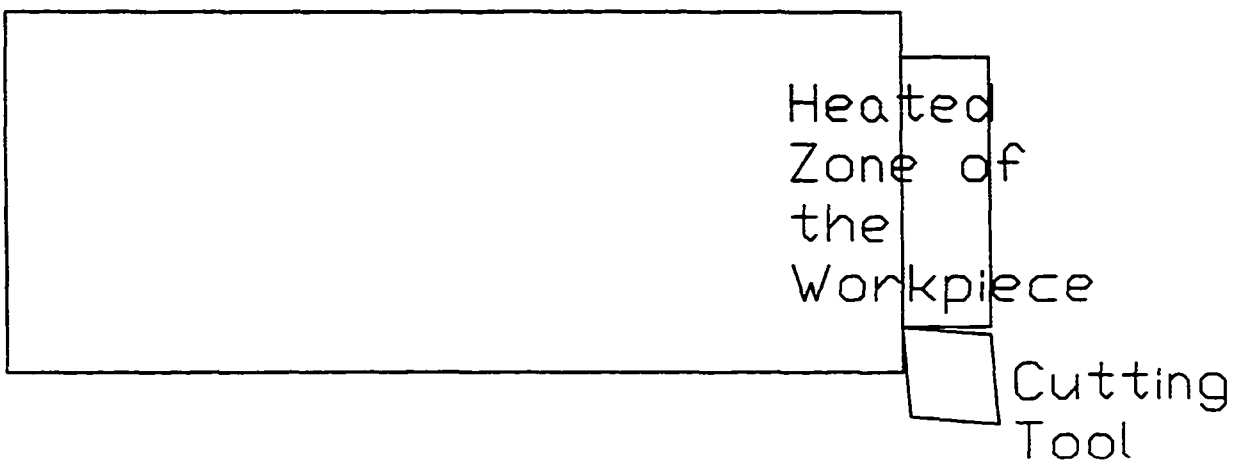

Figure 3.1 General hot machining arrangement

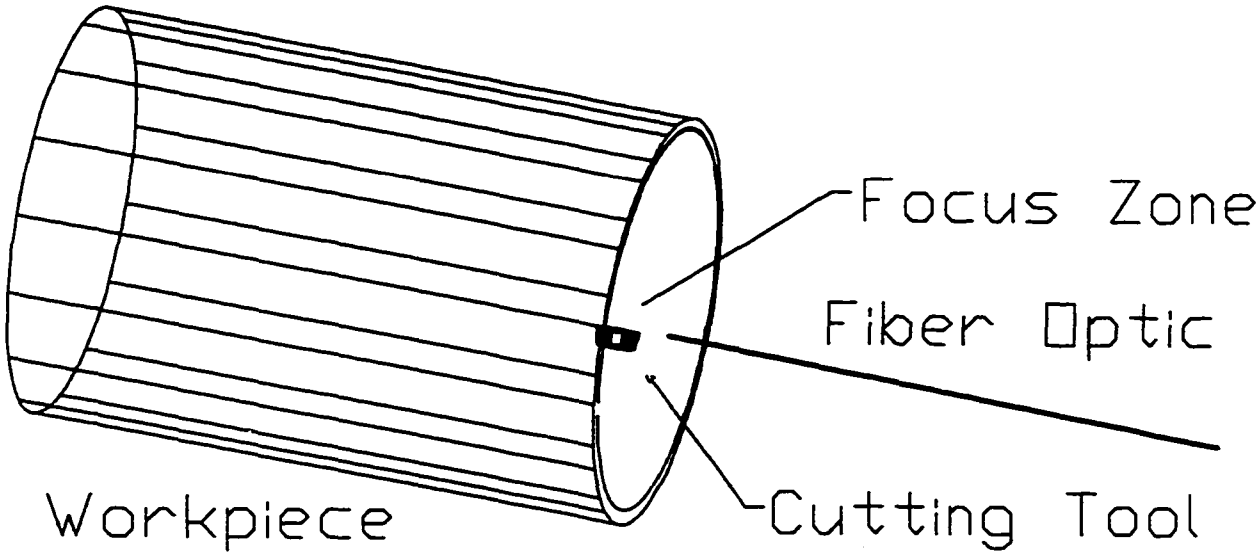

Figure 3.2 Laser hot machining arrangement

approximately 14% cobalt were used to produce chips 5/16 inch thick and 2 3/4 inches wide with slabs going directly to milling from the furnace [47].

Improvement in the machining of "impossible" materials was reported by Gillette of Battelle in 1944. In 1946, Sam Tour and Company began research in "hot spot machining" [47]. Oxyacetylene torches and induction heaters were used for heating. Research into the machinability of cobalt-chromium-molybdenum-tungsten materials was performed. Machinability increased in the range of 125 times by heating the steels to 1088 K prior to machining. Forces decreased substantially with a heating of the surface to about 1106 K (833^{o}C). Findings on the machining of V grade nickel steels included that material removal rates were increased between 200 and 300 percent . Surface finishes were noticeably improved. No degradation of the remaining material was evident.

Research published by Roubik and Schmidt of Kearny and Trecker in 1949 reported the milling of SAE 4340 die blocks with a room temperature hardness of 280 BHN [48]. High strength materials could be milled at higher feed rates and speeds with no reduction in tool life when heated to approximately 940 K (667^{o}C). Tool life was equal in time even though the room temperature milling was performed with a feed of 1/8 of the 1033 K milling. The milled surface indicated no temper color or discoloration demonstrating temperatures of less than 467 K (350 ^{o}F). Microscopic analysis revealed no difference in the microstructure between those milled at room temperature and those at elevated temperature. Spindle power requirements were reduced while feeds were increased. Application was limited to cases where machining could not be economically by any other method.

Work performed by Krabacher and Merchant at Cincinnati Milling Machine Company reported that two material factors were important to the hot machine processing: the ability of the tool material to tolerate abrasion of the workpiece, and the tool/chip interface temperature [9]. In effect, there is a competition between the tool material and the work material involving the temperature effects. If the tool material loses its hardness and strength faster than does the workpiece material, hot machining is not advantageous. If the workpiece loses strength, hardness and abrasion resistance at lower temperatures than does the tool material, then hot

machining is advantageous. Hot machining may increase or decrease the tool life depending on the workpiece material and tool material properties.

Materials that were researched were AISI 3145, Inconel X, Timken 16-25-6 and S816. The AISI 3145 was chosen in two conditions for comparison purposes: hardened and as- received. The three others were chosen due to the difficulty of machining and the belief that the hot machining technique would improve the machinability of the materials.

Induction heating was used for the early tests but was found to have insufficient power densities for nonmagnetic high temperature materials. Distributed oxygen propane flames heated the material through flame nozzles moving with the cutting tool up to 1085 K (812 ^{o}C). One very interesting note was that the tool-workpiece interface temperature "actually runs cooler at 533 K (260 ^{o}C) (preheat temperature) than it does when the work is done at room temperature" [9]. This is due to the reduction of plane strain energy. Abrasion is the enemy of the thermal-assisted machining process. Thermal-assisted machining is difficult due to normal cutting tool limitations.

The ability of the tool material to withstand abrasion decreases with increasing temperature. The ability of the workpiece to abrade the tool also decreases with increasing temperature. If the abrasion resistance of the tool is decreased more rapidly than the strength of the material, then the hot machining process is not recommended. If the ability of the workpiece to abrade the tool decreases rapidly due to the temperature causing a brittle-to-ductile transition or a minor phase change, then hot machining would be recommended. Problems associated with bulk heating of the entire material were noted. It was noted that reduced cutting forces were due to the reduced shear strength of the work material at higher temperatures.

Metals are considered as good candidates for hot machining if they have high modulus of strain hardening. If metals have high modulus of strain hardening, the layer immediately below the cut hardens greatly making it more difficult to shear the work-hardened layer of material. The energy needed to induce shear at the shear plane is reduced at higher temperatures.

The hot machining process reduces the stress at the shear plane, which reduces the strain hardening. The strain associated with chip deformation is highest at the top of the edge of

the chip and lowest at the chip/ tool interface. The temperature distribution is highest at the chip/ tool interface. The thermal weakening is highest at the point where the strain is lowest. The basic ideas behind hot machining, especially with a moving heat source, are to weaken the material most where the strain is highest and to reduce stress at the shear plane of machining [9, 11].

In the case of the AISI 3145 when the material was machined in the as-received condition, the machining at room temperature was superior to hot machining at 1075 K (800 ^{o}C). When the material was heat treated to a hardness of 350 BHN from its as-received hardness of 200 BHN, the hot machining was superior with a drop in hardness to 340 BHN. Tool forces and shear strength are actually higher at 1075 K (800 ^{o}C) than at room temperature for the as received AISI 3145 steel. Tool failure using carbide tools was due to gradual wear at higher speeds and to chipping of the carbides at lower speed particularly those involving intermittent cutting such as milling.

Krabacker-Merchant's research concluded that the primary mechanism for hot machining ability to increase material removal rates with reduced power requirements was the reduced shear stresses of the workpiece [9].

A report on work carried out at Cincinnati Milling Machine Company under the Air Material Command in 1961 continued the work reported by Krabacker-Merchant. Four materials were chosen based on common usage; AISI 4340 alloy martensitic steel, 17-7 precipitation hardening stainless steel, Uniloy 17-4 Mo precipitation hardening stainless steel, and Theromold J hot-work die steel. Temperature was related to shear strength on the shear plane, shear angle, mean coefficient of friction, cutting forces, machining efficiency, and tool/chip interface temperature. As a result of this research, flame, arc, and high frequency induction heating techniques were applied to turning and milling. This research noted several significant results and conclusions as given below [49].

First, the research found that increasing the part temperature did improve material removal rates, reduce tool forces, and reduce the work done. Also, tool temperatures did not necessarily increase as rapidly as workpiece temperatures. Next, limiting temperature is reached when

welding occurs at the tool tip with the workpiece. In addition, high frequency induction is limited in concentrations but is acceptable for maintaining and controlling temperatures. Also, radio frequency resistance can control and localize heat without the problems of arc, induction, or flame heating. Continuous roughing operations were better suited for thermal-assisted machining. In addition, thermal distortions could be minimized with better localization of heat. Next, higher cutting temperatures increase the plastic deformation of the workpiece material. There was no microstructural differences between hot machined workpieces and those more conventionally machined. Finally, lowering the temperature produced less plastic chip formation.

In 1970 Cutfast [3, 50] patented a plasma-assisted hot machining process utilizing high machining rates, lower feed rates and high temperature ceramic cutting tools. Thermal-assisted machining or hot machining using an argon plasma- assisted machining demonstrating increases in material removal rates of 300% have been reported by Cutfast with corresponding reductions in machining times of 40%. The Cutfast process has gained acceptance as most suitable for machining hardened tool steels, Nimonics, cast cobalt, maganese steels, tough alloys and tough stainless steels. Improvements in cutting time have ranged from 4.6 times for stainless steel rolls to 20.6 times for high speed steel [51]. In every case of difficult-to-machine materials, cutting forces were reportedly decreased by 25 to 50 %. The plasma-assisted hot machining frequently utilizes the workpiece as the anode for the machining. This practice works well for metals but fails when the workpiece is a ceramic or insulator. Improvements in hot-machined surface finish were reported in all cases. In one case, final grinding was eliminated as unnecessary.

The research concluded that the ideal heat source would heat only the material to be removed and not the underlying material. It would "quickly raise the temperature so that it can keep ahead of the cutting tool, and this requires a high specific heat input (watts/sec cm^3). Such a method should provide a wide range of constant temperatures, and its results should be reproducible" [3]. A perfect fit of this description might be a high power laser [52]. Smith states that an ideal heating method would heat the work piece material, only as it passes through the chip forming zone, and would leave the remaining material unheated, and

unaffected, by the heating source [51]. This heating source is best available from a high power laser.

Rajagopal used a 15 kilowatt carbon dioxide laser in experiments with Inconel 718 and Ti-6Al-4V [53, 54]. The Ti-6Al-4V with a hardness of 40-42 HRC was machined twice as fast with a 12 kilowatt carbon dioxide laser as without. Carbide tools were negatively affected by thermal-assisted machining when machining Inconel 718. Tool wear decreased 50 % for nose wear, by 35 % for notch wear, and flank wear actually increased by a factor of 2.5. Ceramic tools are not as sensitive to thermal heating and performed better with laser-assisted machining. Microcracks were eliminated by a light finishing operation following heavy machining.

Copley reported on the results of laser-assisted turning plain carbon 1090 steel and Udimet 700 [55, 54]. He concluded that heating the material on the shear plane may change chip formation mechanism to continuous from discontinuous or reduce built up edge. Also, improvements may include reduced cutting forces, enhanced material removal rate, tool life, and surface conditions (flaws, residual stresses, and smoothness). In addition, heating the surface in contact with the cutting tool decreased tool life. Finally, improvements were noted with ceramic tools over carbide tools. Hot machining was successful in increasing tool life and decreasing surface roughness in the case of Udimet 700. Tool forces for the case of hot machining 1090 increased rather than decreased due to austenitizing the undeformed chip but the undeformed austenitized chip was converted to martensite before the chip was cut form the part. Hot machining has continued as both a practical technique for some materials and as a research topic.

Costs of the laser-assisted machining of P/M Rene 95, and low carbon steel, and Ti-6AL-4V has been analyzed for the economics by Tipnis [56, 57]. The conclusion that under those conditions and costs, laser assisted machining was economically unviable based upon ROI. Payback under costs were 30 years. Assuming a reduction of 75% in the cost of the required equipment for laser-assisted machining, the economics are still not viable with a payback time of 10 years.

Ovseenko in 1983 reported on the application of high frequency induction heating for hot machining of high alloy cast irons having a hardness of 50-62 HRC. Temperatures of up to 573

K were controlled within 25 K [58] . Plastic deformation was observed in the surface layer which left a favorable compressive stress. Surface roughness decreased by a factor of approximately 2.5. Preheating by less than 300 K resulted in a reduction of cutting temperature. Preheating by more than 300 K at speeds of over 60 m/min does not result in any improvement because the tool/workpiece temperature is elevated. Continuing research has focused on high specific energy systems such as lasers, plasma heating, and arc heating.

Carbon dioxide lasers were used by Bass and Copley in 1979 in the turning of Udimet 700 and 1090 plain carbon steel [59]. Improvements in tool life and surface finish were reported for the Udimet 700 but tool forces were not reduced as would be expected. The lack of tool force reduction indicates that workpiece strength was not sufficiently reduced. The increase in tool life is likely due to decrease in tool abrasion.

Jau, Bass, and Copley in 1980 used carbon dioxide lasers in researching laser-assisted turning of Inconel 718. Increases in material removal rates were reported with no decrease in tool life by heating the material on the shear plane. In order to make this process economical, an increase in absorption of the laser irradiation must be increased, the optical system loses must be decreased, or the power must be economically increased [59].

Copley and Bass in 1985 used carbon dioxide lasers on Udimet 700 and 1090 carbon steel. The 1090 steel required more power to machine due to the steel being austenitized and then transforming to martensite [60]. Surface finish and tool life were improved for the Udimet 700.

Bass reported results of hot machining of Inconel 718 and Ti-6Al-4V precipitation hardening materials in 1985. Addition of the carbon dioxide laser was observed to decrease the cutting forces. Reducing the velocity also lowered the cutting forces.

A 15 kilowatt carbon dioxide continuous laser was used with ceramic cutting tools. Difficulties in the absorption of 10.6 micrometer wavelength limited the low power applications on Ti-6Al-4V and Inconel 718. Absorption could be increased by the use of Neodymium Yttrium Aluminum Garnet (Nd:YAG) lasers with a wavelength of 1.06 micrometers.

Berenov in 1985 researched plasma torch—assisted turning of steels and carbide cutting tools in which an optimal cutting tool geometry was analyzed [61]. Berenov et al performed

plasma arc-assisted machining in 1989 of austenitic high maganese steels [62]. Plasma arc-assisted machining consists of plasma arc heating of the material to be removed followed immediately with a subsequent machining by cutting tool. Findings were that if the material to be removed could be heated without melting, then the surface finish improved by .2 to 3 micrometers. This was explained by a reduction in the coefficient of friction and a lack of buildup "braked" layer preceding the tool surface. Difficulties in the control of the uniformity of the arc were noted. Work hardening was not observed when high feed and low depth of cut were used. Compressive residual stresses indicated that the machining was in the plastic region. A more favorable microhardness was observed where work hardening was not to be permitted such as with nonmagnetic austenitic steels.

Takeshita and Uehara researched oxygen / acetylene- assisted machining of ceramics including alumina (Al_2O_3), zirconia (ZrO_2), mullite, and silicon nitride (Si_3N_4) [63]. The machinability of zirconia and alumina did not improve with hot machining [63]. Both silicon nitride and mullite behaved similar to metals in hot machining. Both materials displayed optimal cutting temperatures with respect to minimum cutting force. These researchers concluded that "the effect of hot machining concerning the cutting force and chip form in the ceramic cutting is just the same as that of metal cutting" [63]. Surface roughness improved to the point that feedmarks could be easily distinguished. Tool wear was improved and cutting forces were reduced.

Kitagawa and Maekawa in 1984 reported that use of plasma arc- assisted machining in 18 % Mn steel and 0.46 % C steel resulted in improved machinability [64]. This improved machinability consisted of reduction of built up edge, an improvement in surface finish and tool wear, and reduction in tool chatter.

Akasawa, Takeshita, and Uehara in 1987 continued experimentation with oxygen-acetylene heated hot machining on carbon steels using cooled TiC and coated cermets [65]. The multi-coating cermets produced the best tool life with the lowest wear. The cermets had the highest oxidation resistance at 1273K. Cooling the cutting tool resulted in longer tool life under all tested condition.

Kitagawa, Maekawa, and Kubo in 1988 researched continued plasma hot machining of chilled cast iron (372 HB) [66]. The chilled cast iron was successfully machined with a 300 K (300^o C) preheat. The chilled cast iron with a hardness of 380 HRC produced much less chipping of the tungsten carbide tools. The drop in hardness and abrasion resistance with hot machining rather than a drop in strength was credited with the reduction in forces. The drop in hardness resulted in significantly less tool chipping and flank wear. Cutting costs decreased 50 percent for chilled cast iron.

Kitagawa and Maekawa in 1990 reported that the use of plasma arc- assisted machining in fully dense ceramics resulted in improved machinability [46]. Alumina and zirconia showed no improvement. In the case of silicon nitride, the increase in tool life was eight-fold. Chip formation changed from brittle to ductile chip formation at about 1323 K (1050^o C). Ionic ceramics such as alumina and zirconia [67] did not improve in machinability with hot machining. Chip formation generally becomes ductile or plastic chip formation above the glass transition points [68]. Tool life was increased with hot machining for cubic boron nitride and polycrystalline diamond. Cemented carbides did not withstand the use. Reduction of built up edge, an improvement in surface finish and tool wear, and reduction in tool chatter was observed. Silicon nitride exhibited a clear improvement in machinability above 1373 K. The glass transition temperature is in the range of 1075— 1275 [69]. It was reported that tool costs can comprise up to 95% of the total cutting costs. The relationship of tangential (F_t) to normal forces (F_n) in machining is reversed in hot machining. Surface roughness is optimal at $F_t/F_n = 1$. Large defects due to brittle machining disappear.

Konig and Zoboklicki in 1993 [70] used carbon dioxide and Nd:YAG lasers with polycrystalline diamond and cubic boron nitride for turning of Stellite 6, and hot pressed silicon nitride. Cutting forces for the cutting of Stellite 6 was reduced by 70 % and tool wear decreased 90%.

4 HEAT SOURCES OF HOT MACHINING

4.1 Flame sources

Flame sources (see Figure 4.1) were the first and cheapest source of thermal energy at the cutting zone for hot machining. The disadvantage of the flame source is that the process is limited by the adiabatic flame temperature as the maximum temperature possible. The energy intensity can not be increased. The energy flux can only be increased by higher flow rates. The additional disadvantage of flame sources is that since the reaction is a chemical one, the material can chemically react as well.

4.2 Induction heat sources

Induction heating (Figure 4.2), by contrast, is a non-contaminating process. Induction heating of a material requires the magnetic coupling between the electromagnetic source and the material being machined. Induction heating heats from the surface down, with the depth of penetration being partially controlled by the frequency of the induction source. Higher frequencies will result in a smaller heating depth. However, most ceramic materials are non-magnetic and therefore, they are not capable of being heated by induction heating.

4.3 Plasma heat sources

Plasma heat sources usually consist of a charged ionized gas between the nozzle and the workpiece. Plasma sources can be divided between transferred versus internal (non-transferred) plasma arcs. Transferred plasma arcs (see Figure 4.3) operate between the plasma gun's electrode and the workpiece. The nozzle is usually used as the anode and the workpiece is

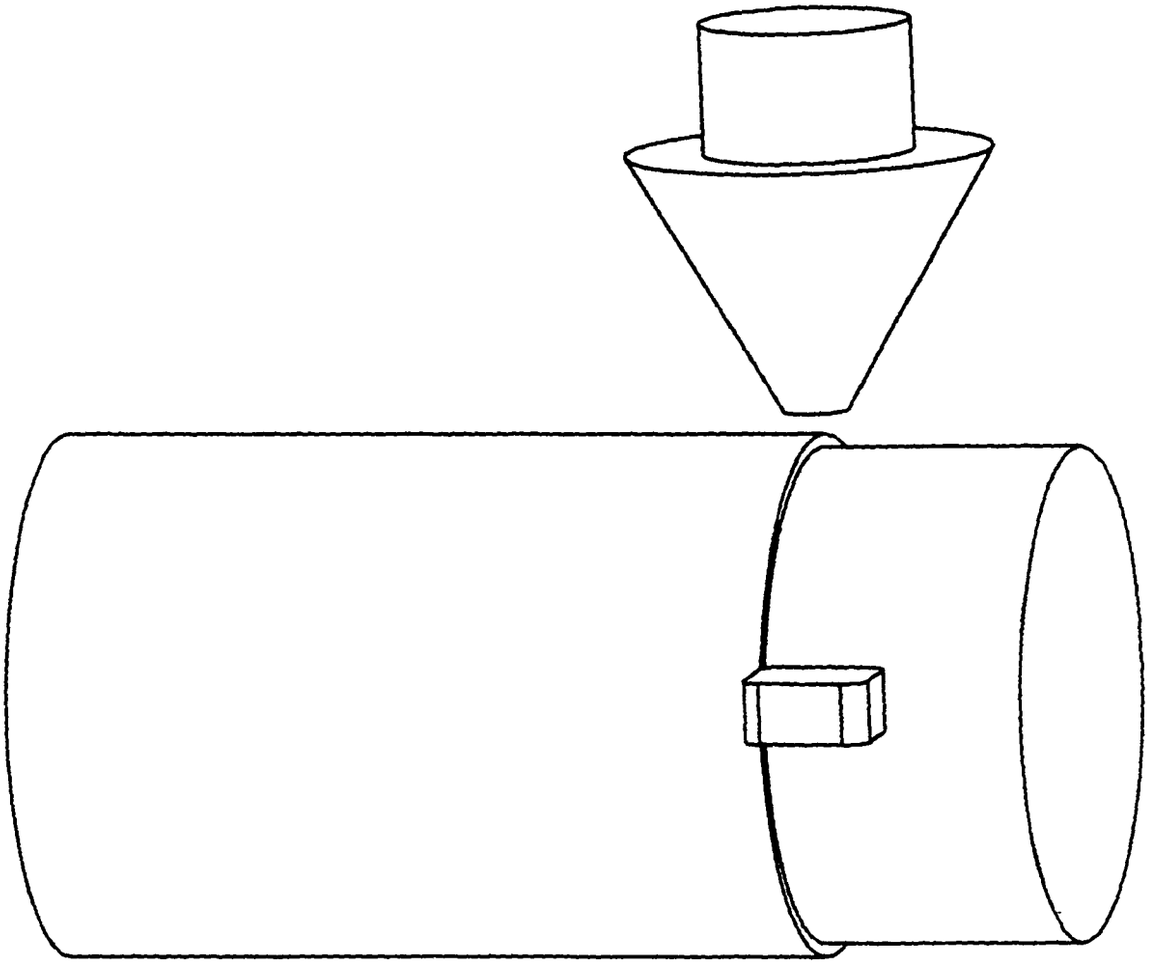

Figure 4.1 Flame heating arrangement

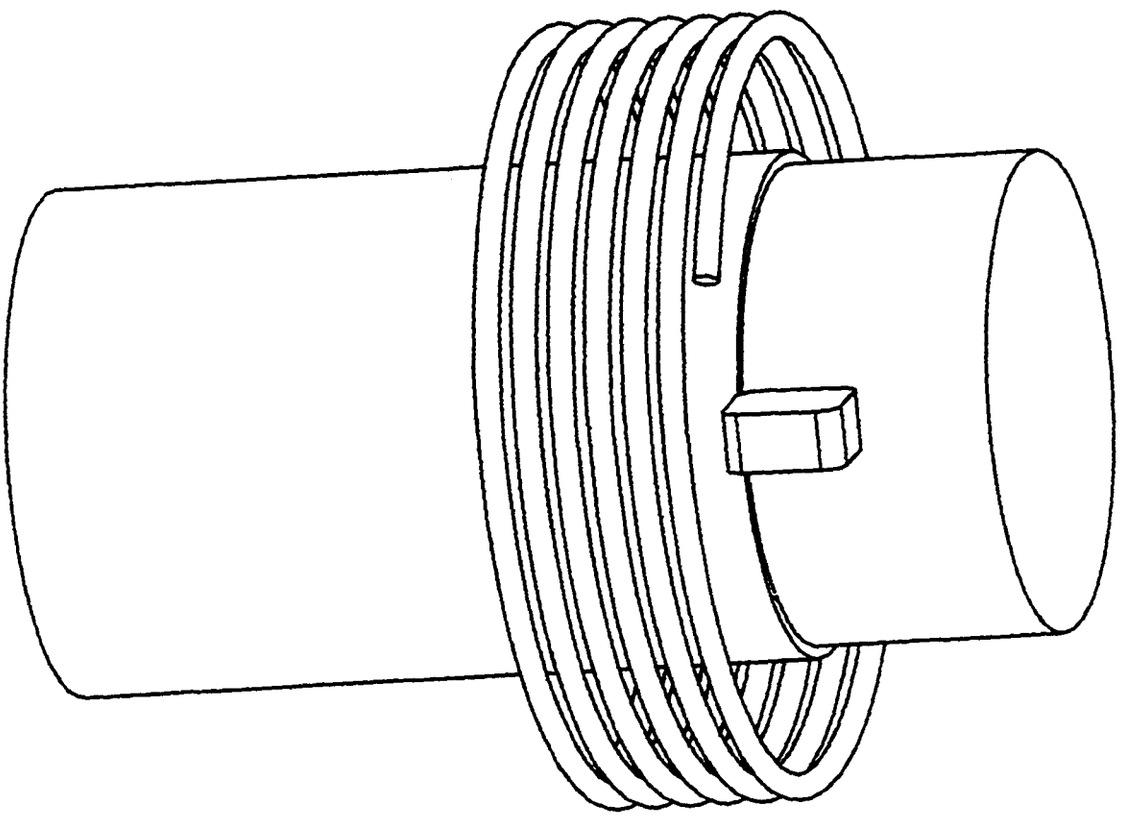

Figure 4.2 Induction heating arrangement

generally used as the cathode. In ceramic materials, this is not the case due to the low electrical conductivity of the materials. The plasma must therefore be an internal arc, produced and contained within the plasma gun itself. The internalized plasma arc (see Figure 4.4) is less efficient than the transferred plasma arc, requiring more cooling, and transferring less energy to the workpiece. The size of the interaction zone is larger and the interaction time thus is longer. It may be problematic to heat just the material to be removed. Additionally, reactions between the plasma gases and the workpiece material must be considered.

4.2 Laser heat sources

Lasers as heat sources provide monochromatic, spatially and temporally coherent energy sources that are highly intense. The coupling of the laser light to the workpiece is a function of the absorptivity of the material to that particular wavelength of light and the angle at which it is incident [71].

4.4.1 Carbon dioxide lasers

Carbon dioxide lasers are reliable workhorses in industry. Common powers of these lasers are 1–3 kilowatts operating continuously producing a wavelength of 10600 nanometer. The absorption of carbon dioxide laser light by silicon nitride is known to be .23 and machining of silicon nitride has been carried out using only carbon dioxide laser radiation. However the strength of the material after being cut dropped due to the presence of thermally damaged material layer [72, 73].

4.4.2 Nd:YAG lasers

Neodymium Yttrium Alumina Garnet lasers can lase at 1060 nanometer. Experiments showed that silicon nitride absorbs the 1060 nanometer wavelength readily. Tabulated values for absorption of silicon nitride are given as 0.7 in contrast to .23 for CO_2 laser. The power of Nd:YAG lasers has been limited to 400 watts when operating in the continuous wave region in earlier days. Recently, Nd:YAG slab lasers capable of producing continuous emissions up to

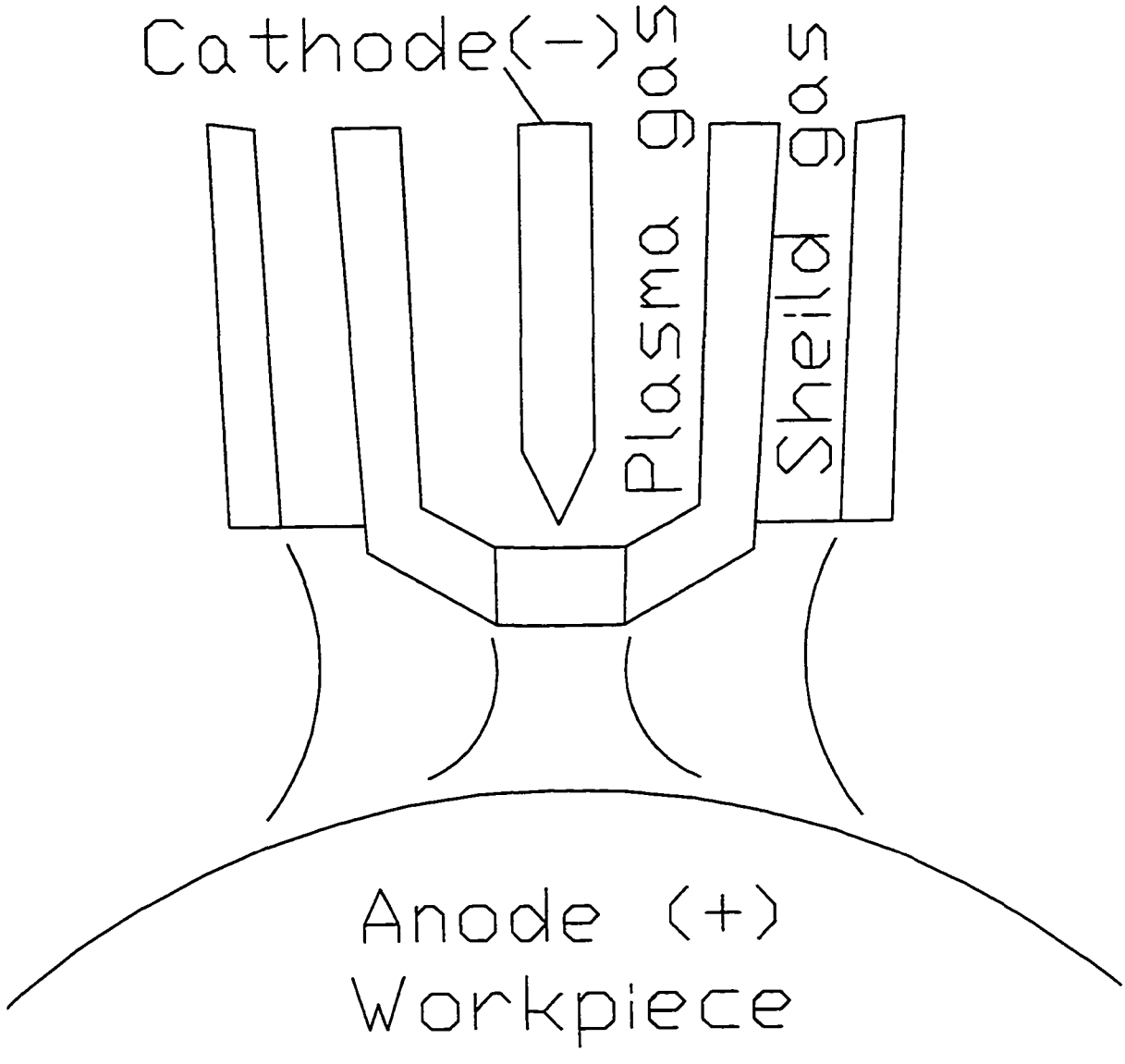

Figure 4.3 Transferred plasma—arc arrangement

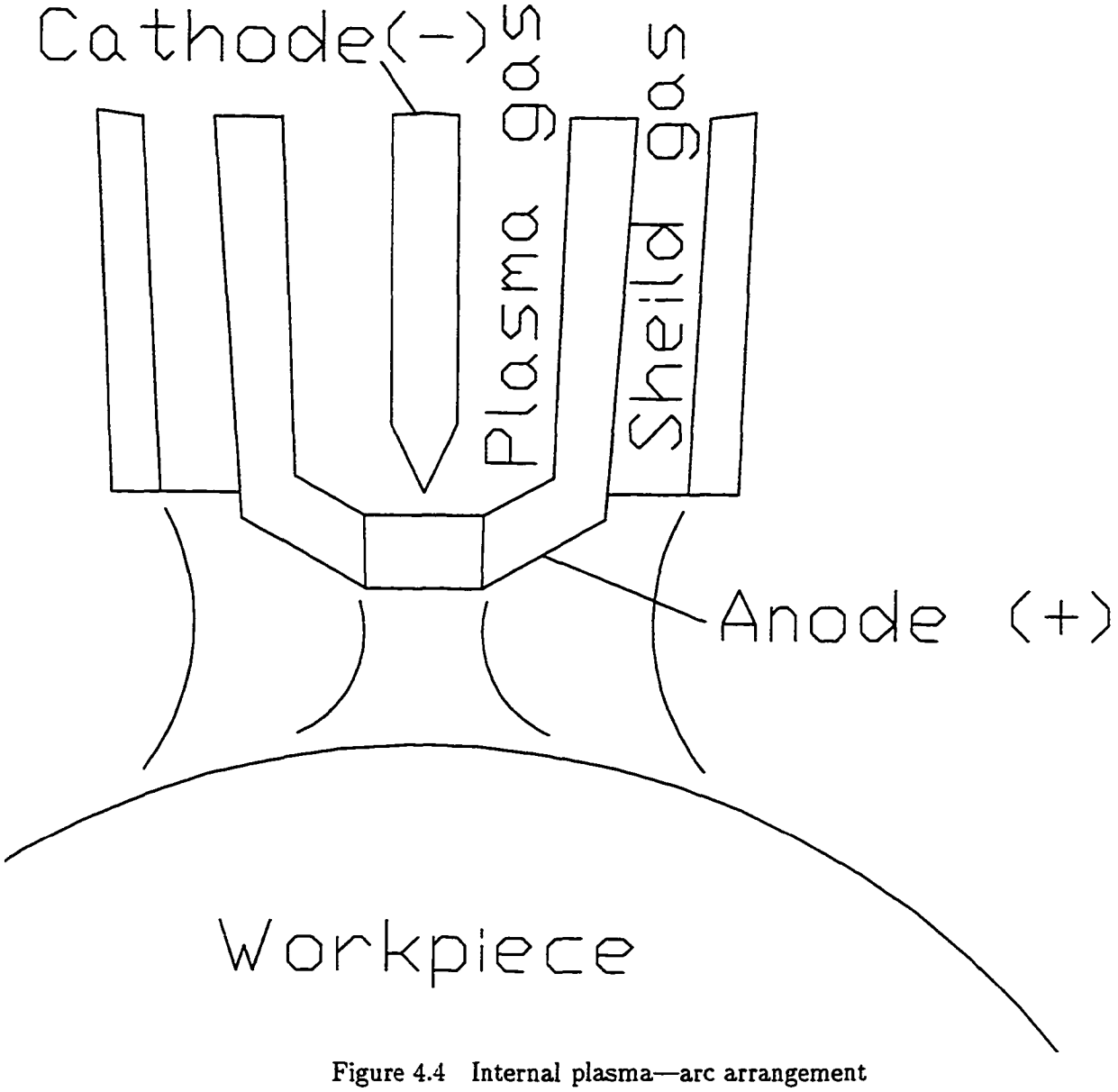

Figure 4.4 Internal plasma—arc arrangement

powers of 2.5 kilowatts have been developed [74]. According to *The Industrial Laser Review*, purchase costs for continuous wave Nd:YAG lasers are $100/watt and operating costs are $10/hr with an average uptime of 90 % [75].

4.4.3 Comparing Nd:YAG and CO_2 on absorption and penetration

In a comparison of the absorption and penetration of different frequency of light on a material, one must look primarily at the wavelength or frequency. For example, copper reflects carbon dioxide wavelengths, and absorbs Nd:YAG laser energy. Ceramic materials as a general class absorb carbon dioxide wavelength better than Nd:YAG wavelength. But silicon nitride absorbs Nd:YAG laser spectra better than carbon dioxide laser beams.

4.4.4 Fiber optics

Fiber optics capable of carrying higher energy density are becoming available primarily for Nd:YAG lasers. The use of high power fiber optics for delivery of laser beams greatly reduces the complexity of optical systems. Fiber optics for carbon dioxide lasers exist but suffer from severe attenuation. Fiber optics for carbon dioxide lasers currently suffer an energy loss of 50 % for short distances. The losses on carbon dioxide laser fiber optics, combined with high cooling requirements for the power losses, eliminated the possible application of carbon dioxide beam for this research.

5 SILICON NITRIDE

Silicon nitride materials are desirable for their high strength, high rigidity, chemical inertness, and high hardness [17, 67, 3]. Silicon nitride (Si_3N_4) is used in primarily two forms: reaction bonded and hot isostatic pressed. Reaction bonded is commonly ground or machined first in the green state and then nitrided and is gray in color. Powders are sized to allow full nitriding of the silicon powder to keep distortion to less than 1 percent while allowing a volumetric expansion of 20 percent. Strengths of reaction bonded silicon nitride are at most one half of the hot isostatic pressed [17, 76, 77]. Reaction bonded densities are approximately 70 % of the hot isostatic pressed. Reaction bonded silicon nitride fails catastrophically. Reaction bonded silicon nitride is processed at 0.2 to 10 MPa N_2 and high temperatures of 2073 K (1800 ^oC) [78].

Hot isostatic pressed material (or HIP) is formed by compacted powder methods and subsequently hot isostatic pressed at pressures and temperatures to form a near full density part. Hot isostatic parts are black in color. Distortions of approximately 1 percent (non-uniform) expansion of the part occur with hot isostatic pressing. Silicon nitride can only be densified to 85% theoretical density without any additional binders [79, 80, 81].

Diamond forming conditions are required to achieve this density. To obtain nearly full density (approximately 98%), sintering binder aid(s) must be added. These binders aid in increasing the density of the material and improving material properties. However, the cost of using these binders is a reduction in theoretical maximum hardness and strength properties due to the solidification of these binder aids in the intergranular areas. The binders often remain as a glassy or amorphous phase layer segregated between the grain structures.

Silicon nitride has two primary structures: the α (Figure 5.1) structure and the β (Figure

5.2) structure. The density of α ABCDABCD and β ABAB are approximately the same. The difference is in the stacking arrangement. (see Figures 5.1 and 5.2). In the hot isostatic pressing process, a mixture of more than 80 percent α silicon nitride is mixed with a few percent of rare earth oxides such as yttrium, and the remainder β silicon nitride powder. The powder is first compacted and pre-formed. The preform is then placed in a hot isostatically press at temperatures of generally 2123 K and pressures of 200 kilopascals pressure of nitrogen or argon for 5 hours. A glassy or liquid phase of the rare earth oxides is formed. The α silicon nitride dissolves into the rare earth oxide. The silicon nitride precipitates out as the β phase and interlocks the existing and growing β grains [82]. A one percent non-uniform expansion results. If the process was started with mostly β silicon nitride, the intergranular interlocking would not occur. The result would be a much more friable and less tough ceramic.

Strength of silicon nitride is strongly dependent on the density (see Figure 5.3). Fracture toughness is temperature dependent for the intergranular material (see Figure 5.4) but not for the silicon nitride only [83, 84]. In full density silicon nitride with a density of 3.19 g/cm^3, the strength is 1.1 GPa. If the density is reduced to 3.0 g/cm ^{3}, the strength is 0.5 GPa. A loss in density of 5 percent results in reduction in strength by one-half [85]. Youngs modulus of up to 300 GPa have been reported for full density material(3.3 g/cc) at room temperature. A strength of 900 MPa was reported for such a material at room temperature. The strain rate of $20\text{x}10^{-6}$ per hour was used with a fixed stress of 77 MPa for determining the strength. Hardness of silicon nitride is approximately 20 GPa Knoop at 1500 K.

After grinding, the strength of silicon nitride is highly dependent on the surface finish of the finished part. In research carried out at England in 1985, tensile specimens were broken utilizing spherical bearings for pure tensile loading [17]. The specimens failed below manufacturer's values, the cause of failures being due to surface imperfections created during machining. Higher strength is obtained with better surface finish. A typical silicon nitride (HS130) requires a surface finish of 1-2 μ meters to preclude surface initiated failure. Hardness is higher for pure α silicon nitride but fracture toughness is much higher for pure β silicon nitride. Rocker arm inserts and rocker rams require a surface finish less than 0.01 micrometers [86].

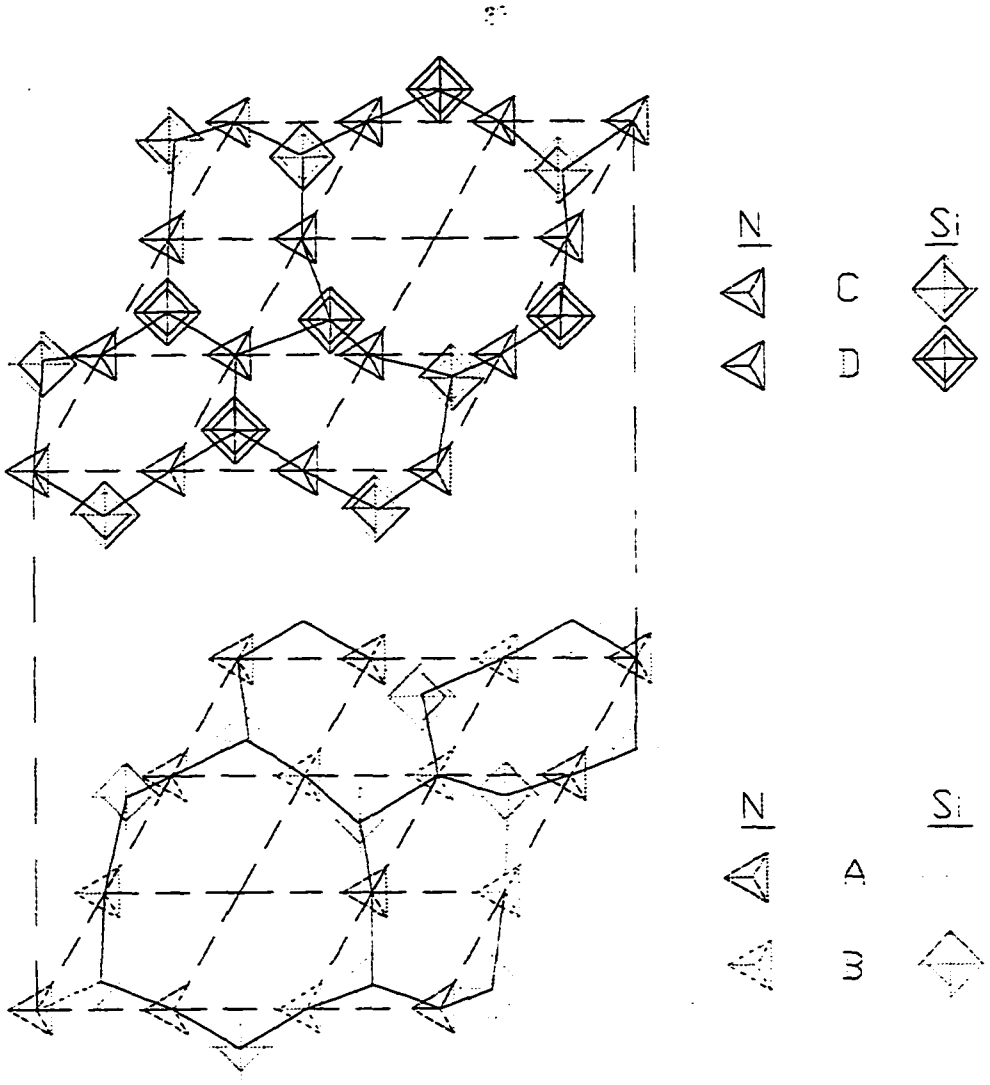

Figure 5.1 Structure of α Si_3N_4

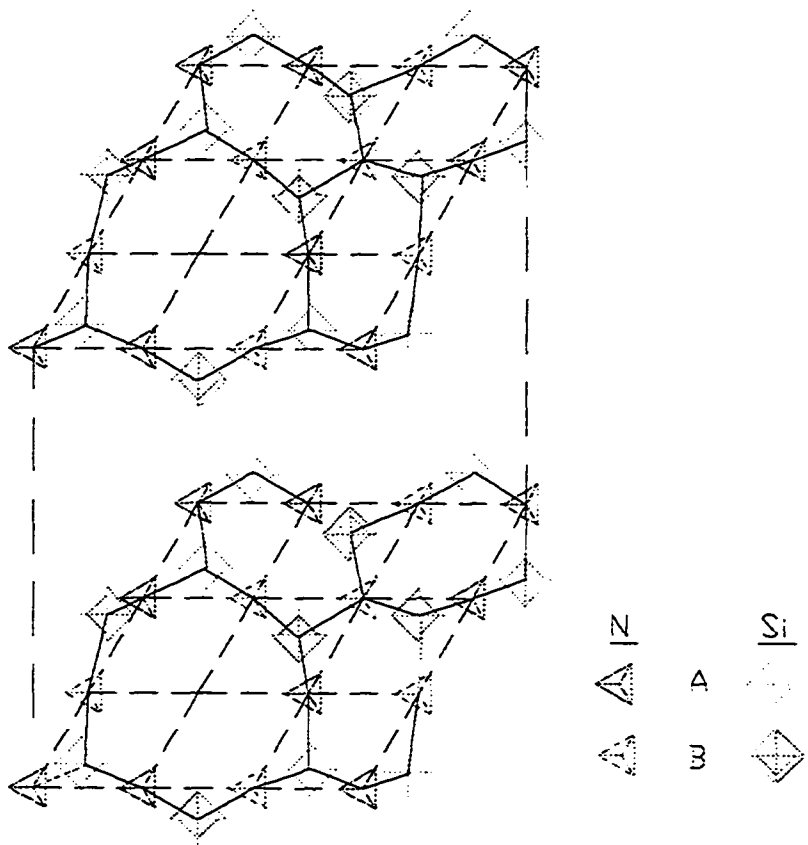

Figure 5.2 Structure of β Si_3N_4

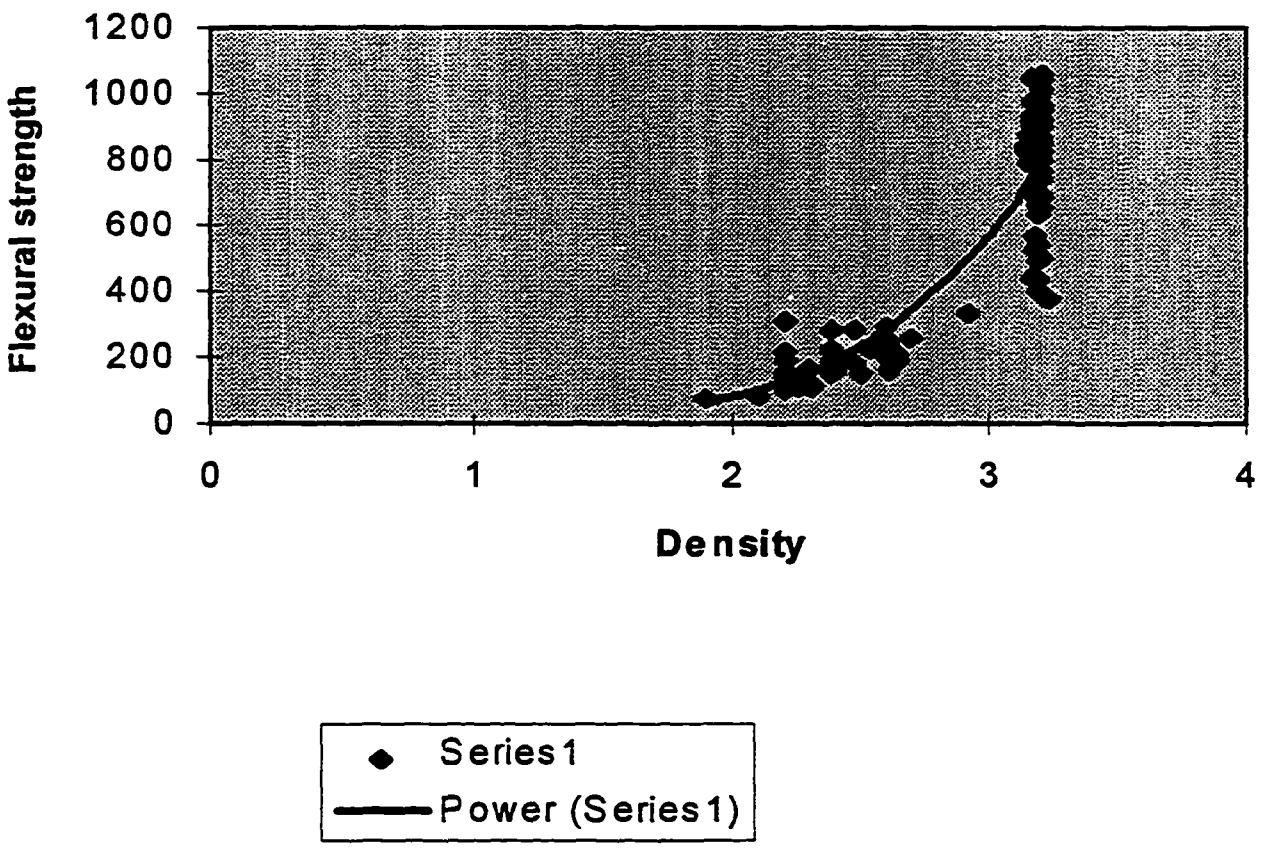

Figure 5.3 Flexural strength vs density of Si_3N_4

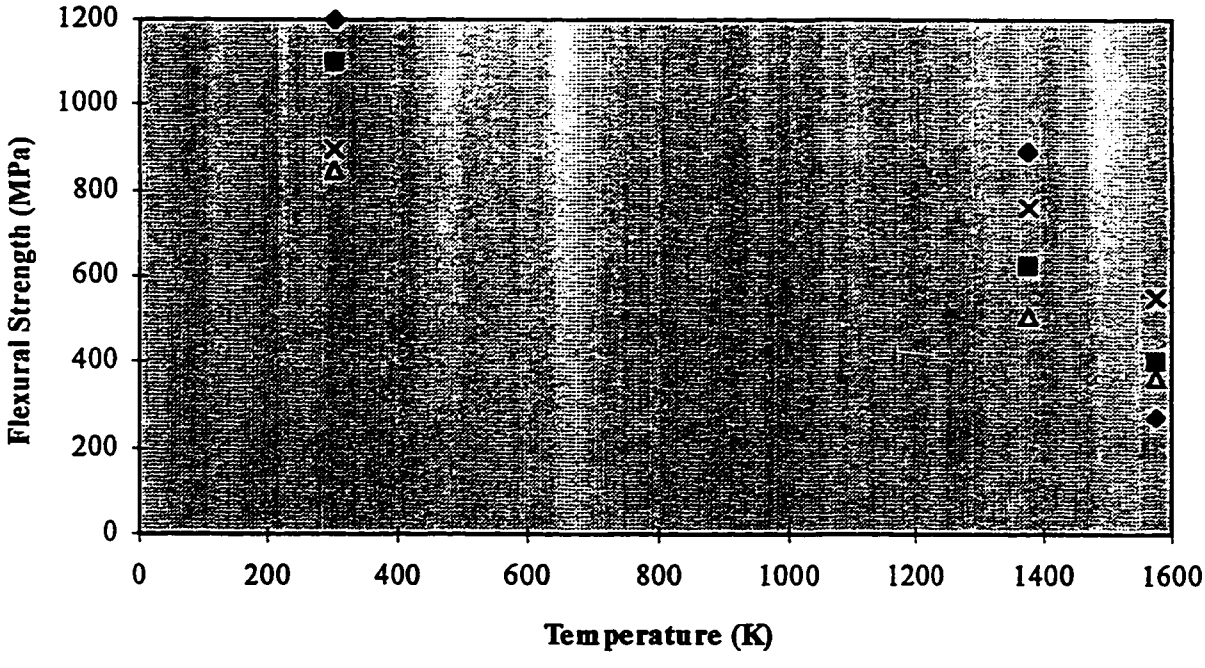

Figure 5.4 Strength vs Temperature of HIP Si_3N_4

Thermal conductivity is influenced by β content and the amount of rare earth oxide glassy phase. The highest thermal conductivity is obtained after complete α to β conversion and with 3% rare earth oxide. Thermal conductivity of silicon nitride is very temperature dependent. The thermal conductivity is higher at room temperature and decreases to about 1/1000 of the room temperature conduction at a temperature of 1273 K. As the silicon nitride heats up, the temperature gradient increases, the thermal conductivity decreases, and the heated zone transfers less energy into the bulk workpiece. The energy flux at the surface is essentially unchanged, which heats the material further. The material heats to a higher temperature, which decreases the thermal conductivity. If the material were at 1273 K (1000 ^{o}C) with a gradient of 1000 K, the thermal flux would be the same as one degree K gradient at room temperature. The transfer of energy within the bulk material is limited and a high gradient will occur between the surface and the bulk material. Per Carslaw and Jaeger, heat transfer by conduction follows the equation [87];

$$\dot{q} = \Delta(T) * k;$$

$\dot{q}$ = the energy transferred

$\Delta(T)$ = the temperature gradient

and k = the coefficient of thermal conductivity which is temperature dependent in this case.

6 Nd:YAG LASER - SILICON NITRIDE INTERACTIONS

6.1 Development of lasers and their unique properties

In order to understand laser - silicon nitride interactions, one must begin with reviewing the development of lasers and their unique properties.

Einstein developed the concept of stimulated emission in 1917 [52]. He proposed that an excited atom could be stimulated to return to its lower energy state by releasing a fixed quantum of electromagnetic energy. The principle of conservation of energy demands that the quantum of energy be equal to the difference of the energy states. The energy relationship is defined as:

$$\Delta\epsilon = h\nu = h\ c\ /\lambda$$

where $\Delta\ \epsilon$ = energy difference,

c = speed of light,

h = Plank's constant,

v = frequency, and

λ = light wavelength.

The practical application of this relationship was by Charles Townes in 1954 with a microwave amplification by stimulated emission of radiation or maser [52]. This work was extended into the visible spectra in 1960 when Theodore Maiman at Hughes Aircraft [88] developed a practical device producing coherent monochromatic light at 694 nm. Maimain's invention was first referred to as an optical maser. Today, this invention is better known by its acronym - laser. Maiman's laser was a solid state ruby rod optically pumped or energized by a flashlamp.

The unique properties of lasers include high intensity, monochromacity, temporal coherence, spatial coherence, and the ability to focus to a fine point [52, 89, 90]. The high intensity of a raw laser beam provides high specific power to area output of electromagnetic radiation. To expand, monochromacity means the light spectral line width is very small, but not without minor variation in light frequency and wavelength. The temporal coherence occurs when the waves of light in time are in phase. In phase, each quantum of light is additive to the intensity of a focus spot; there is no light cancellation or interference. Spatial coherence implies that if a point is moved along the path of the light, the light intensity will remain constant. Due to the temporal and spatial coherence, the intensity of light from a laser is additive. A large plane of parallel light rays to a single fine point. The point size is limited by the diffraction of the optical elements and the light wavelength.

Light is a form of electromagnetic energy. Absorbed electromagnetic energy is dissipated as heat. A determination of the laser's power is made by measuring the temperature rise of a non reflecting, non transmitting block (or 'black body') of a known mass in the laser's beam. An individual photon with a quantum of energy striking a surface may be absorbed, reflected or transmitted. Whether one particular photon is absorbed, reflected or transmitted can not be determined [52, 91]. On a stochastical level, a percentage of the incident photons are reflected, a percentage of photons are absorbed and the remaining photons are transmitted. Thus, the absorption of the material at a particular wavelength is the percentage relationship between absorbed and incident energy. The coefficient of absorption gives a measure of how deep the energy is absorbed into the material.

6.2 Absorption, reflectivity and transmittance

Absorption is the percentage of light energy (or electromagnetic energy) incident on the material which is transferred into joule heating at the material's atomic or molecular level. Absorption is important in understanding laser processing because it determines the effectiveness of a particular laser source in elevating the temperature of a specific material.

Reflectivity is the percentage of electromagnetic energy that is redirected back at the energy

source. Transmittance is the percentage of electromagnetic energy which emerges from the nonsource side of the material [91]. Transmittance is usually assumed to be zero for nonopaque material [91]. From physics, the sum of the absorption, reflectivity, and transmittance is equal to 1 [91]. For nonopaque material, the absorption is equal to:

$$a = 1 - R$$

a = absorption, and

R = reflectivity.

Absorption, reflectivity and transmittance are not constant or temperature independent. Using silicon as an example, a direct, though slight, relationship exists between temperature and reflectivity [92]. For silicon, a slight relationship is given by:

$$T = 213.3\ (R) - 7193.7$$

where T = temperature in K and,

R = reflectivity in

This relationship is valid from 273 K to 1573 K. The relationship can be rewritten as:

$R = (7193.7 + T)/213.3$.

Thus the reflectivity varies between 37 % to 41 % over this temperature range.

From equation 6.3, absorption varies between 59 % and 63 % over this temperature range. The conclusion for silicon is that as temperature is increased, the reflectivity increases and the absorption decreases slightly. The decrease in absorption is not highly significant.

6.3 Coefficient of absorption

Silicon nitride absorbs Nd:YAG laser wavelength (1,064 nm) much better than carbon dioxide laser wavelength (10600 nm) [93, 94]. The coefficient of absorption for silicon nitride for a Nd:YAG laser is given as $\epsilon = 0.7$ [95]. The coefficient of absorption for silicon nitride for a carbon dioxide laser is given as 0.23 [95]. Empirical tests with lasers also demonstrated that silicon nitride is unaffected by a raw unfocused carbon dioxide laser beam but the material surface is heated rapidly by a Nd:YAG laser beam.

In a study of carbon dioxide laser-silicon nitride interactions, the flexure strength of the material dropped dramatically with increasing energy of the beam. There was no intensity of the beam that did not demonstrate a reduction of the flexure strength [96]. At slower transverse speeds, all silicon nitrides exhibited reduced flexural strength. All silicon nitrides retained at least 40 % of the original flexural strength.

Silicon nitride exposed to rapid heating using the Nd:YAG laser does not tend to crack (See Section 6.5 for further explanation). Focused continuous carbon dioxide laser beams shatter silicon nitride surfaces [97]. The tendency for brittle fracture is directly related to the volume of material that is stressed. Nd:YAG laser beams provide less thermal shock to the material during heating [97]. The thermal shock in hot isostatic pressed silicon nitride by carbon dioxide laser beams may be due in part to the silica. Silica is present at the grain boundaries of Si_3N_4 and is not transmissive to carbon dioxide laser wavelength. Silica has such a high absorption value that 99 % of the incident energy in less than 10 μ meters for wavelengths greater than 7000 nanometer. For carbon dioxide lasers it is not possible to produce a thin enough sample of silica that the absorption could be accurately measured. In hot isostatic pressed silicon nitride, there is intergranular silica material. This silica material is not transmissive to carbon dioxide laser beams as is witnessed by the fact that silica lenses when used in carbon dioxide lasers shatter immediately at all power levels. Thus, the intergranular cracking which effects the carbon dioxide laser machining may be a greater function of the materials between the grains than the material in the grains. An analogous example is the failure of a grinding wheel due to overheating of the bonding material and not the failure of the grit itself.

The silicon nitride surface has a Stephan-Boltzmann temperature of approximately 7500 K (7277 ^{o} C) [91]. The Stephan Boltzman temperature is characterized by the surface temperature that is necessary to exist if all the transferred energy is transmitted by pure radiation of energy. This temperature is only seen at the surface or the surface in the plume. The substrate temperature as a function of depth is limited by the amount of energy which can be transferred into the material from the surface before the Stephan-Boltzman temperature source is removed. Plasma formation is expected at energy flux of 10^8 watts / cm^2 [52]. Energy flux in

these experiments was four orders of magnitude lower. No plasma formation was observed at the incident energy level of 1.27 x 10^4 w/cm^2 even though the duration of heating was much longer than during turning. This lower energy flux is typical of the energy flux used for heating and heat treating of metals.

The absorption coefficient for silicon nitride is in the range of 2 - 15 nm $^{-1}$ for krypton floride (KrF) which is 248 nm. We would expect the penetration depth for a Nd:YAG laser beam to be $\sqrt{1063/248}$ or twice the penetration depth of a KrF excimer laser beam [98]. Carbon dioxide laser beams would have an effective penetration depth six times greater than a KrF excimer laser beam.

With carbon dioxide laser beams, a plasma layer is inevitably generated which tends to non—uniformly heat the workpiece surface. The plasma temperature disassociates the nitrogen but does not vaporize the silicon. The plasma temperature merely melts it. The silicon reacts with oxygen and resolidifies as a mixture of SiO_2 and Si. The resolidified material microcracks. The microcracks extend into the base material, thus weakening the material. These reactions will be further explained in Section 6.4.

6.4 Laser—silicon nitride surface interactions

Laser-silicon nitride interactions can be broken down into several cases as summarized in this paragraph [95]. Case 1 produces no silicon nitride decomposition. Case 2 decomposes the silicon nitride producing liquid silicon and diatomic nitrogen gas. The liquid silicon remains as a recast layer on the workpiece surface. Case 3 decomposes silicon nitride into silicon gas and monatomic nitrogen gas. The silicon does not resolidify on the workpiece surface. Case 4 produces a gas composed of silicon and nitrogen atoms. The reaction products of Case 5 are atomic nitrogen and ionized atomic silicon. Case 6 produces ionized atomic nitrogen and ionized atomic silicon. The first four cases are the most applicable to this research; thus they are discussed in further detail below.

Case 1 - The silicon nitride is heated to a temperature below the sublimation temperature [95]. The incident energy is absorbed in the form of thermal energy only; no chemical reaction

occurs. Increased atomic mobility and diffusion occur. Stresses on the grain boundaries are more easily tolerated due to increased slip along the grain boundary lines. Crystal softening results from a combination of these factors. No nitrogen is released from the workpiece surface; thus no nitrogen evolution occurs.

Case 2 - The silicon nitride is heated to 2100 K, the point where the following chemical reaction occurs [95]:

$$Si_3N_4(s) \longrightarrow 3Si(l) + 2\,N_2(g).$$

Each mole of silicon nitride reacts to produce two moles of diatomic nitrogen gas from the workpiece surface. The diatomic nitrogen gas is considerably lower in pressure on the silicon than atomic nitrogen gas since the volume of diatomic evolved gas is about half of atomic nitrogen gas. Silicon liquid remains on the workpiece surface and resolidifies. Case 2 interactions are typical of carbon dioxide laser interactions [95].

Case 3 - At higher photon energy levels, the appropriate chemical reaction of decomposition is:

$$Si_3N_4 \longrightarrow 3\,Si(g) + 2N_2\,(g).$$

Each mole of silicon nitride reacts to produce two moles of diatomic nitrogen and three moles of silicon vapor from the workpiece surface [95]. Thus, five moles of gas evolve from the surface. An important feature of this reaction is that the silicon is removed from the surface as a gas. No recast silicon liquid layer remains on the workpiece surface. Case 3 interactions are typical of Nd:YAG laser interactions [95, 34].

Case 4 - The silicon nitride is heated to the point where the following chemical reaction occurs [95, 99]:

$$Si_3N_4 \longrightarrow 3\,Si(g) + 4N(g).$$

The energy of the laser - silicon nitride interaction produces complete disassociation but not ionization of the silicon nitride. No charged particles are released. Each mole of silicon nitride produces a total of seven moles of silicon and nitrogen gas. The gas pressures at the

workpiece surface are significant and remove the ejected material away from the surface. Case 4 interactions are typical of excimer laser interactions [95].

The gas evolution is most pronounced for excimer laser interactions. The gas evolution for Nd:YAG laser interactions is less pronounced. Yet, this process for Nd:YAG laser interactions is more pronounced than for carbon dioxide laser interactions. Since the energy of the photon striking the material is inversely proportional to the wavelength, or directly proportional to the frequency, the excimer laser has the most energy transferred in a single interaction [52]. Nd:YAG laser photons have slightly less energy and carbon dioxide laser photons have still less.

One important factor is to distinguish between the power of an individual photon interaction and a stochastical laser interaction. The individual photon interactions of excimer, Nd:YAG and carbon dioxide lasers have been given above. The stochastical or average power of each laser is based more on the ability to produce photons than on the energy of the photons. The average power of the carbon dioxide laser is highest. The Nd:YAG laser power is less and the excimer laser has the lowest power of the three. Note: this is in the opposite order of the energy of the photons.

By selective use of a Nd:YAG laser on the silicon nitride, a small highly heated zone of material is created which dictates the cutting process. The aim of laser-assisted turning is to make both the zone of heating and the zone of cutting occur simultaneously and coincidentally. The material to be removed is heated while minimizing the heat impact on the surrounding base material. The strength of Nd:YAG laser heating is the selectivity and control of the thermal energy source.

When using a Nd:YAG laser for laser-assisted turning, the use of an oxygen assist-gas is not recommended. By using oxygen-assist gas, additional energy from the silicon oxidation following the nitrogen gas evolution is generated. However, increased oxide products have a highly detrimental impact on the finished part. An alternative reaction for the decomposition of silicon nitride in the presence of oxygen is given by the following equation:

$$2\,Si_3N_4 + 7\,O_2 \longrightarrow 6\,SiO + 8\,NO.$$

The top layer has rapid evolution of SiO and NO gases which causes more porosity and voids as the gases rise in the material. A pore is due to the evolution of gas in the material. A void is caused by the slip of material away from its current site without replacement by other material or by gas. The top surface of the workpiece with an oxygen- assist gas would rapidly react and leave a layer of silica on top of the unreacted silicon nitride.

A factor complicating laser-assisted turning is that silicon nitride is not a completely homogeneous material. Hot isostatically pressed silicon nitride is by its very nature a collection of β silicon nitride grains separated by an amorphous or glassy phase composed of yttrium oxide and silicon dioxide or silica. The silica has optical properties of its own. The silica absorbs very little energy in the operating wavelength of Nd:YAG lasers. In fact, silica is used for lenses and fiber-optics in Nd:YAG lasers. Silica absorbs readily in the operating wavelength of carbon dioxide laser [100, 101, 102]. The absorption by silica at 10600 nm is 10,000 times higher than the absorption at 1064 nm. The silicon oxide generated would further combine with oxygen as given by the following equation:

$$6\ SiO + 3\ O_2 \longrightarrow 6\ SiO_2$$

to form silica.

This silica does not absorb the Nd:YAG laser wavelength but will melt by pure conduction of thermal energy from the absorbing silicon nitride. This silica will resolidify on the surface. The resulting resolidified layer is detrimental to the workpiece surface's integrity and strength.

Sialons (SIlicon ALuminium Oxygen Nitrogen) can be thought of as a derivative of silicon nitride with aluminum and oxygen in a one-to-one substitution. Generally, the formula follows the form:

$$Si_3 - xAl_xO_xN_4 - x$$

with $0 \leq x \leq 2$

to remain in the solid solution range [104, 105, 103, 106]. Sialons are actually a class of ceramic "alloys" of silicon nitride. The sialons can also be thought of as having the form:

$$Si_6 - zAl_z0_zN_8 - z$$

where z denotes the number of nitrogen atoms substituted in the material [103, 77, 82]. Sialons break down into two classes: sialons with a large glass phase and sialons with a continuous intergranular crystalline phase of yttrium aluminum garnet (YAG).

Sialons have improved low temperature properties at the cost of the high temperature properties [104, 105, 103, 106]. The high temperature properties began to degrade at 1073 K, significantly before the high temperature properties of silicon nitride degrade. Low values of z (nitrogen substitutions) result in materials similar to silicon nitride [107]. Higher values of z result in dramatic decreases in both hardness and toughness [108]. The fabrication of sialons is greatly eased by the ability to perform green machining prior to sintering and a very linear shrinkage factor. Green machining is the ability to cut or machine a part in its green or unfired state. Due to the extremely linear shrinkage factor, shapes can be formed oversized and will shrink to a very precise and predictable final shape. Sialons can be thought of as a subclass of silicon nitride with easier green machining and sufficient conductivity in cases for electrical discharge machining (EDM). Electric discharge machining results in a surface finish several times rougher than diamond grinding.

Silicon nitride's good oxidation resistance is due to the presence of a protective silica (SiO_2) layer. Silicon nitride has two major crystalline forms (alpha and beta) which are both hexagonal in structure. The alpha is made up of alternating layers of beta and its mirror image. The beta is thought to be more stable thermodynamically at all temperatures and pressures. Alpha silicon nitride is meta- stable (stable at certain temperatures and pressures). The addition of oxides improves transformation processing of alpha silicon nitride to beta silicon nitride. Silicon nitride is only stable against oxidation at partial pressures of 10^{-21} atmospheres of oxygen. Silicon nitride forms a layer of SiO_2 rapidly, which is tenuous and protects against further oxidation [67].

The boundary oxides are necessary for three reasons. The first reason is to aid in the dissolving of alpha silicon nitride which will subsequently reprecipitate as beta silicon nitride. The second reason is to bind the resulting grains together with a thin layer of intergranular material [109, 110]. The final reason is to provide protection against further oxidation of the

silicon nitride. The intergranular layers form an amorphous glassy layer which can be heat treated into a vitreous ceramic layer. The intergranular material also can transfer thermal energy preferentially to the silicon nitride grains. Attempts have been made to increase the densities of the silicon nitride above 85 % without the use of binders and oxide additives [111]. The attempts have required the use of substantially higher temperatures and pressures to achieve the densities. Attempts were also made using a fine grain beta powder as the precursor. However, lower strengths at room temperature were the result of these attempts.

The absorption of silica and silicon nitride at the two wavelengths, taken together, can best be summed up as follows: when Nd:YAG lasers are illuminating the surface of silicon nitride, the energy is being absorbed by the silicon nitride grains and is transmitted by the oxide material in the grain boundaries. The grains of silicon nitride are capable of absorbing the energy by heating and by sublimation. The β silicon nitride is capable of withstanding the thermal shock. When the surface is illuminated by the carbon dioxide laser, the energy is not absorbed by the silicon nitride, due to its low absorption. Instead, the laser energy is absorbed by the intergranular layers of oxides. The silica will crack to the depth of 40 nanometer and is sensitive to thermal cracking. The silica has a much higher thermal conductivity than does the silicon nitride. The result is the institution of a fatal flaw in the material. This is equivalent to overheating the bond of a grinding wheel and is just as damaging.

The critical crack size as given by the Griffith relationship is 40 micrometers for opacity of HIP silicon nitride [112, 76]. The result is that for Nd:YAG illumination, the grains are heated and are able to be machined while the intergranular material remains glassy. In comparison, the intergranular silica is shattered by the high energy carbon dioxide laser illumination and the grains of β silicon nitride are not significantly heated to any temperature approaching the brittle to ductile transition temperature.

6.5 Thermal diffusivity of silicon nitride

The key to understanding the silicon nitride-laser interaction lies in the composition and structure of silicon nitride. To review, the hot isostatic pressed silicon nitride begins with α

silicon nitride powder, a percentage alumina, a small percentage of a rare earth oxide or a small amount of silica ($Si0_2$). The oxides are necessary as binder phases and for proper sintering to occur. During the hot-isostatic press operation, the α silicon nitride dissolves and reprecipitates as β silicon nitride. The binder phases serve as catalysts during the dissolving and reprecipitating of the grains. The binder phases are the materials left on the grain boundaries as glassy amorphous intergranular materials [79, 113]. The laser interactions are between the grains of β silicon nitride and the laser beam or the glassy (amorphous) solvent and the laser beam. The intergranular material will control a large portion of how the hot isostatic pressed silicon nitride behaves.

The decomposition of the solvent to β silicon nitride can be written as:

$$2\ Si_2N_2O\ (s) \longrightarrow \alpha \text{ or } \beta\ Si_3N_4(s) + SiO_2(s).$$

At hot isostatic temperatures and pressures, the tendency for silicates to form increases. Silicates are important glass forming liquids. Residual oxygen will be incorporated into the material by the reaction [114]:

$$\beta Si_3N_4(s) + 3\ O_2(g) \longrightarrow 3\ SiO_2(s) + 2N(g)\ .$$

The thin intergranular phase tends to be transformed into silica (SiO_2). This transformation depends upon the purity and types of binders and sintering additives.

The intergranular boundaries completely surround each grain boundary. The intergranular boundaries can be as thin as eight angstroms but remain continuous even at that dimension [115, 116, 117]. The film thickness is dependent on the quantity and type of material sintering agents and impurities.

The presence of the intergranular material controls high temperature strength but has a beneficial effect of increasing the fracture resistance above the value expected from single crystal fracture resistance [118]. A further factor is the thermal expansion dissimilarity between silicon nitride and the intergranular material.

Further examination shows a brittle-to-ductile transition temperature for the hot-isostatic pressed silicon nitride intergranular material is considerably lower than that of the material

grains. The intergranular material is much more susceptible to thermal cracking than the grains themselves. The coefficient of thermal expansion for the intergranular material is much higher than the granular material.

Looking at the above factors taken as a whole, if the intergranular material is heated more than the grains, the material will expand. The expansion combined with the susceptibility to thermal cracking will cause the intergranular material to fail. Since the intergranular material completely encloses the grain, the bulk material will quickly fail due to the crack susceptibility and the lack of high temperature strength in the intergranular material.

If the grains are heated, the effects are quite different. The grains exhibit a lower coefficient of thermal expansion that the intergranular material. So as the energy is transferred to the intergranular material, both materials expand. The coefficient of thermal expansion for the grains is higher and the temperature in the grains (by the laws of the heat transfer) will be higher. So even though the grains are at a higher temperature, the effect is negated by the coefficient of thermal expansion mismatch. The brittle-to-ductile transformation temperature for the grains is much higher than the intergranular material. The temperature differential, combined with the transformation temperature mismatch, will cause the materials to again behave similarly if the granular material is at a higher temperature than the intergranular material. If the grains are heated rather than the intergranular material, the grains are much more tolerant of thermal gradients than is the intergranular material.

The total effect of these factors is that the heating of the grains produces an environment for machining of the bulk material. If the intergranular material is heated, the environment is one in which the material can rapidly fail.

Table 6.1 Thermal conductivity of HIP Silicon Nitride (W/m^{o}K)

Temperature	AY6	PY6	SNW-1000	SNW2000
300	31.8	32.3	27.6	27.6
550	24.3	24.3	21	21
825	18.4	18.4	17.2	17.2
1100	0.037	0.037	0.037	0.037
1375	0.03	0.031	0.033	0.033

The thermal diffusivity (κ) of silicon nitride is given by the equation [52]:

$$\kappa = K/\rho C$$

where K = the thermal conductivity (watts/cm K)

ρ = the density (g/cc) and

C = the specific heat (joules/g K).

The depth of heating (D) is given by the equation:

$$D = (4\kappa t)^{(1/2)}$$

where κ = the thermal diffusivity, and

and t = the interaction time.

The depth of heating is limited by thermal diffusivity. Thermal conductivity (K) is extremely temperature dependent, and the specific heat (C) is nearly constant (see Table 6.1, data from Lewis [119]). The result is that the thermal diffusivity is extremely temperature dependent. This allows the energy to start heating the material near the surface but quickly limits the rate of energy transfer through the silicon nitride. The glassy phases (YtO_2, SiO_2, ...) are not limited and heat preferentially. The amorphous or glassy phases soften and become liquid. The softened material is pushed into the cracks by the cutting tool.

The zone that is thermally heated to the point where ductile machining can take place is approximately the same as the depth of heating. This is due to the high instantaneous surface temperature (7500 K) and the temperature necessary for ductile machining (approximately 1500 K). The result is that the surface layer of the silicon nitride is heated into the ductile machining region but the substrate after machining remains sufficiently cool to avoid damage and thermal cracking. The silicon nitride material at the surface which is melted is machined away by the following cutting tool. As noted in Case 3 of S ection 6.4, there is no recast silicon nitride layer at the new surface.

The material's surface can be thought of as a control volume. In this control volume, there must be conservation of energy. The law of conservation of energy defines that the total energy is a constant. Thus, in the control volume, any energy that enters by radiation must reradiate out, be conducted out, or be stored as thermal energy within the control volume. Absorption of energy is dependent on the material's temperature. Absorption of radiant energy improves as the temperature increases due to a large decrease in the material's thermal conductivity. A cycle of improved absorption, with decreases in conduction, rapidly heats the control volume. The material can heat thermally until such time as the silicon nitride decomposes. When the silicon nitride decomposes, liquid silicon remains on the surface, while the nitrogen is transformed to diatomic nitrogen gas. The sublimation temperature of silicon nitride is given as 2173 K [120].

The liquid silicon absorbs Nd:YAG radiation better than does silicon nitride. Some of the silicon nitride will evaporate off the material surface. Silicon dioxide (or silica) is almost transparent to Nd:YAG radiation, and is commonly used as the transport media of optical fibers for Nd:YAG lasers. The silica will remain on the workpiece surface unless removed by secondary heating of the workpiece surface. By secondary heating, it is meant that the laser is heating the silicon nitride and the silicon nitride is transferring energy and heating the silica. The low direct heating of silica by the Nd:YAG laser is advantageous in that silica is not thermal shock tolerant.

While the surface is heated, the material is worked with the turning tool. The surface

heating reduces the strength and increases the ductility of the workpiece material. The heating is most pronounced nearest the surface. The specific energy of cutting is the energy necessary to cleave or separate the material. This is the energy necessary for the stresses on the material to exceed the yield strength of the material. When the material strength is reduced due to elevated temperatures, the cutting energy is reduced. The frictional energy needed for the turning operations is reduced due to the increased ductility of the material. The frictional energy is further reduced due to the presence of liquid material on the surface with the provision that the surface material does not weld to the cutting tool or create built-up edge problems [121, 122].

Silicon nitride melts and forms silica. When this silica resolidifies, a recast layer of silicon oxide and silicon is formed. This resolidified layer typically has microcracks which extend into the base material. The microcrack length is dependent on the interaction time. In the case of laser- assisted machining, the liquid layer is removed from the surface as is the upper heated workpiece layer. This reduces the potential number and significance of microcracks forming.

6.6 Effects of laser silicon nitride interactions on strength

Grain boundary strength appears to be the controlling factor in the strength of silicon nitride. Boundary strength of silicon nitride generally drops at 1123 K (850^o C) [72]. Creep resistance has been shown to be controlled by sintering aid material. Compressive strength of silicon nitride may be traded off for greater fracture resistance, hardness, or increased electrical conductivity in the case of sialons.

The oxides in the grain boundaries are necessary in order to obtain more than 85% theoretical density. These same oxides provide the intergranular slip that is necessary for ductile machining. The intergranular oxides also heat preferentially to the bulk of the grains of β silicon nitride at high temperature due both to the grain's mass and to the decrease in thermal conductivity of β silicon nitride. Attempts to achieve higher theoretical densities by starting with fine grained β silicon nitride rather than the usual practice of α silicon nitride as the precursor have been unsuccessful. Lower strength resulted from these attempts. The oxide

additions are both the boon and the bane of silicon nitride. Too much oxides cause the material to suffer from poor high temperature strength. Due to the inability to exude the glassy amorphous layer between the grains and a lack of oxides, the material can not achieve density greater than 85% theoretical density.

The α β transformation is necessary to form a high strength material. One cannot just start with powder β silicon nitride and achieve good material properties. The strength of the silicon nitride ceramic comes from the interlocking grains of silicon nitride. If β silicon nitride was used as a precursor, the hot isostatic pressed material would be held together by the binders rather than the interlocking grain formation and grain growth. A fine distribution of β silicon nitride is necessary in the precursor in order to have a large number of grain growth initiation sites for nucleation and to produce a fine grained material from the liquid. In regards to the strength of silicon nitride, there is an optimal temperature and pressure for sintering or hot isostatic pressing [123].

Due to the lack of coherency between silicon nitride and the amorphous or glassy region, the grains have higher strength than the boundaries. Decreasing the amount of glassy amorphous material increases the binding energy at the grain intergranular boundaries and produces a higher strength material. Decreasing the amount of glassy amorphous material also reduces the ductility of the material. The decrease in the ductility reduces the applications that a high temperature material is suitable for. Expected advantages of a fine finishing operation using a laser pretreatment are reduced cutting forces, increased tool life, ability to use inexpensive tools, improved surface integrity, higher material removal rates and the ability to machine materials which can not be machined by any other means [25].

6.7 The importance of creep in laser silicon nitride interactions

Creep is one portion of the machining process. Initial theories of turning were that a crack was propagated ahead of the cutting tool. Later research indicated that turning was not the propagation of a crack but the extension of a tear. The tear was caused by the tensile forces of the chip which were caused by the cutting tool. The highest forces are located immediately

before the cutting tool tip. Creep is directly related to machining. Creep modeling for silicon nitride was first done by Drucker in 1964 [124]. Drucker assumed a two dimensional model of hexagonal cells with a continuous glass layer between the cells. Drucker's first model has been extended to include the effects of viscosity as denoted below by the formula:

$$\dot{\epsilon} = \sigma_a ve/(\nu\sqrt{3})\ (\mathrm{h/a})^3$$

where ν = viscosity,

h = film thickness, and

a = grain size or facet-length.

Drucker's model first assumed an incompressible material in order to calculated the forces on the grains and at the inter phases.

In a non-linear viscous material,

$$\dot{\phi} = \theta\ \tau^n$$

where $\dot{\phi}$ = shear strain rate,

τ = shear stress and

θ and n are material constants.

Creep is due to the intergranular material being compressed by the grain. Maximum strain in compressions occurs when all glassy material has been squeezed from between the grains and the direct grain to grain contact occurs. Tension requires twice as much force to remove the glassy material from between the grains.

Additional effects on creep are those of oxidation and crystallization of the partial grain boundaries. In the case of silicon nitride, oxidation of the exposed grain boundaries occurs almost instantaneously. In annealing of alumina, the amorphous phases tended to devitrify. Lange formed a variety of silicon nitride materials with varying amounts of glass [125]. The material with the minimum glass had values of n close to one, which are substantially equal to that value where diffusional creep predominates. Samples with larger values of glass had values of n = 2 which is substantially equal to that where cavitational creep is the predominate mechanism in the amorphous glassy material. Partial devitrification would change the

mechanism of creep from diffusional to cavitational. At low levels of stress when the amount of devitrification is large, the value of n would increase from one to below two. Chadwick found that devitrification was partial for silicon nitride and that by annealing, a large portion of the material would neither crystallize nor oxidize in the center of the material [124]. At lower stress rates and high temperatures (1473 K), little crystallization of the amorphous material was observed. The viscosity value of the silicon nitride reached a plateau or constant value at low stress levels. The general behavior of silicon nitride under low stress was a rapid strain when first under load, followed by a sharp drop in the strain rate as the material is squeezed out from between the grains. Pre-annealing and partial grain boundary devitrification were found to have little effect on the initial values of creep in the amorphous material. Of all high strength high temperature materials, silicon nitride had the greatest resistance to spalling and delamination [41].

Yttrium oxide sintered silicon nitride materials exhibit slow crack growth due to surface connected porosity from about 1073 K (800^{o} C) until 1273 K (1000 ^{o}) [124]. From 1273 K. the boundary phase devitrification becomes the primary failure mode. Above 1373 K (1100 ^{o} C), creep fracture becomes the primary mode of low strength failure. Creep fracture is the primary failure mode for ductile machined metals.

Creep in metals is given by the Larson-Miller parameter equation [76]:

$$P = f(\sigma) = T\ (C + \log tr)$$

where σ = stress (mPa),

T = the absolute temperature

tr = the time to creep rupture

and C = a constant.

The higher the value of P, the more plastic the material will turn. Higher temperatures aid in turning the silicon nitride in a ductile manner.

For metals, the value of C is usually about 20 for steels [3]. For silicon nitride, C is between 30 and 44 [76]. From the fracture maps of silicon nitride, it is observed that slow crack growth

becomes the dominant failure mode at 1273 K (1000^{o} C) and is replaced by creep as the dominant failure mode at higher temperatures and higher allowable stresses [76].

7 EXPERIMENTAL APPARATUS AND DETAILS

7.1 System integration

The system used for these experiments is comprised of a continuous wave 100 watt Nd:YAG Laser Sonics model 6000) laser interfaced with a two axis computer numerical controlled Dyna Myte model 3000 1 1/4 horsepower lathe. The Nd:YAG laser radiation was delivered immediately before the cutting tool through a 600 micron 3M Powercore high power, low attenuation optical fiber with a SMA 905 connector. The fiber is capable of transmitting 2.3 kilowatts of continuous 1063 nanometer wavelength laser light. Near normal incidence was selected to provide near optimal coupling of the laser to the material. Normal incidence was not utilized to avoid potential reflected backscatter damage to the laser crystal.

Hot isostatic pressed silicon nitride samples 150 mm in length and 52 mm in diameter were turned using TP15, TP40, and M20 Carboly inserts. TP15 are multi Al_2O_3 coated inserts, coated with TiN, Al_2O_3, TiC, and TiCN. TP40 is coated with TiN, TiC, and TiCN. M20 is an uncoated carbide tool. High power 600 micron transmission fibers were used to deliver the laser power to the workpiece surface immediately before the surface zone is rotated into the cutting tool. Parameters of speed and tool type were varied. In all cases of machining without laser assistance, the wear rate of the tungsten carbide tools was equal to the feed rate. In short, without laser assistance, the only material that is removed is cutting tool material machined by the workpiece.

7.2 Laser

Research indicated that carbon dioxide laser illumination results in fracture damage to the surface of the cylinder. Nd:YAG laser illumination does not cause extensive fracture damage

to the surface; however, the illumination from the Nd:YAG laser does heat the surface.

7.3 Lathe

For this experiment, the lathe was selected. Single point turning is continuos in nature while milling or grinding which by their very nature are interrupted cutting processes. The hot machining process must first be proven out on the turning operation [11]. Geometries are more easily controlled in turning and lend themselves to more direct analysis. It is anticipated that the majority of parts manufactured from hot isostatic pressed silicon nitride will consist of rings, cylinder liners, wear pads, and bolts. All these parts are manufactured primarily by turning.

7.4 Material analysis

Quality of the finish was first determined by a Shefield QE model 3 surface profilometer with a skid driven by a Bendix VE model 14 profilometer pilot. Subsequent analysis utilized a Joel scanning electron microscope fitted with both energy dispersive X-ray spectroscopy and electron backscatter analysis. Further evaluation was carried out on a Hitachi V4000 scanning electron microscope fitted to a Quantrax electron diffraction x-ray analysis (EDAX). Further surface analysis was carried out on a Mahler Perthometer. Microstructure was determined by x-ray diffraction.

8 RESULTS AND DISCUSSION

8.1 Principles of machining

Generally, turning is governed by the geometry of the cutting tool, the hardness of the cutting tool, the hardness of the workpiece, the strength of the cutting tool, the strength of the workpiece, the fracture toughness of the two materials, and the chemical compatibility or lack of compatibility of the two materials. The cutting is somewhat simplified for this case since cutting fluid was not used.

8.2 Experimental purpose

The purpose of the experiment is to develop parameters for turning and facing of a part made from silicon nitride. To this end, a series of experiments were run using carbide, coated carbide, and diamond tooling. The material was a fully dense hot isostatic pressed silicon nitride purchased from Cercom Inc. The material was provided in a 150 mm long 52 mm diameter rod. The silicon nitride used is beta silicon nitride with an intergranular layer of amorphous and partially crystallized silica glasses. The rod was placed in a Dyna lathe and was fixtured using an elastomeric material ring between the chuck and the rod. The purpose of the elastomeric ring was to provide a compliant system for absorbing and storing short force transients which might otherwise result in the chuck backdriving and opening due to the high hardness and high Young's modulus of both the rod and the chuck. A Lasersonics model 6000 100 watt continuous wave Nd:YAG laser was used for all trials. The continuous wave Nd:YAG laser was selected to provide a more uniform energy source which could be effectively coupled to the silicon nitride workpiece.

The laser was coupled with a high transmittance high power 600 micron fiber optic pur-

chased from Minnesota Mining and Manufacturing specialty optical products. The silica fiber optics are capable of transmitting 1064 nanometer light with up to 2.3 kilowatts of continuous energy or over one gigawatt of pulsed energy. The fiber optic was fixed to the moving tool holder, and focused immediately in front of the cutting zone. The laser beam was presented nearly normal to the cylinder. Near normal rather than normal was selected to minimize the risk of damage to the laser through back reflectance. The fiber optic provided for flexibility in the optical path without the need for complex mirror arrangements for beam steering.

The coupling equation is given by the radiation heat transfer equation:

$$\dot{q} = \epsilon^* \sigma * (T_1{}^4 - T_2{}^4)$$

where;

$\dot{q}$ = the energy transferred from the beam to the workpiece (source to sink);

ϵ = the emmisivity

σ = the Stephan-Boltzman constant

T_1 = the temperature of the source

T_2 = the temperature of the sink.

8.3 Creep at high temperatures for silicon nitride

The creep constants for materials are useful for machining, because the values given are predictive of the material machining characteristics. Analyzing the data given in an article in MRS K shows creep at high temperatures in silicon nitride follows the characteristic equation of metal creep [126, 17]. The fact that the generalized creep equation is followed for silicon nitride as it is for ductile metals is important since there is a temperature dependence for the creep parameter. This indicates that at higher temperatures, a ductile fracture is expected rather than catastrophic failure of brittle materials.

Laser-assisted machining resulted in initial material removal with all cutting tools used. The HX or M20 grade inserts performed poorly, rapidly failing before a single facing operation was completed. The wear mode was combined flank, nose, and side wear. The uncoated

tungsten carbide tools had a material removal rate of the tool one order of magnitude smaller than the silicon nitride.

TP15 coated tungsten carbide tools performed better and were capable of multiple facing operations. Failure occurred where the coating was first chipped and would grow from that point by removal of the tungsten carbide substrate. If the chipping of the coating was first at the nose, both side wear and flank wear failure would occur. If the chipping was first on the side, side wear would be the failure mode. If the chipping first occurred on the flank, flank wear would be the failure mode. TP40, which is a tougher coating, performed better than did TP15. Once chipping occurred, failure of the tool would rapidly follow.

Experimentation showed that silicon carbide was not appreciably heated by Nd:YAG laser illumination. Further experimentation demonstrated that silicon nitride and silicon carbide were not favorably effected by carbon dioxide illumination. By utilizing the Nd:YAG laser, the carbide tools were able to turn the silicon nitride to a surface finish of 0.1 micrometers. Further there appeared to be a speed which provided a best surface finish (see Figure 8.1)

8.4 Analysis by scanning electron microscopy

A scanning electron microscope was used for analyzing the samples. In the case of the diamond saw cuts on the bulk material, the material cleavage was characteristic of brittle failure (see Figure 8.2, 8.3, 8.4, 8.5, and 8.6). The material was broken out of the surface leaving irregular depressions and small grains loose on the surface. In the case of the carbide-faced samples (see Figure 8.7, 8.8, 8.9, and 8.10), the surface was very regular. The surface appeared to be two distinct phase under backscatter X–ray analysis (see Figure 8.11). One phase appeared to be very crystalline with the other phase smeared between the crystals. The energy dispersive X–ray spectroscopy revealed that the light or smeared material was much higher in oxygen, yttrium, tungsten, titanium and aluminum, than the lighter or more crystalline material (see Figure 8.12 and 8.13). The tungsten, titanium, and aluminum are due to the titanium nitride coated, tungsten carbide inserts which use aluminum as a binder in the cutting tool insert manufacturing process. These impurities are found in the light phase.

This suggests that there is shear plane heating occurring in the β silicon nitride crystals. The impurities are found in the oxide rich smeared material. This material may have softened appreciable or have become liquid to capture the wear products of the cutting tool insert coatings. The harder phase is silicon nitride which is cleaved by the cutting tool with the assistance of laser heating on the shear plane. Surface finishes are recorded in Figures 8.14 through 8.24 for zones 1 through 9 respectively. The smeared material is the yttrium oxide and silicon oxides which liquify and soften at 1500 ^{o} K. EDAX elemental mapping of the elements confirm that smearing of the intergranular material occurs (see Figure 8.25) when compared with the EDAX mapping of the diamond sawn Si_3N_4 (see Figure 8.35). Large particles can clearly be seen on the diamond sawn Si_3N_4 at 250x (see Figure 8.23). The effect of the turning operation on surface finish can be seen by comparing zone 1, zone 2, zone 3, zone 4, zone 5, zone 6 and zone 7 at 1000x (see Figures 8.26, 8.27, 8.29, 8.31, 8.37, and 8.38). Comparing zone 3 at 250x, 1000x, and 5000x (Figure 8.27, 8.28, and 8.29) shows the stradations of machining and the resulting smearing of the grains. Zone 5 shows the cutting and smearing of the intergranular silicon and oxygen in the machining action along with the deposition of trace Cobalt, Titanium, and other materials from the cutting tools (see Figure 8.33, 8.34, and 8.35). Note that the gold shown in 8.34 is from the sputtering operation. Zone 6 and 7 (Figure 8.36, 8.37, and 8.38) demonstrates the effect of turning on the intergranular smearing.

These findings indicate that the mechanism for ductile hot machining is the softening of the grains combined with softening of the grain boundaries. The softening of the grain boundaries provides a built up edge which protects the insulated coated tool edge from wear. The built up edge also fills surface imperfections and cracks which may have resulted and returns a very smooth surface on the laser-assisted turning of silicon nitride.

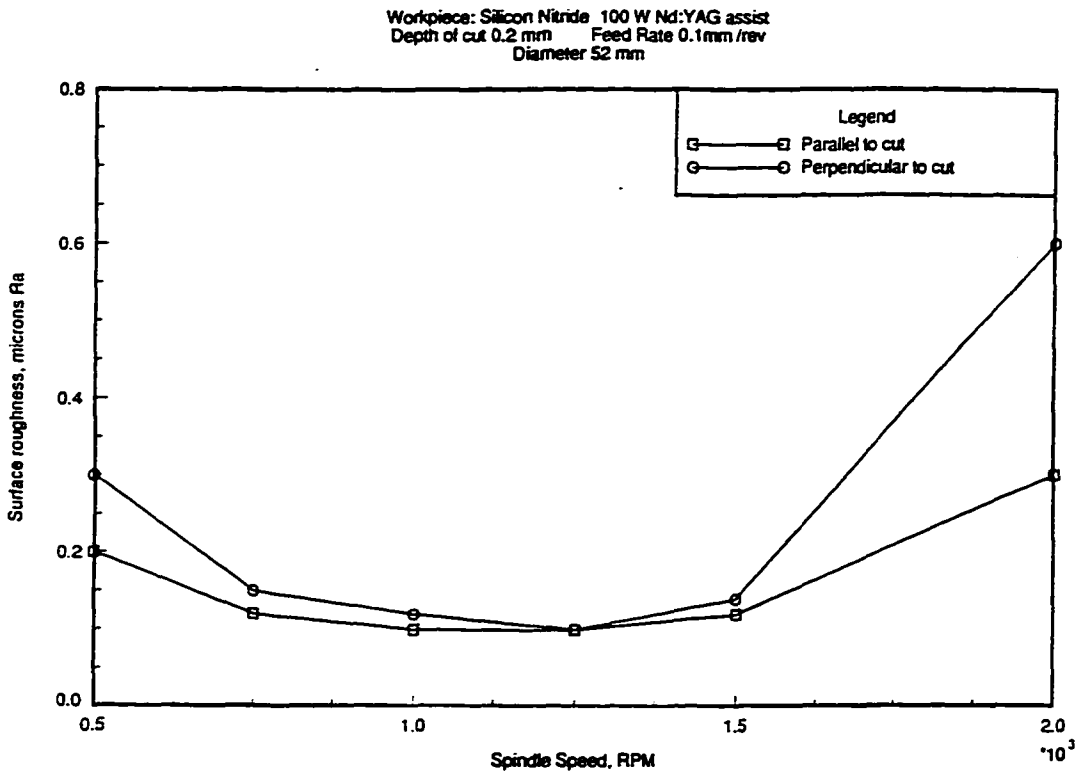

Figure 7. Speed vs. surface finish for Laser assisted–turning of Silicon Nitride

Figure 8.1 Surface finish of carbide faced Si_3N_4

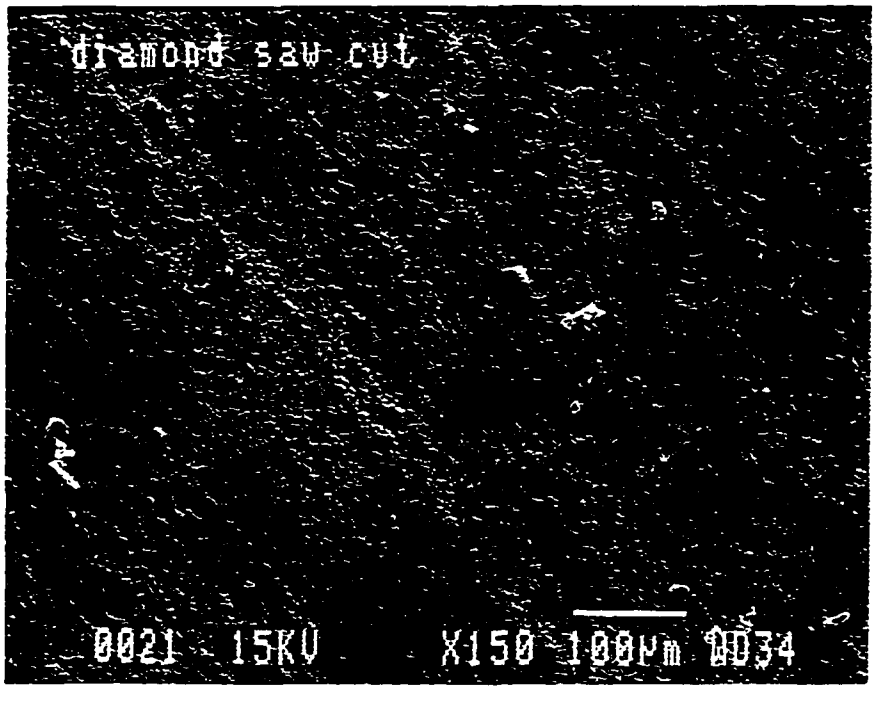

Figure 8.2 Scanning electron photomicrograph of diamond sawed Si_3N_4 X150

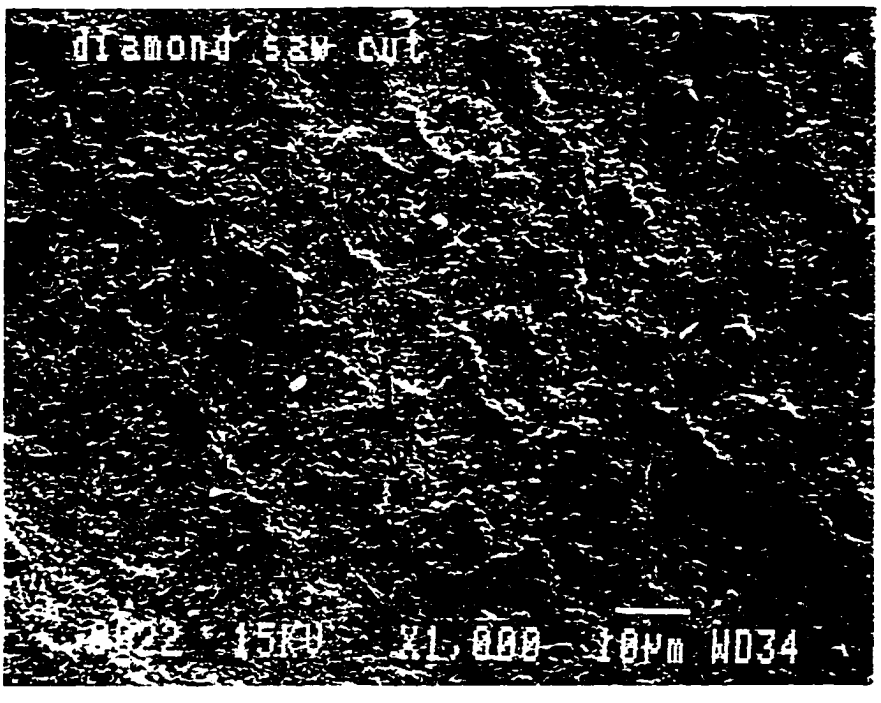

Figure 8.3 Scanning electron photomicrograph of diamond sawed Si_3N_4 X1000

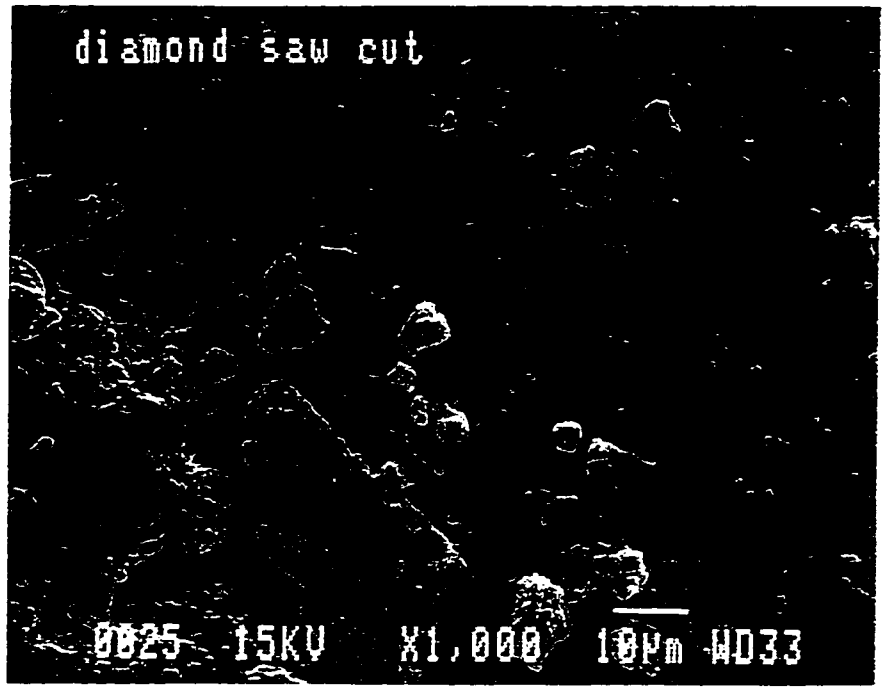

Figure 8.4 Scanning electron photomicrograph of diamond sawed Si_3N_4 X1000

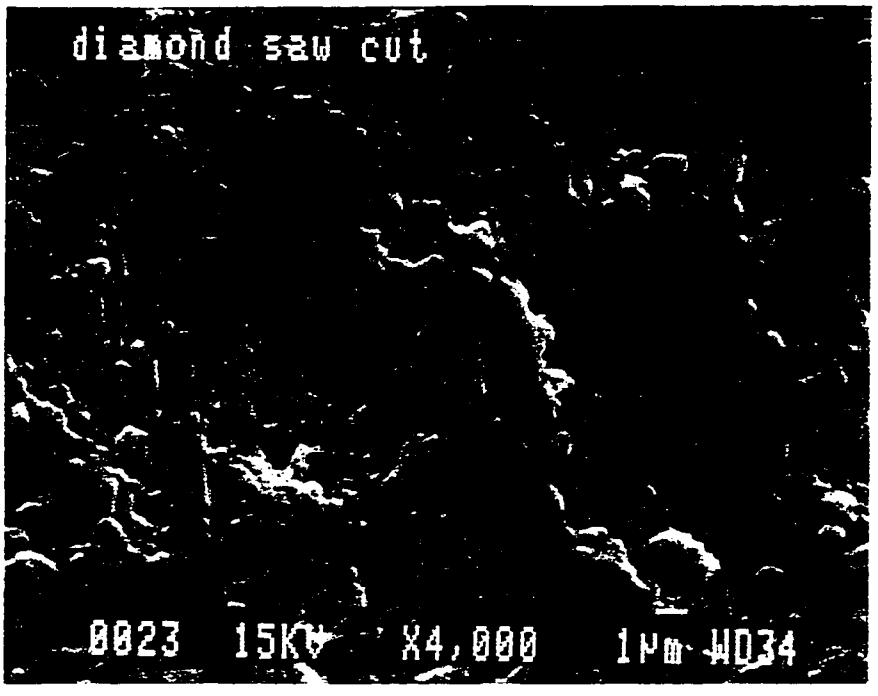

Figure 8.5 Scanning electron photomicrograph of diamond sawed Si_3N_4 X4000

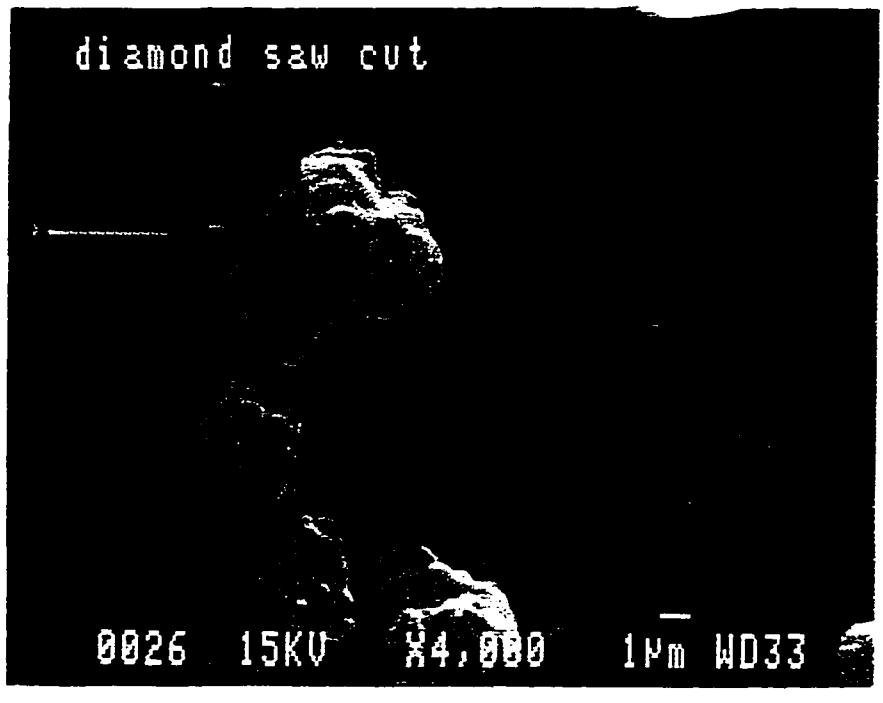

Figure 8.6 Scanning electron photomicrograph of diamond sawed Si_3N_4 X4000

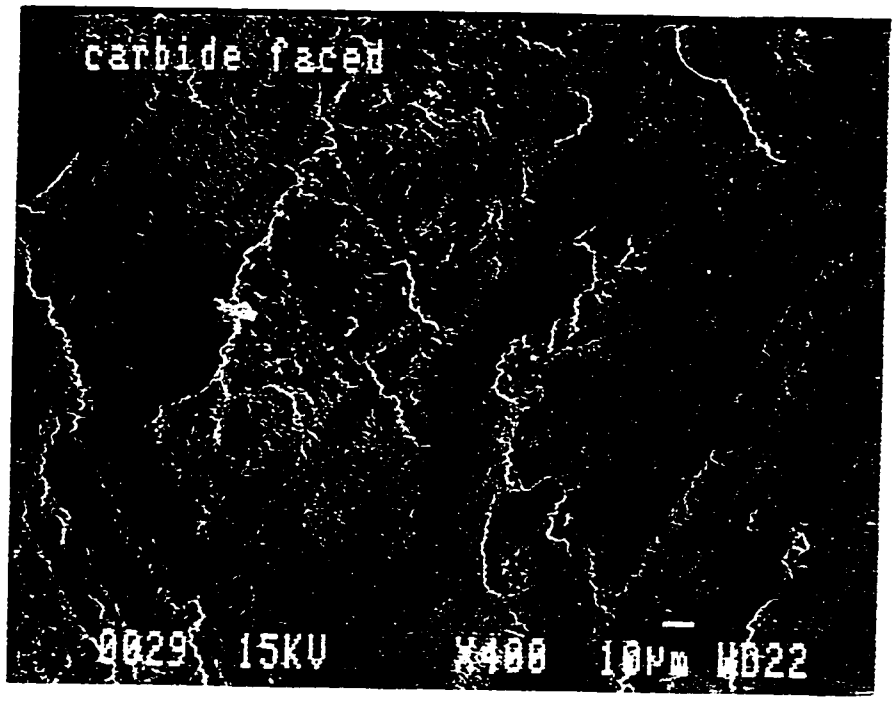

Figure 8.7 Scanning electron photomicrograph of carbide faced Si_3N_4 x400

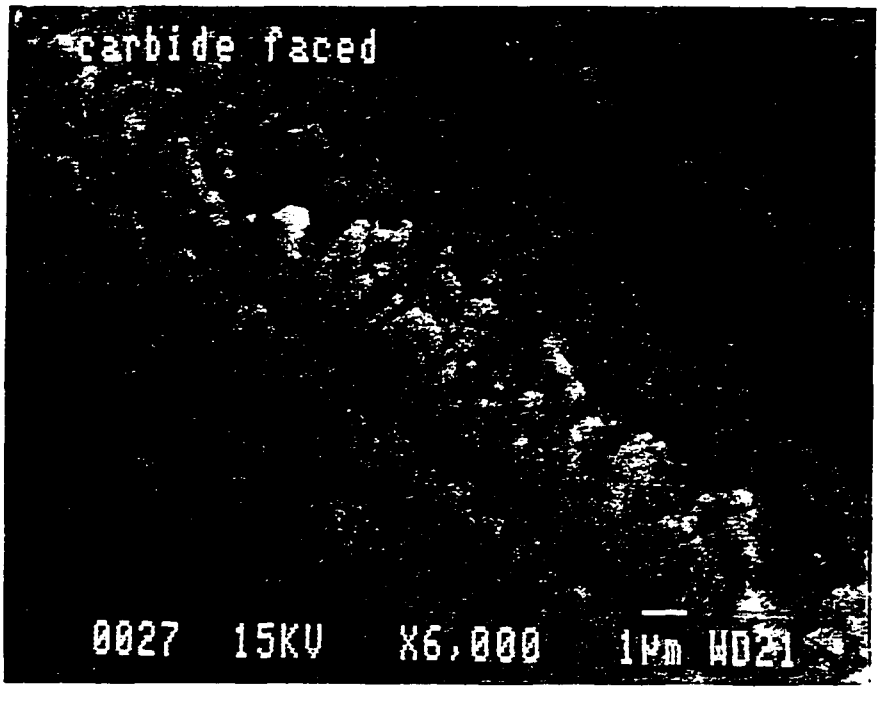

Figure 8.8 Scanning electron photomicrograph of carbide faced Si_3N_4 x6000

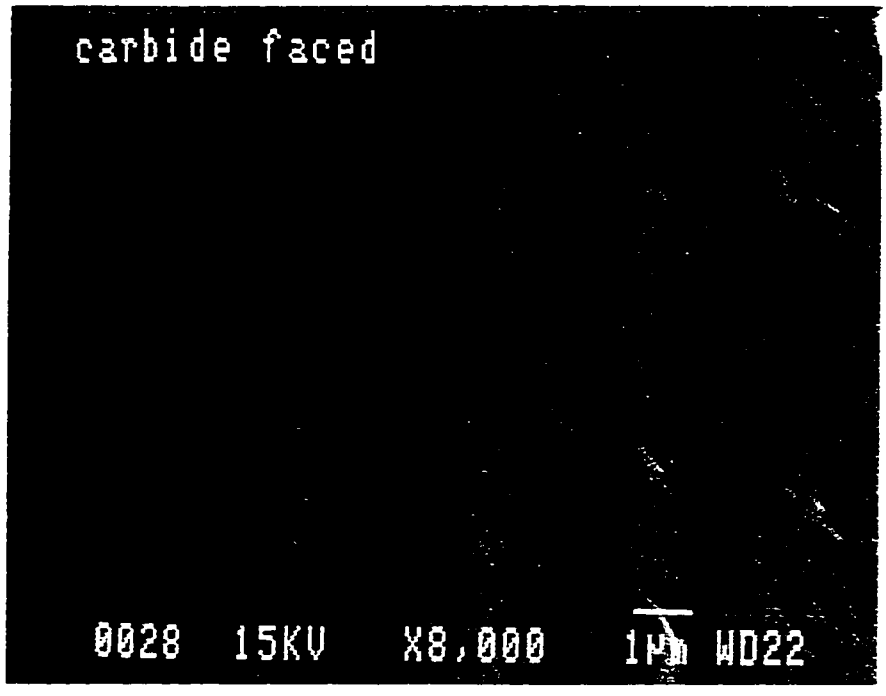

Figure 8.9 Scanning electron photomicrograph of carbide faced Si_3N_4 x8000

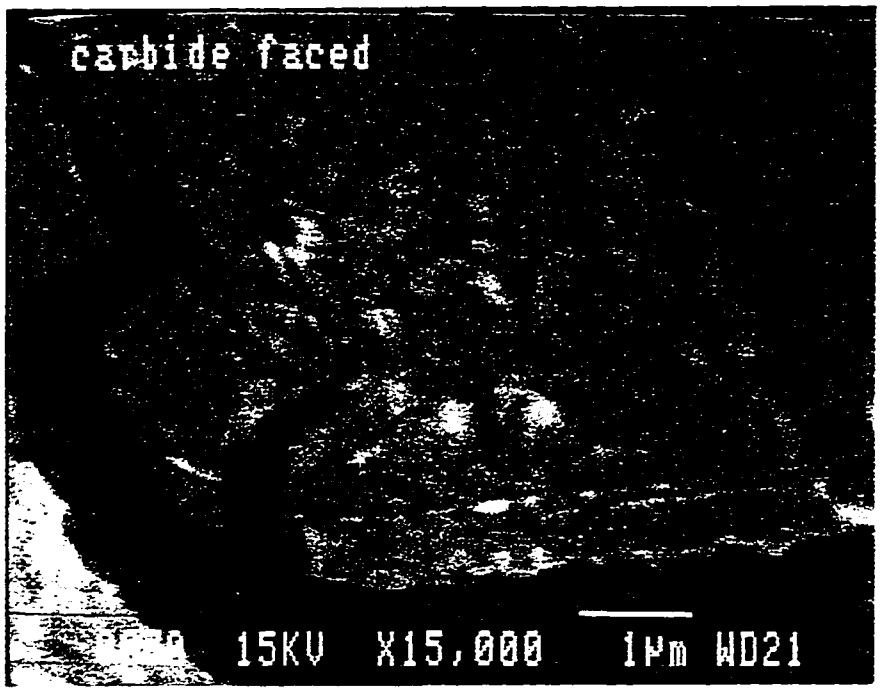

Figure 8.10 Scanning electron photomicrograph of carbide faced Si_3N_4 x15000

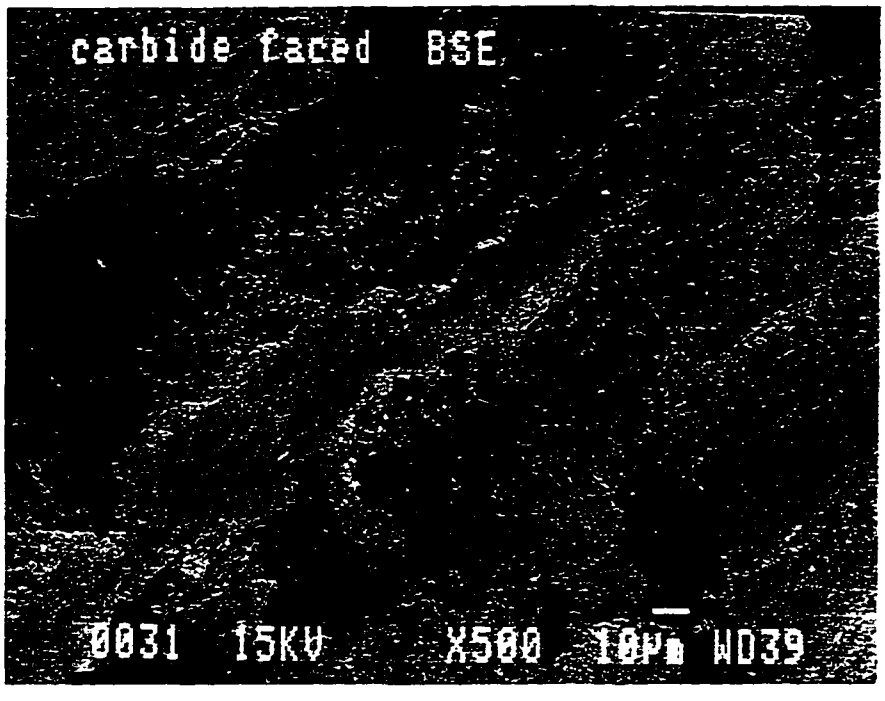

Figure 8.11 Backscatter photomicrograph of carbide faced Si_3N_4

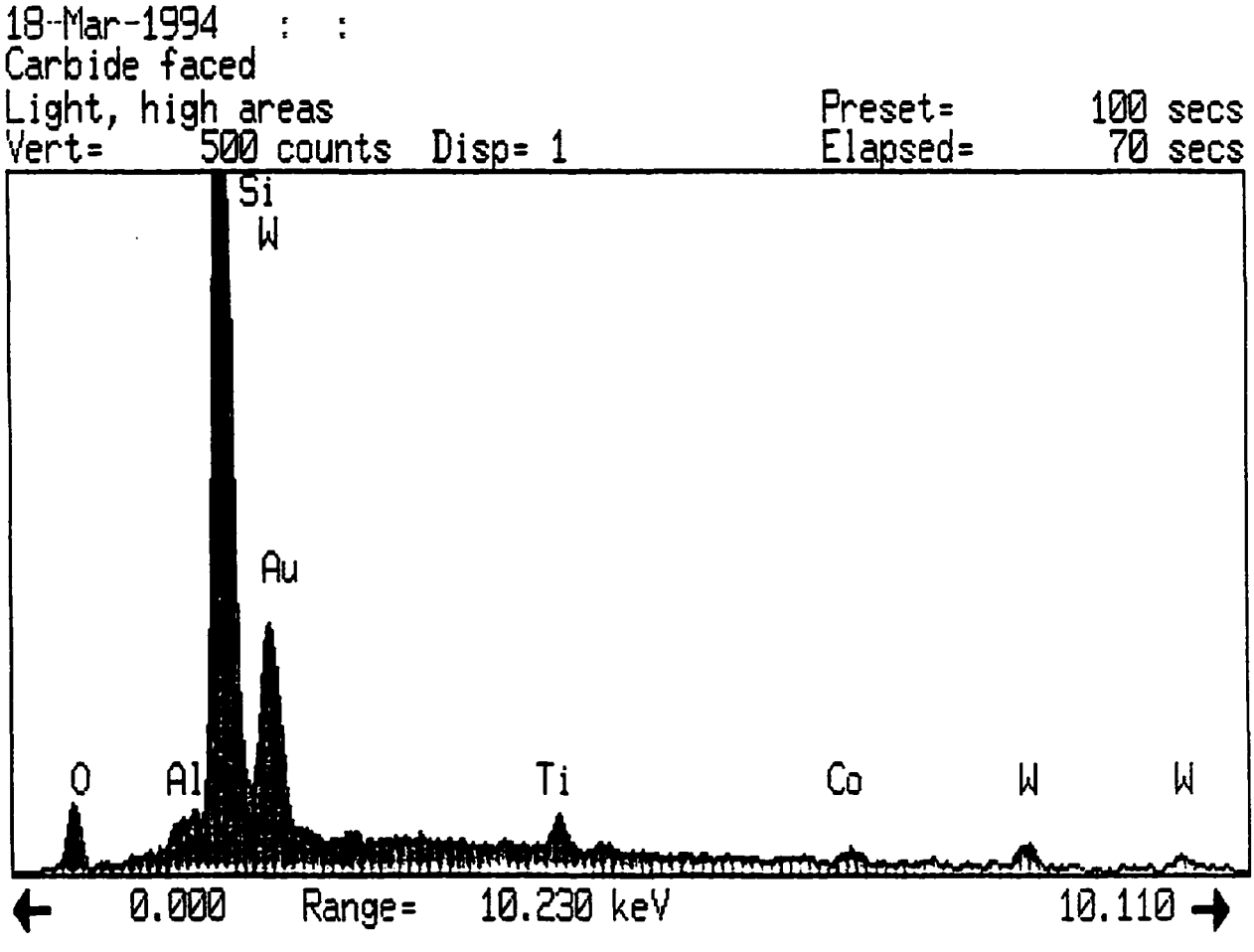

Figure 8.12 Analysis of constituents of light phase of carbide faced

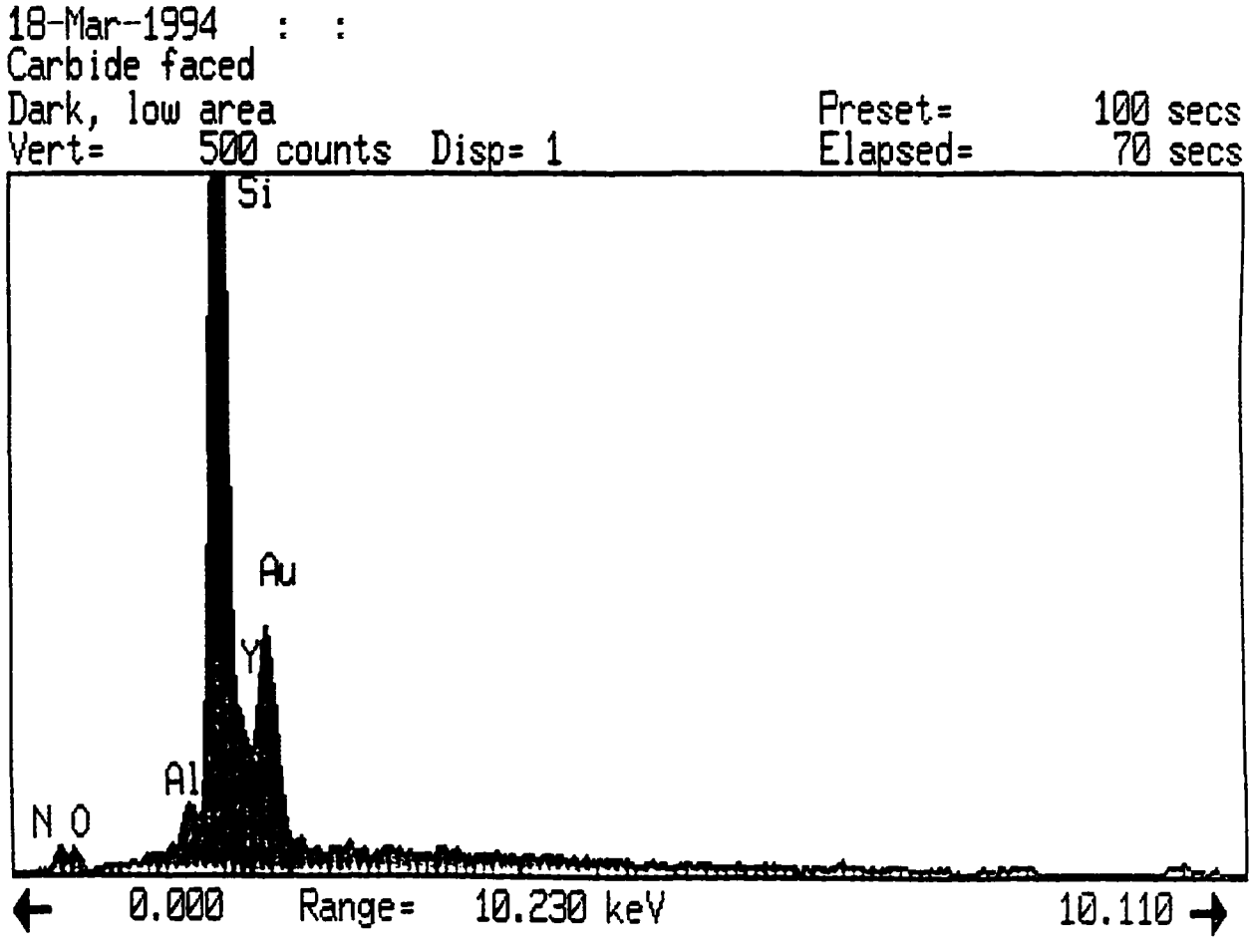

Figure 8.13 Analysis of constituents of dark phase of carbide faced

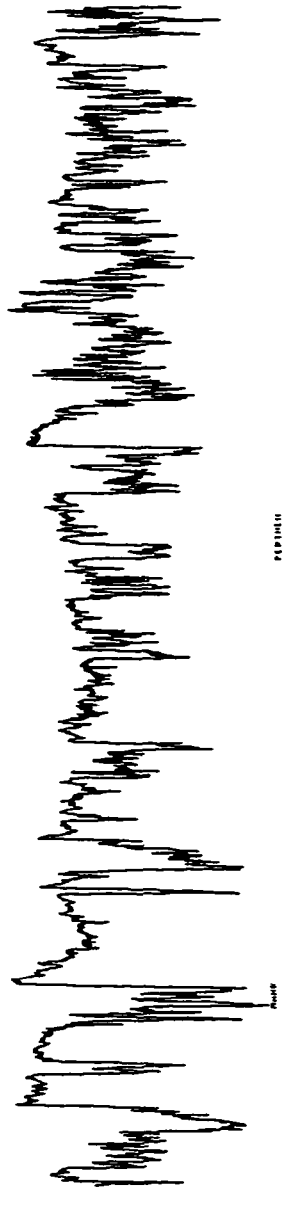

```
PROGRAM                1
MEASUREMENT            1
T1 RFHTB-50     50 CAL
LT              5.600 MM
LM              4.000 MM
VB              25.00 YM

LC   GS         0.800 MM
RA              0.481 YM
RZ              2.676 YM
RK              1.096 YM
RZISO           2.016 YM
WT              1.347 YM
RQ              0.597 YM


R PROFILE           POS
LC   GS         0.800 MM
```

```
PROGR
MEASUREMENT            2
T1 RFHTB-50     50 CAL
LT              5.600 MM
LM              4.000 MM
VB              25.00 YM

LC   GS         0.800 MM
RA              0.444 YM
RZ              3.113 YM
RK              0.487 YM
RZISO           2.020 YM
WT              1.138 YM
RQ              0.607 YM

ISU IMSE DEPT.
QUALITY LAB
301 ENGR ANNEX
  PERTHOMETER S3P

LASER CUT   CER1
RADIAL
```

Figure 8.14 Profilometer trace of Nd:YAG laser assisted machined surface: Zone 1 : Radial and Transverse

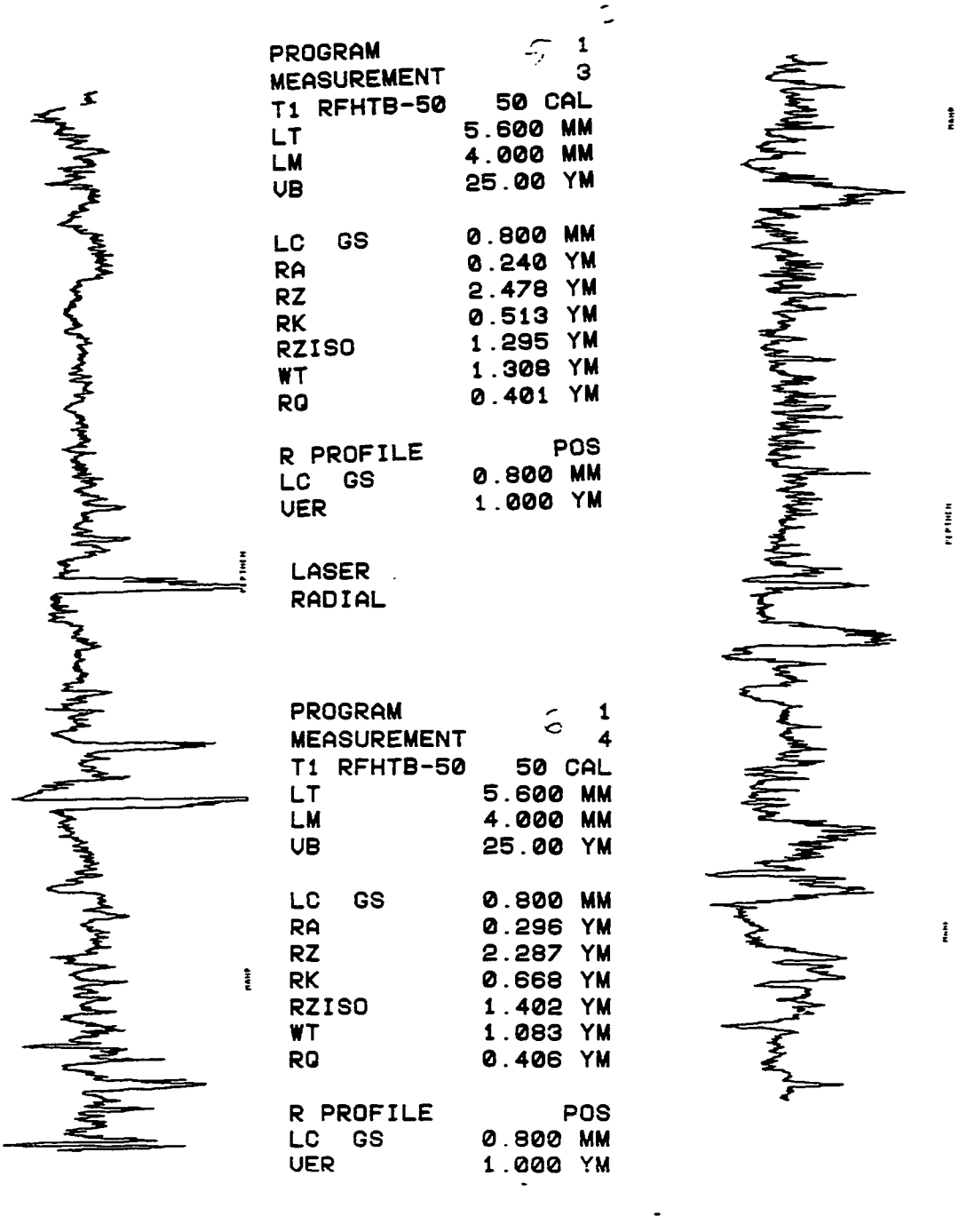

Figure 8.15 Profilometer trace of Nd:YAG laser assisted machined surface: Zone 2 : Radial and Transverse

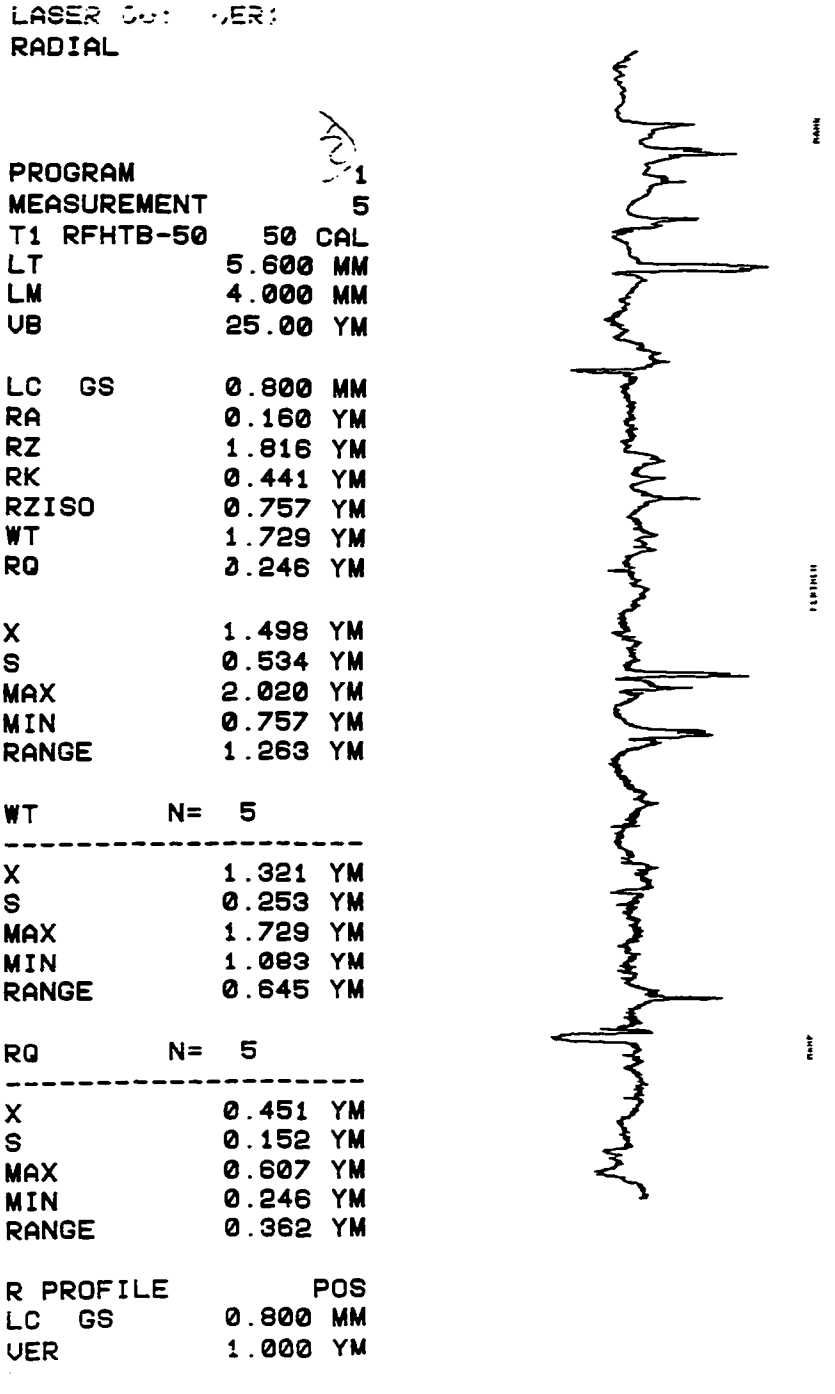

Figure 8.16 Profilometer trace of Nd:YAG laser assisted machined surface: Zone 3 : Radial

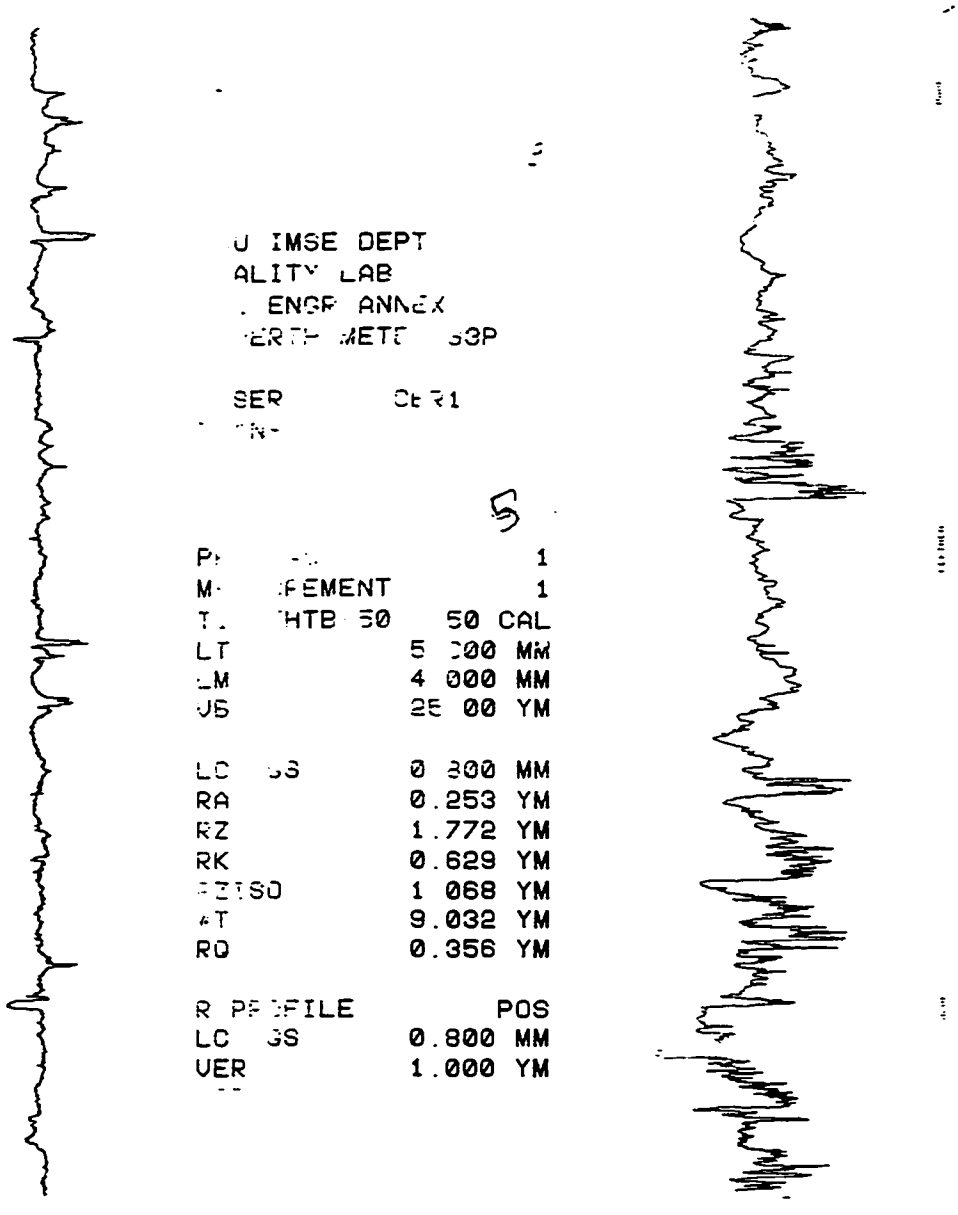

Figure 8.17 Profilometer trace of Nd:YAG laser assisted machined surface: Zone 4 : Radial and Transverse

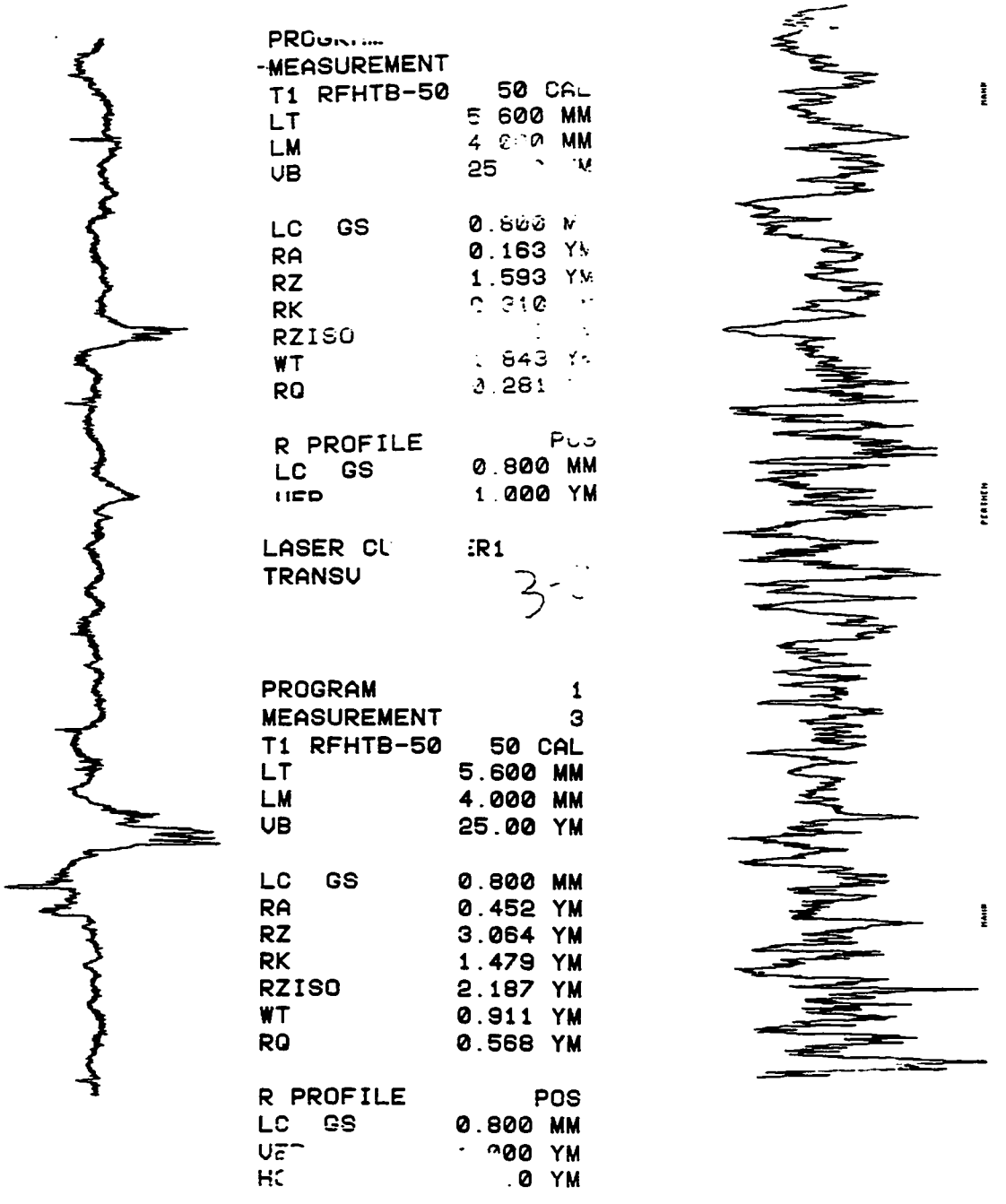

Figure 8.18 Profilometer trace of Nd:YAG laser assisted machined surface: Zone 5 : Radial and Transverse

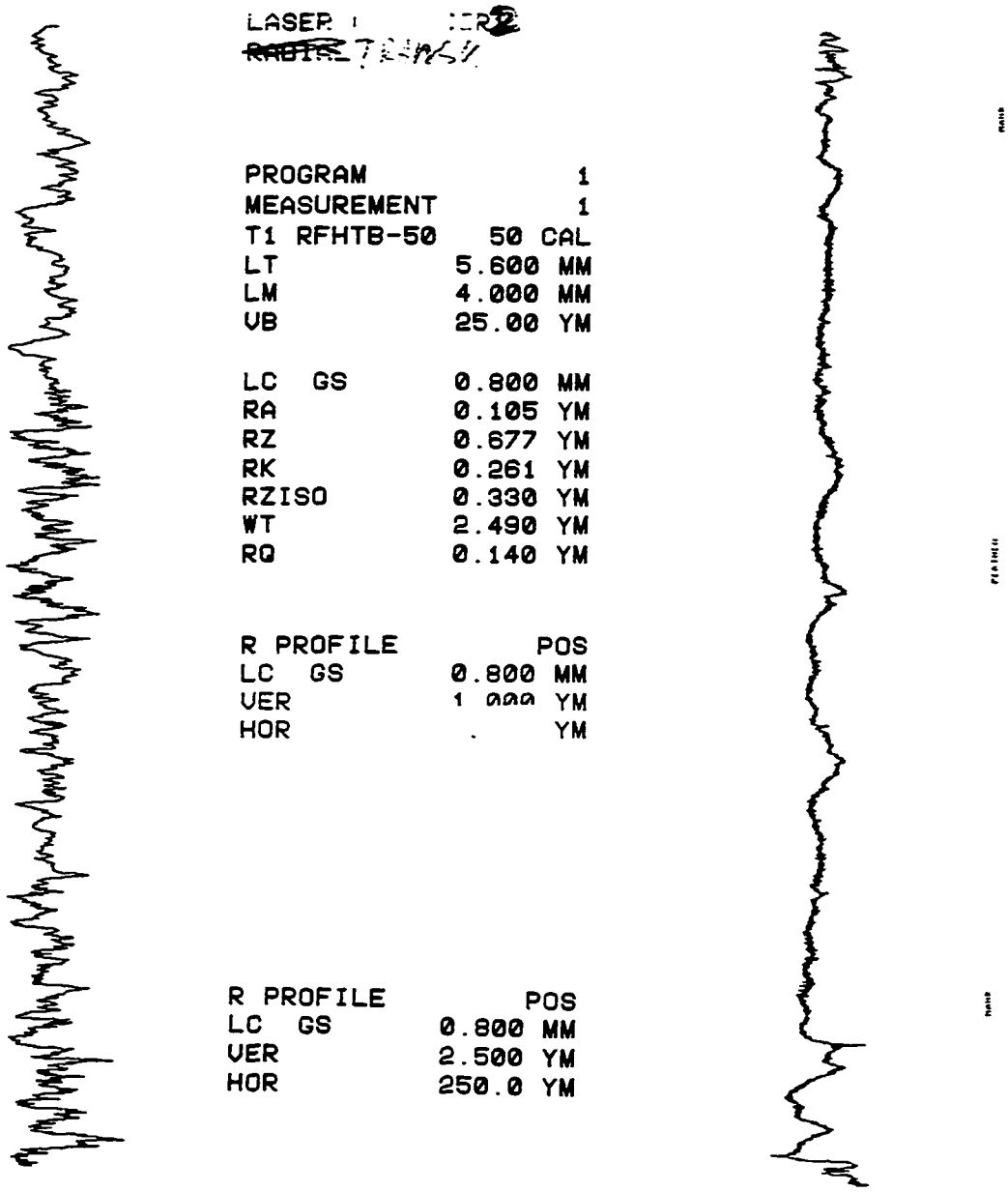

Figure 8.19 Profilometer trace of Nd:YAG laser assisted machined surface: Zone 6 : Radial and Transverse

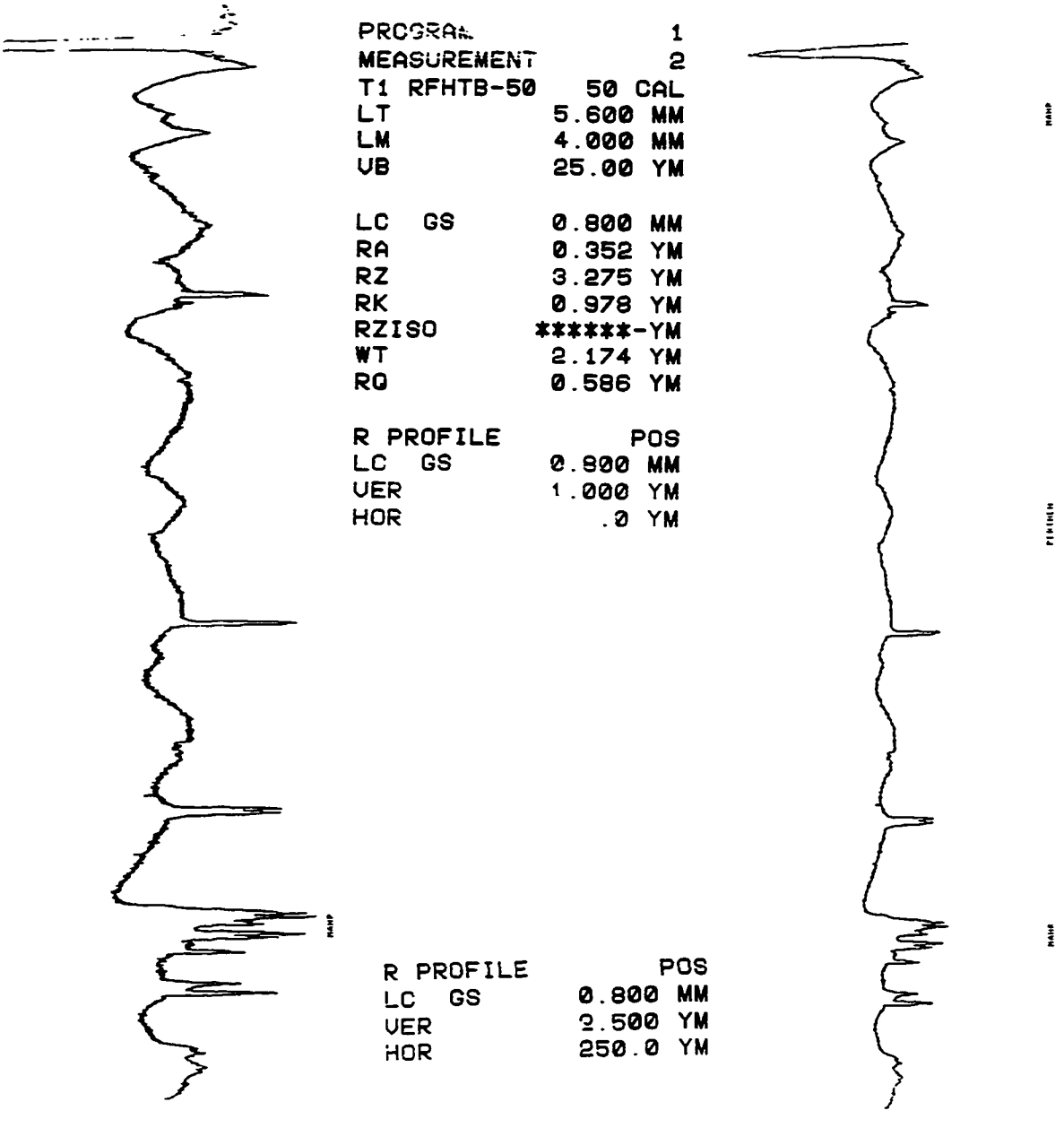

Figure 8.20 Profilometer trace of Nd:YAG laser assisted machined surface: Zone 7 : Radial and Transverse

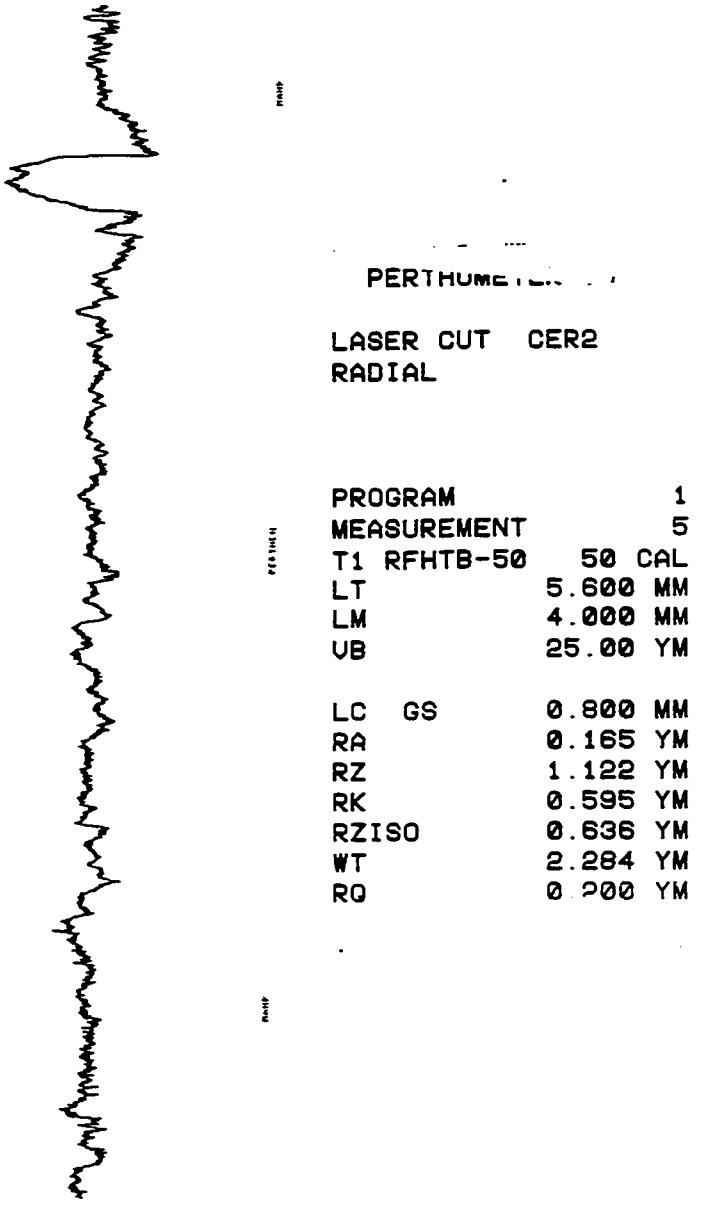

Figure 8.21 Profilometer trace of Nd:YAG laser assisted machined surface: Zone 8 : Radial

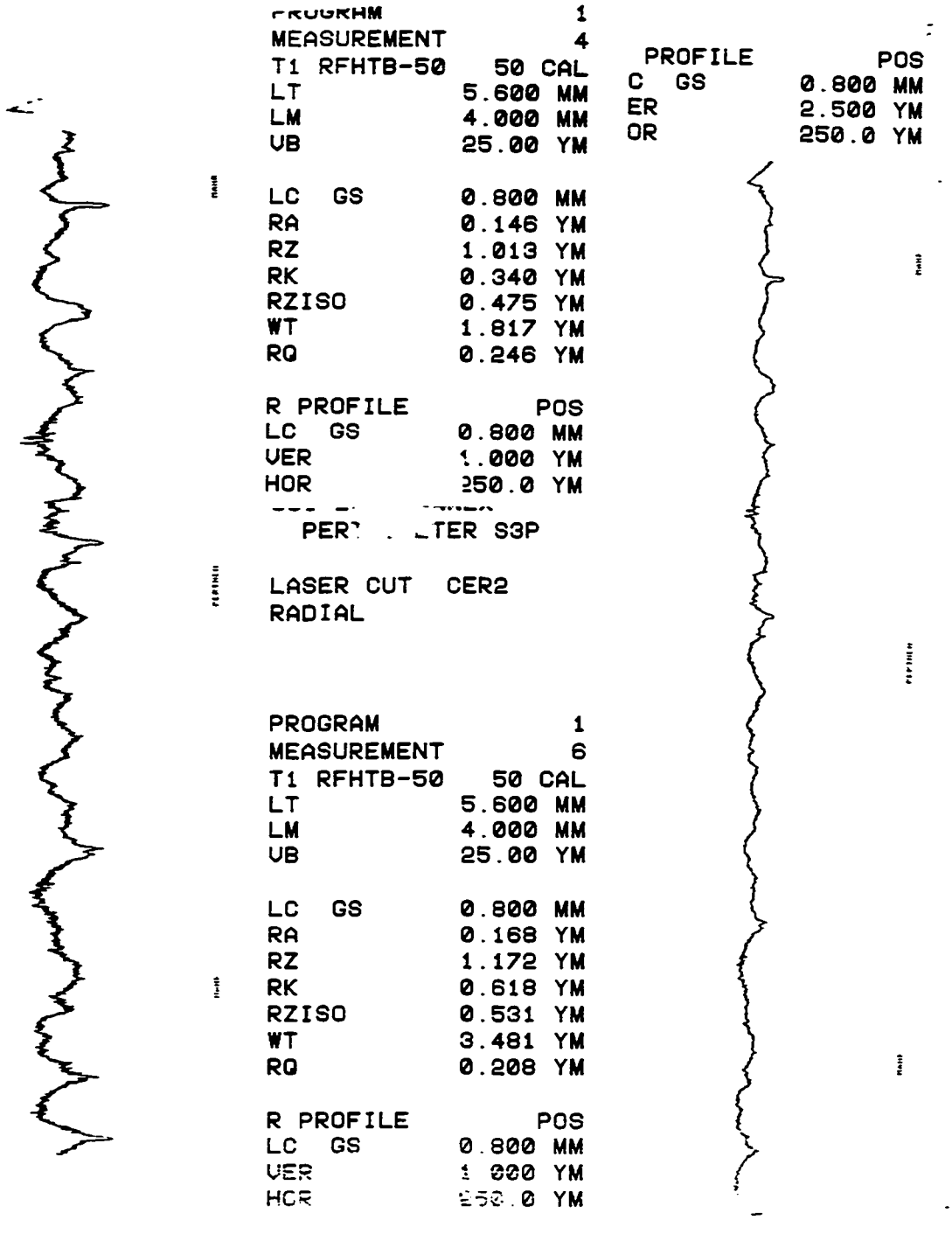

Figure 8.22 Profilometer trace of Nd:YAG laser assisted machined surface: Zone 9 : Radial and Transverse

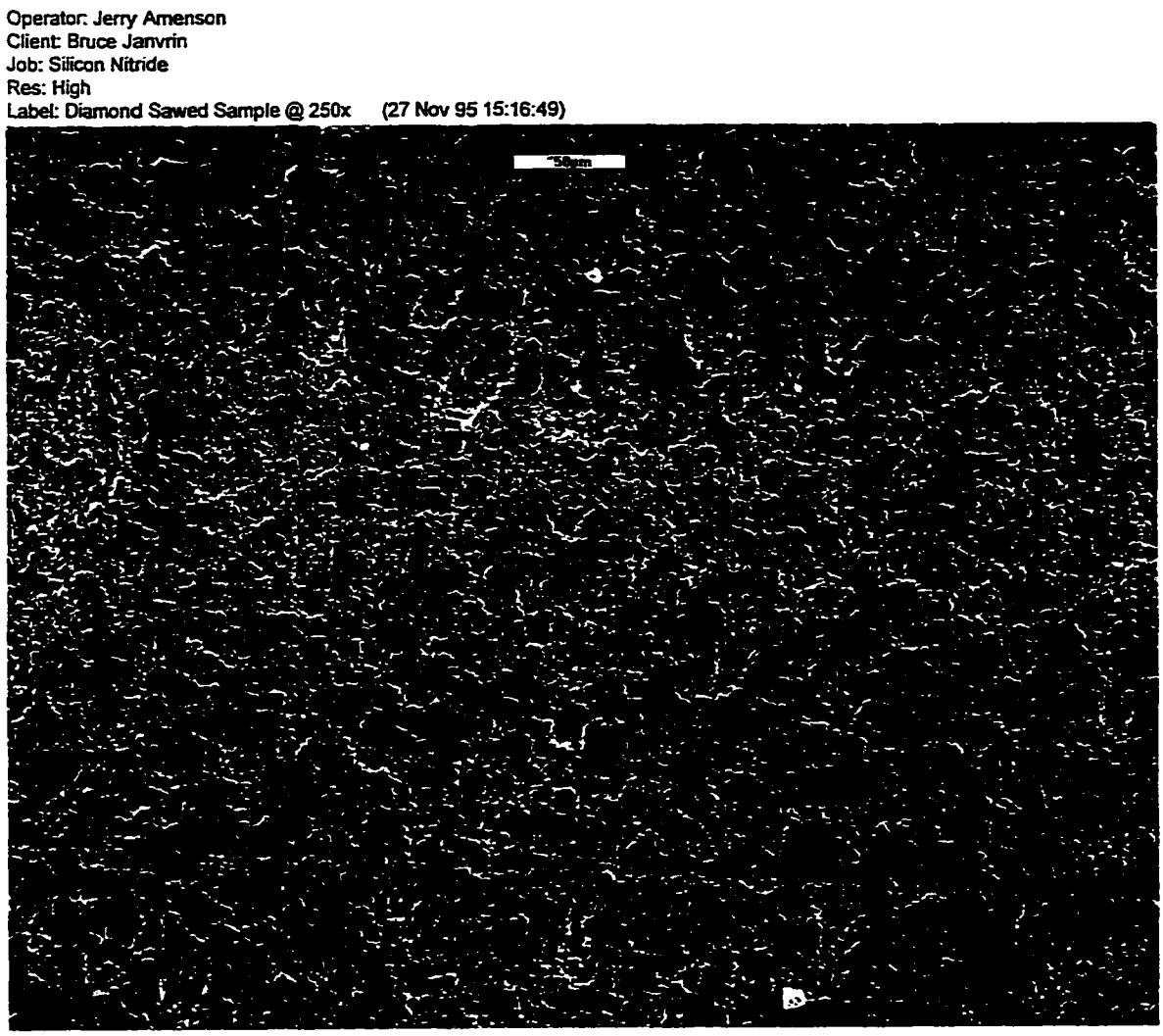

Figure 8.23 Scanning electron micrograph of diamond sawn silicon nitride (250x)

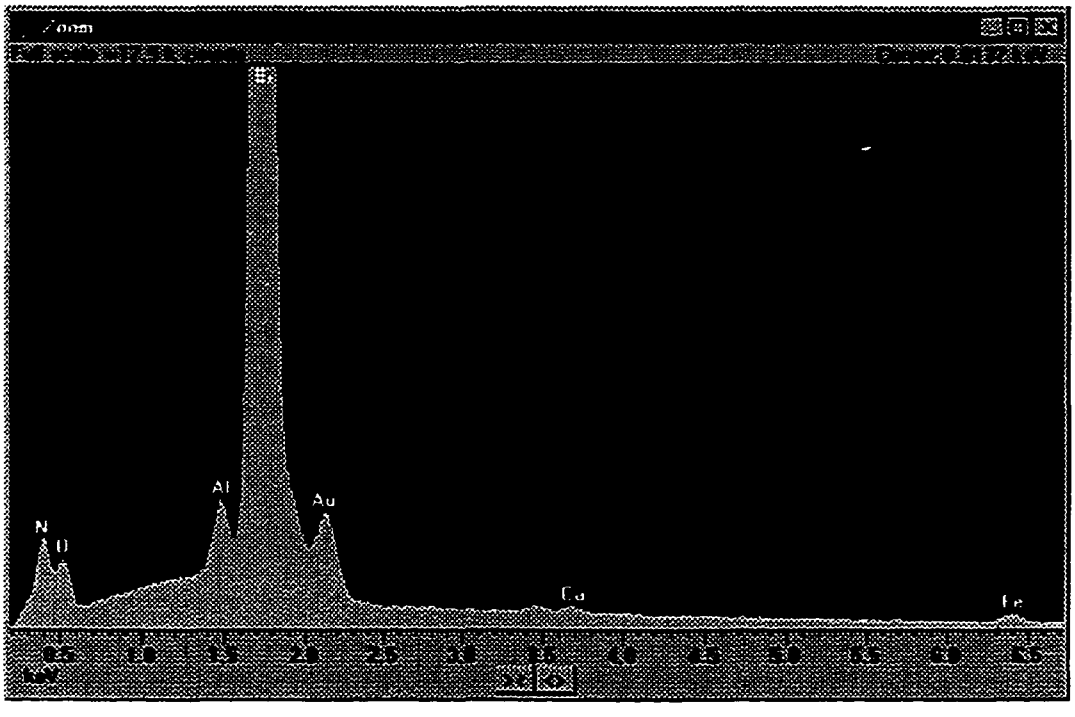

Figure 8.24 EDAX distribution of elements of diamond sawn silicon nitride

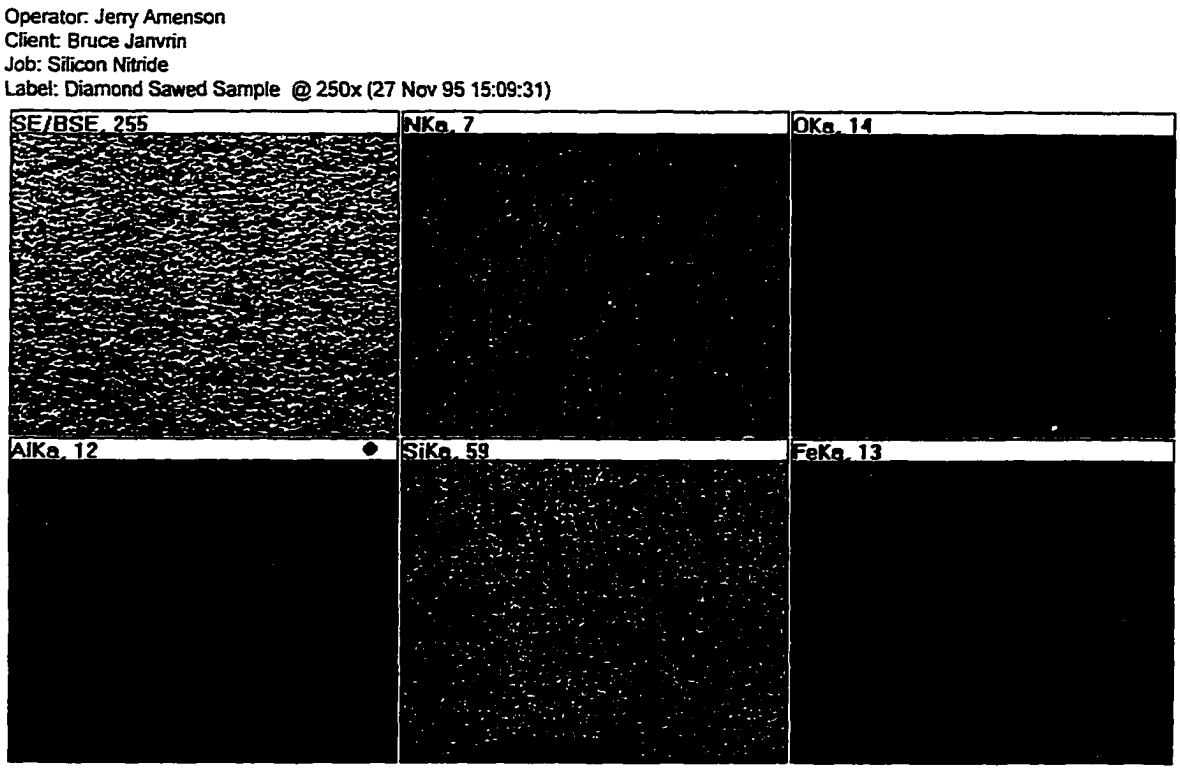

Figure 8.25 Elmental distribution on diamond sawn silicon nitride

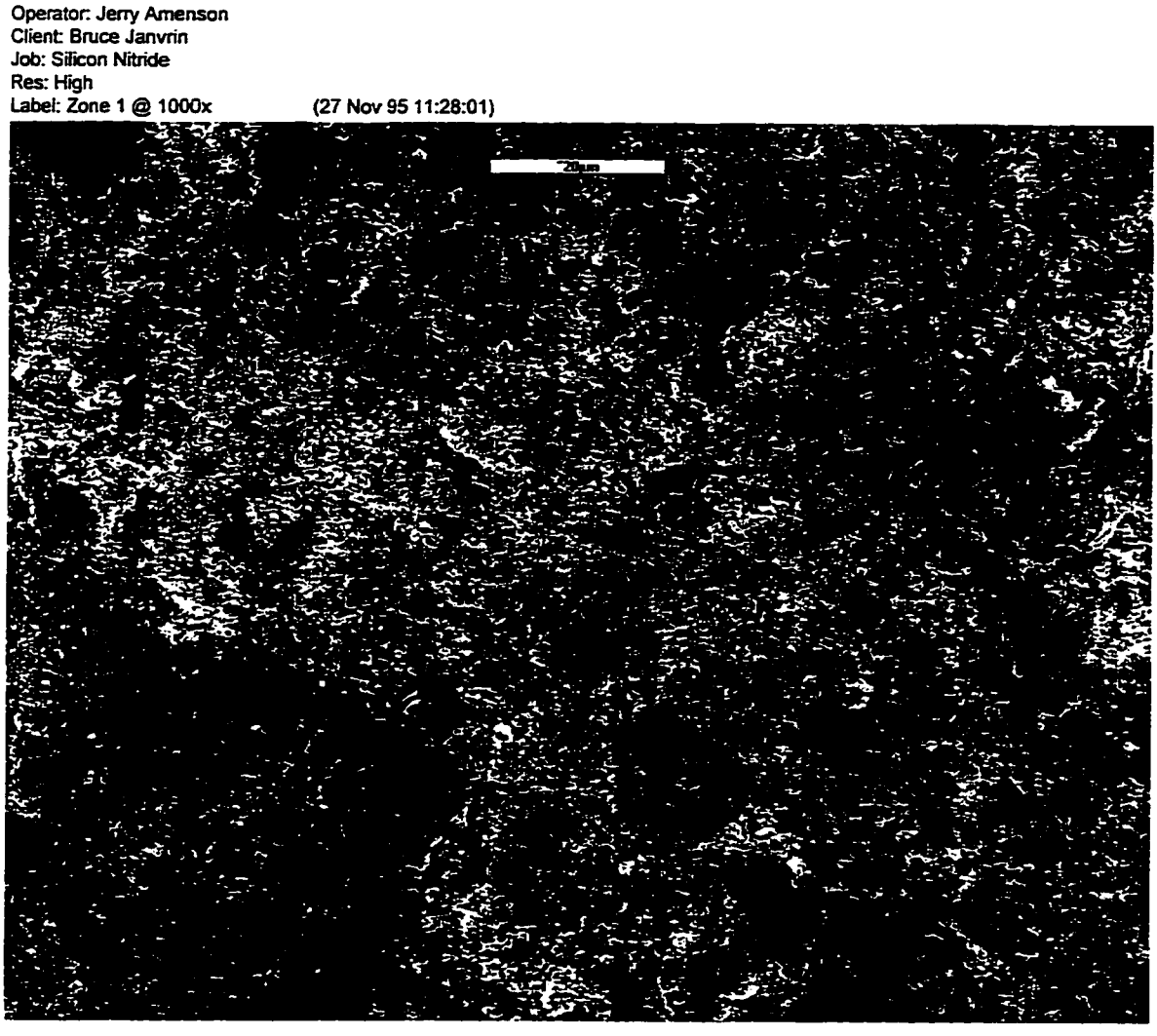

Figure 8.26 Scanning electron micrograph of laser-assisted turned zone 1 (1000x)

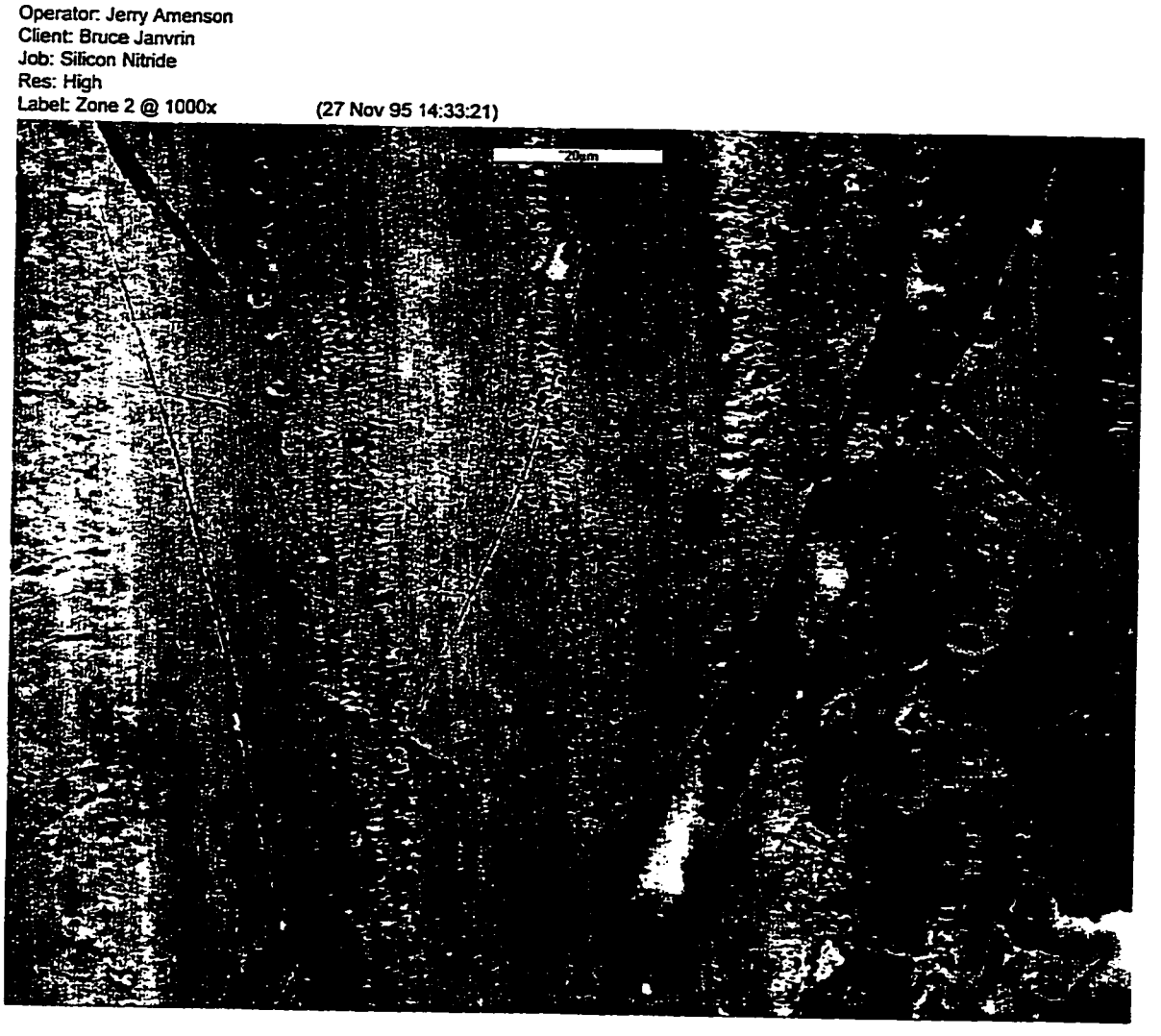

Figure 8.27 Scanning electron micrograph of laser-assisted turned zone 2 (1000x)

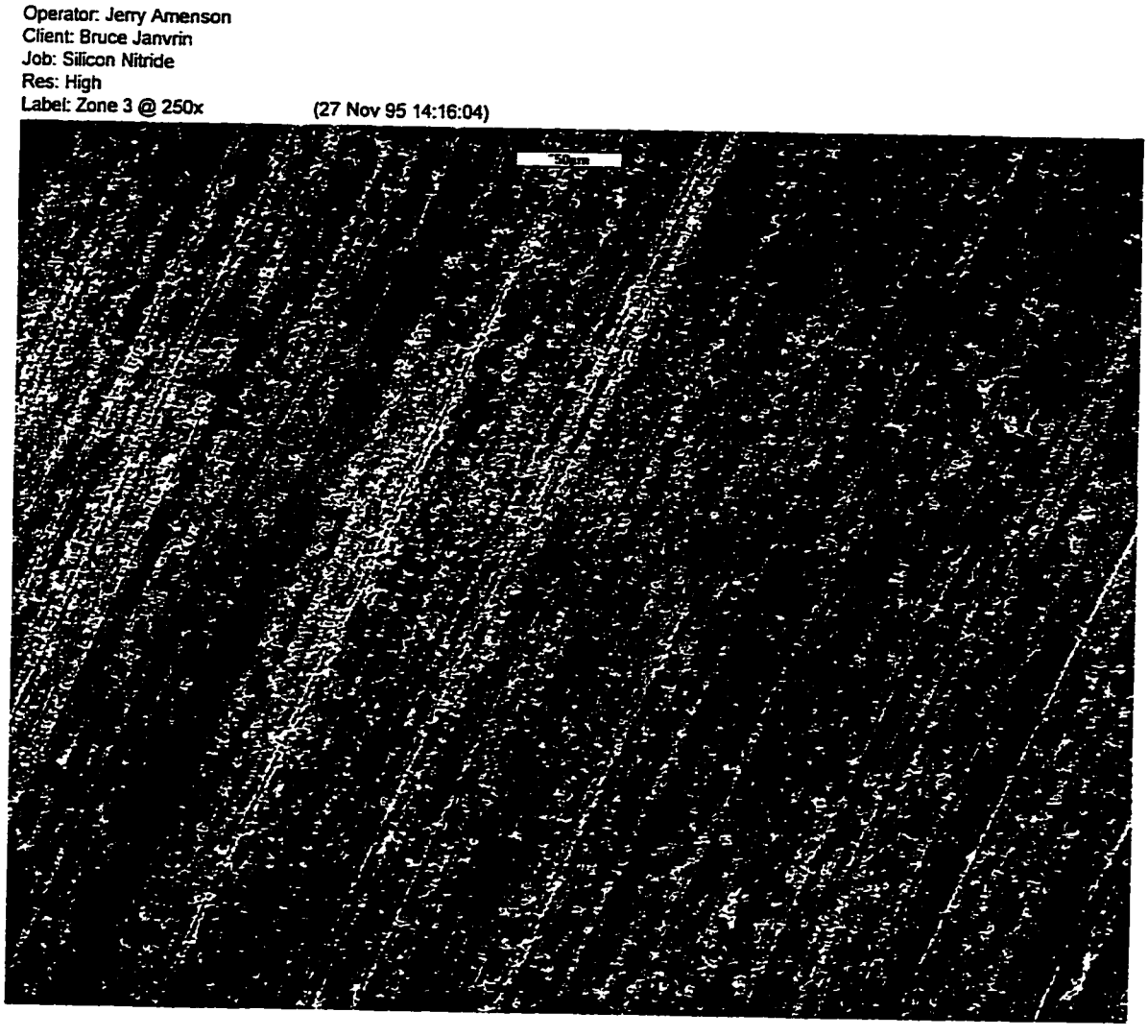

Figure 8.28 Scanning electron micrograph of laser-assisted turned zone 3 (250x)

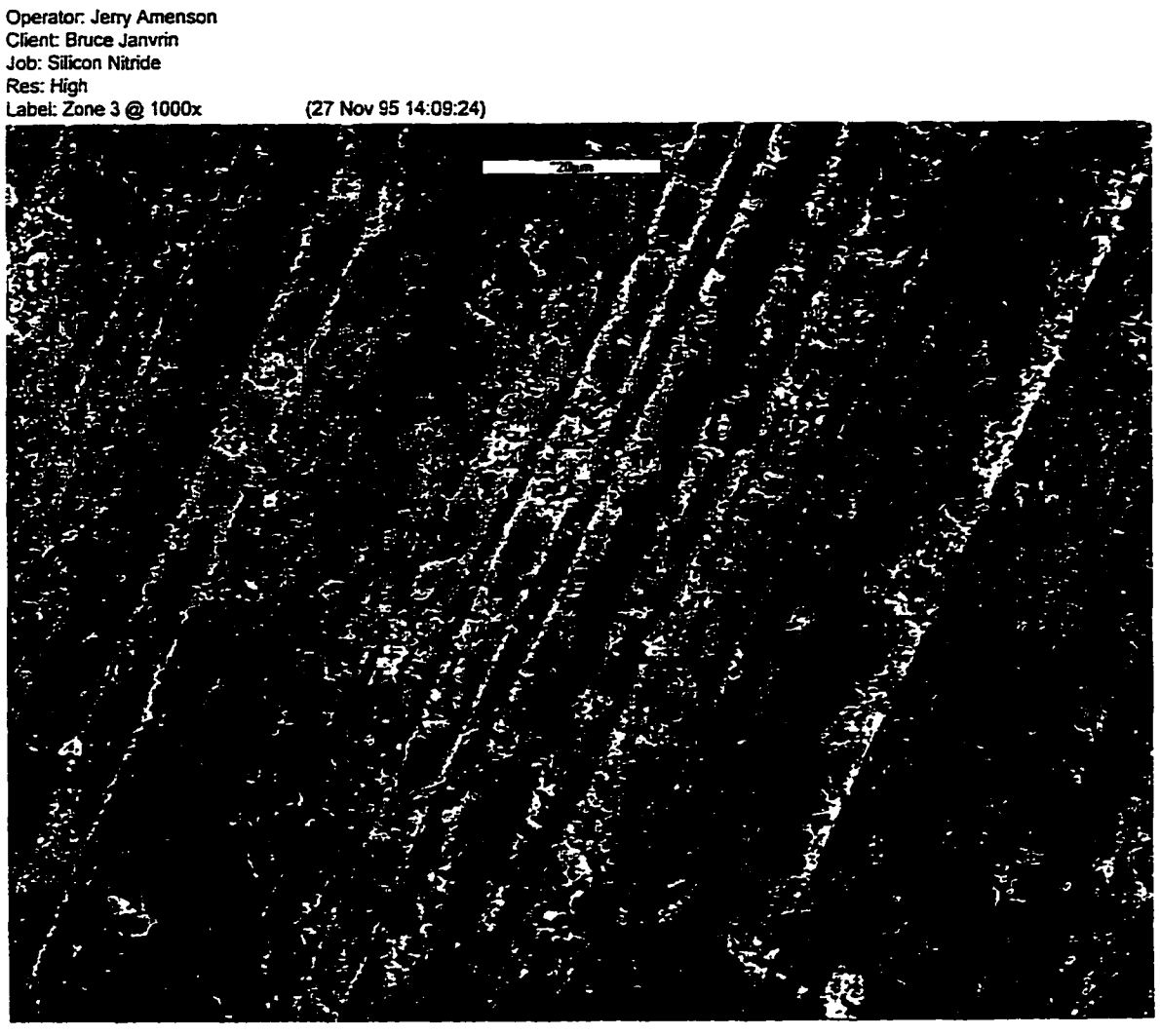

Figure 8.29 Scanning electron micrograph of laser-assisted turned zone 3 (1000x)

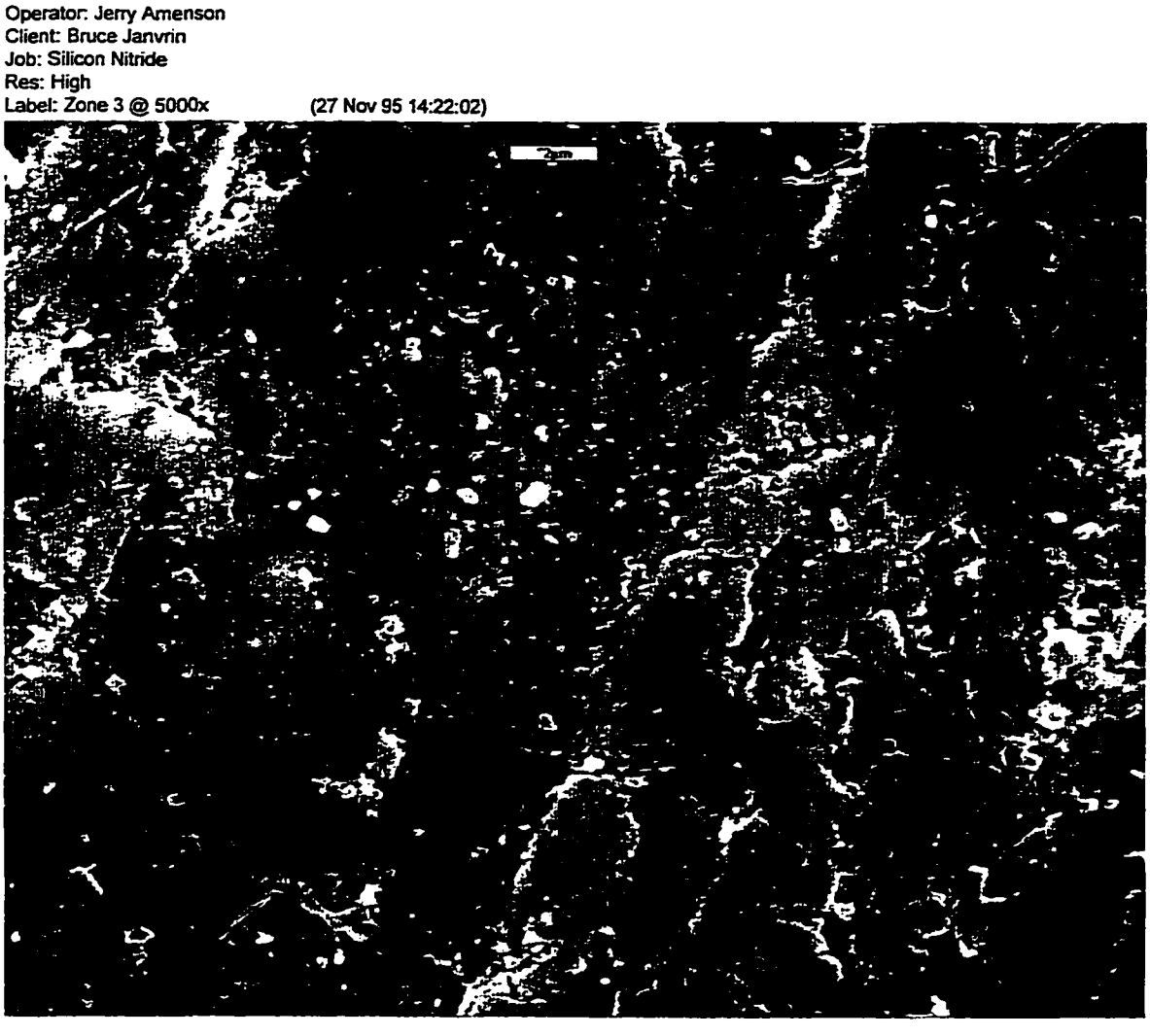

Figure 8.30 Scanning electron micrograph of laser-assisted turned zone 3 (5000x)

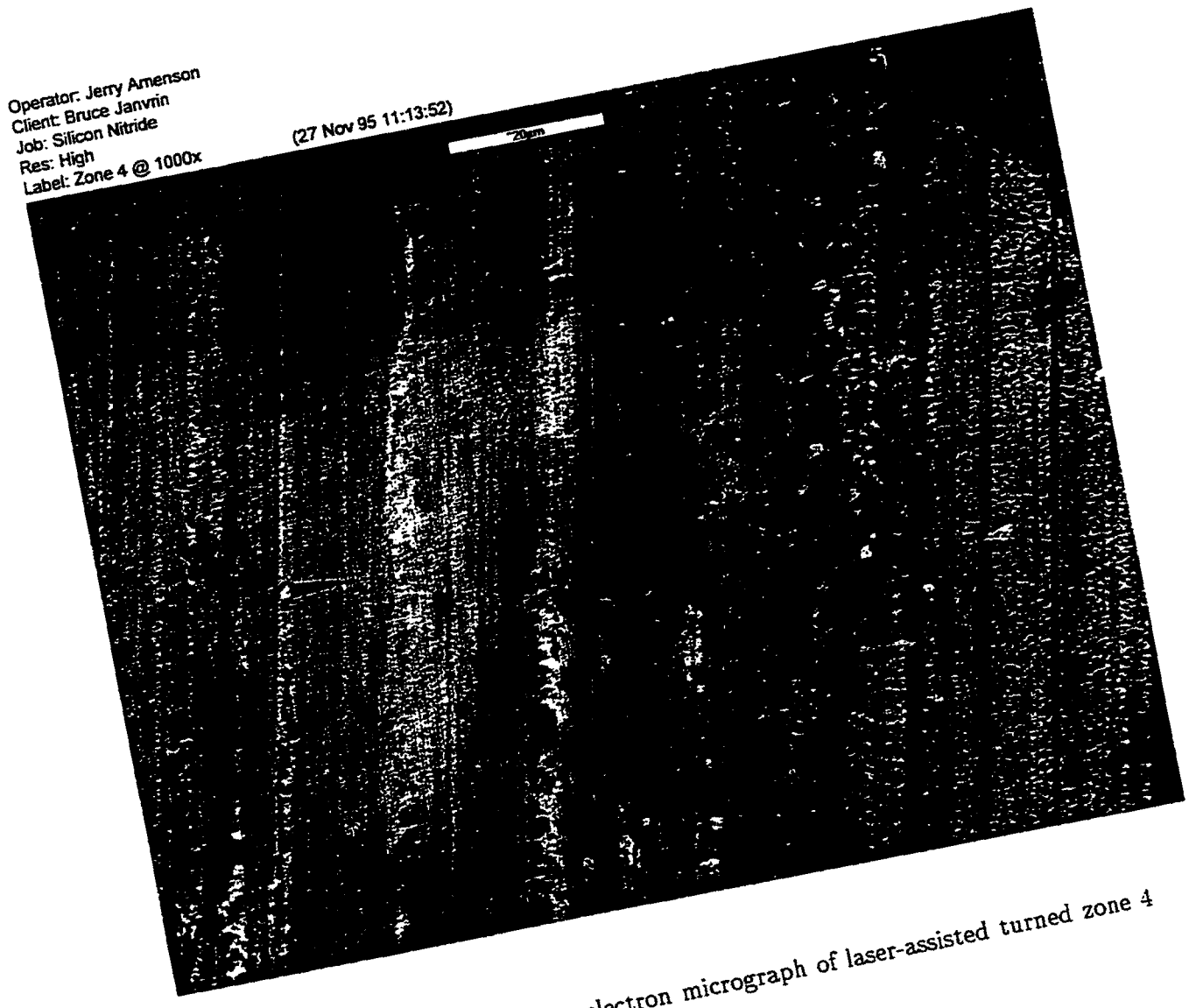

Figure 8.31 Scanning electron micrograph of laser-assisted turned zone 4 (1000x)

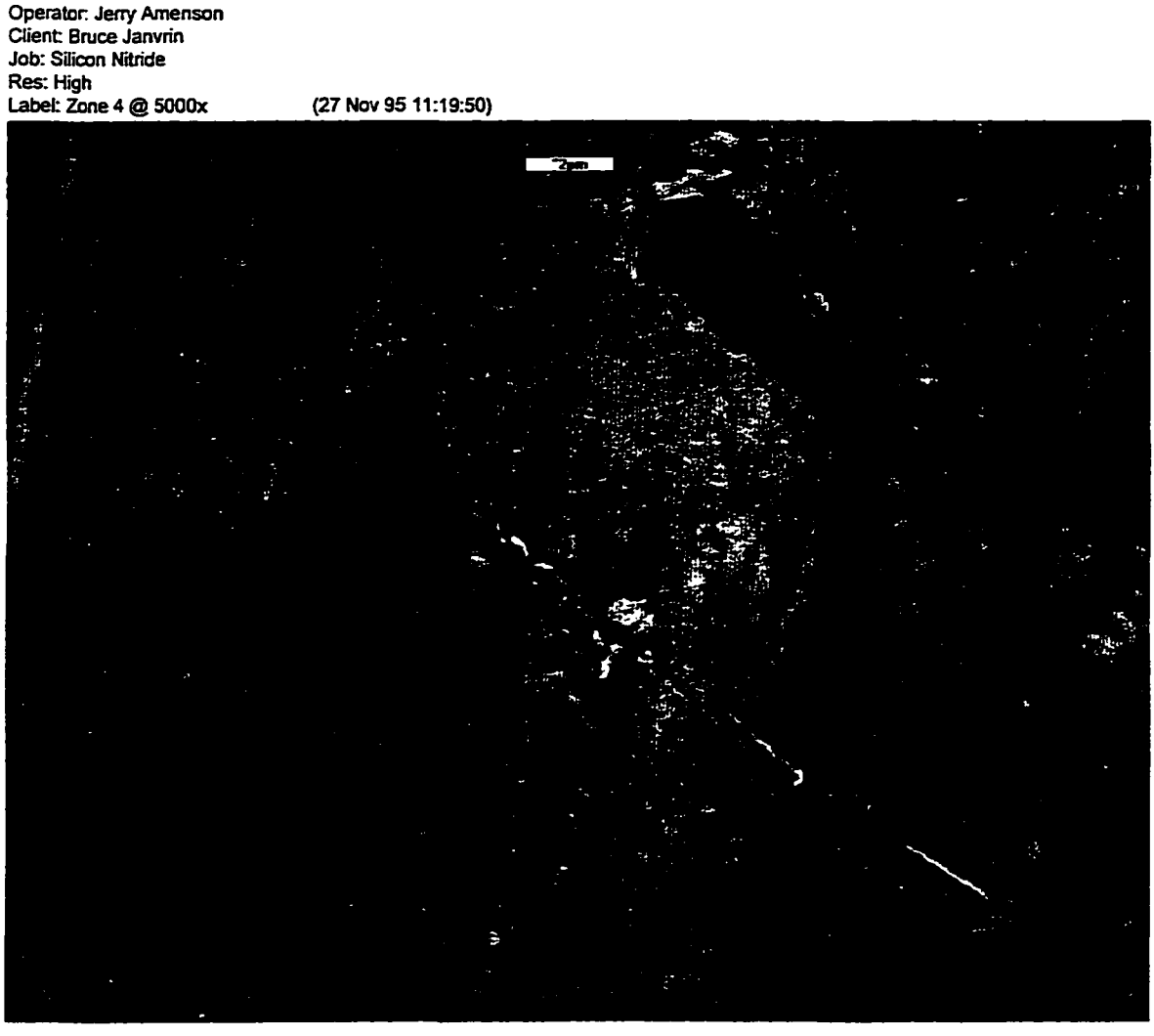

Figure 8.32 Scanning electron micrograph of laser-assisted turned zone 4 (5000x)

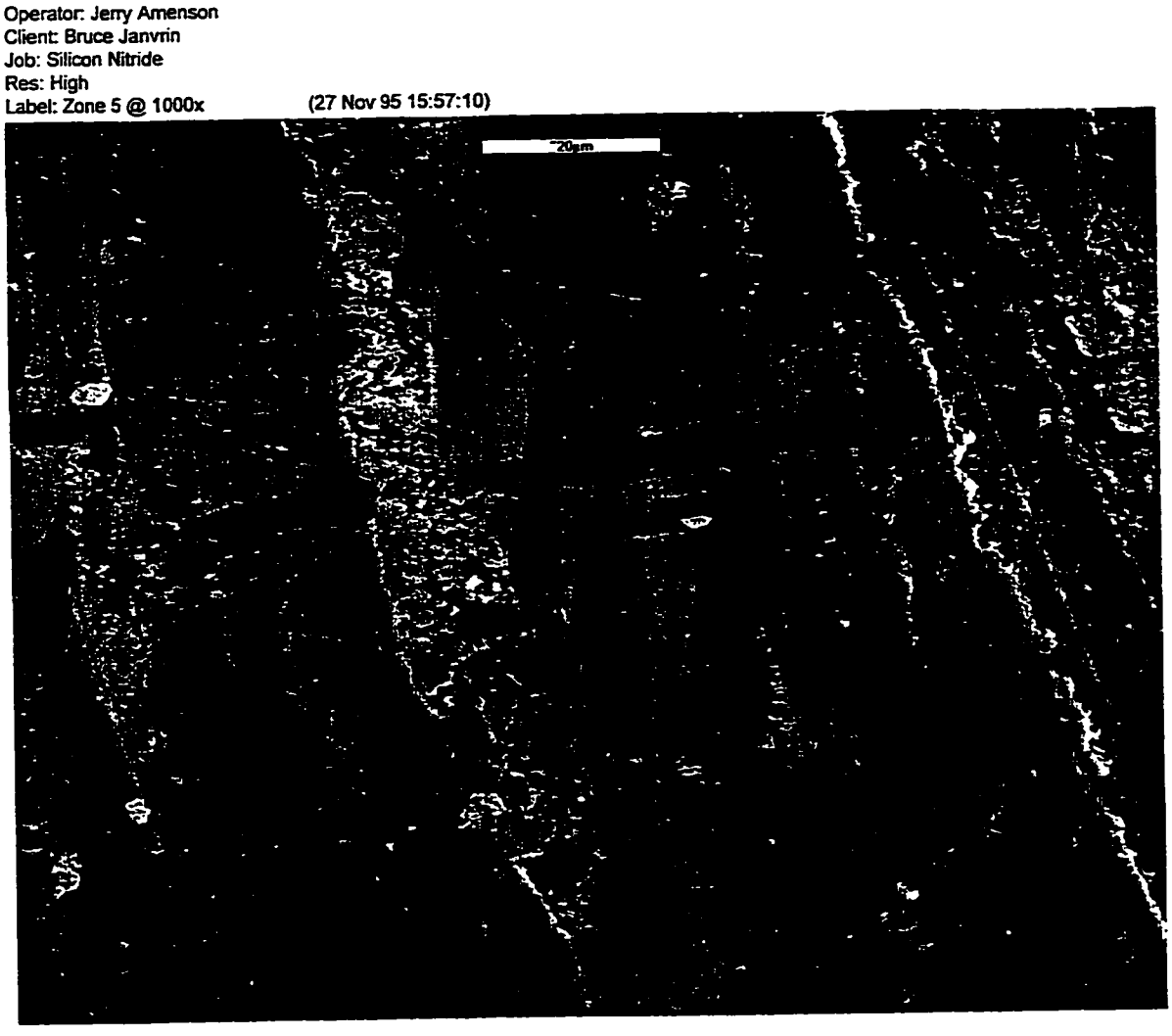

Figure 8.33 Scanning electron micrograph of laser-assisted turned zone 5 (1000x)

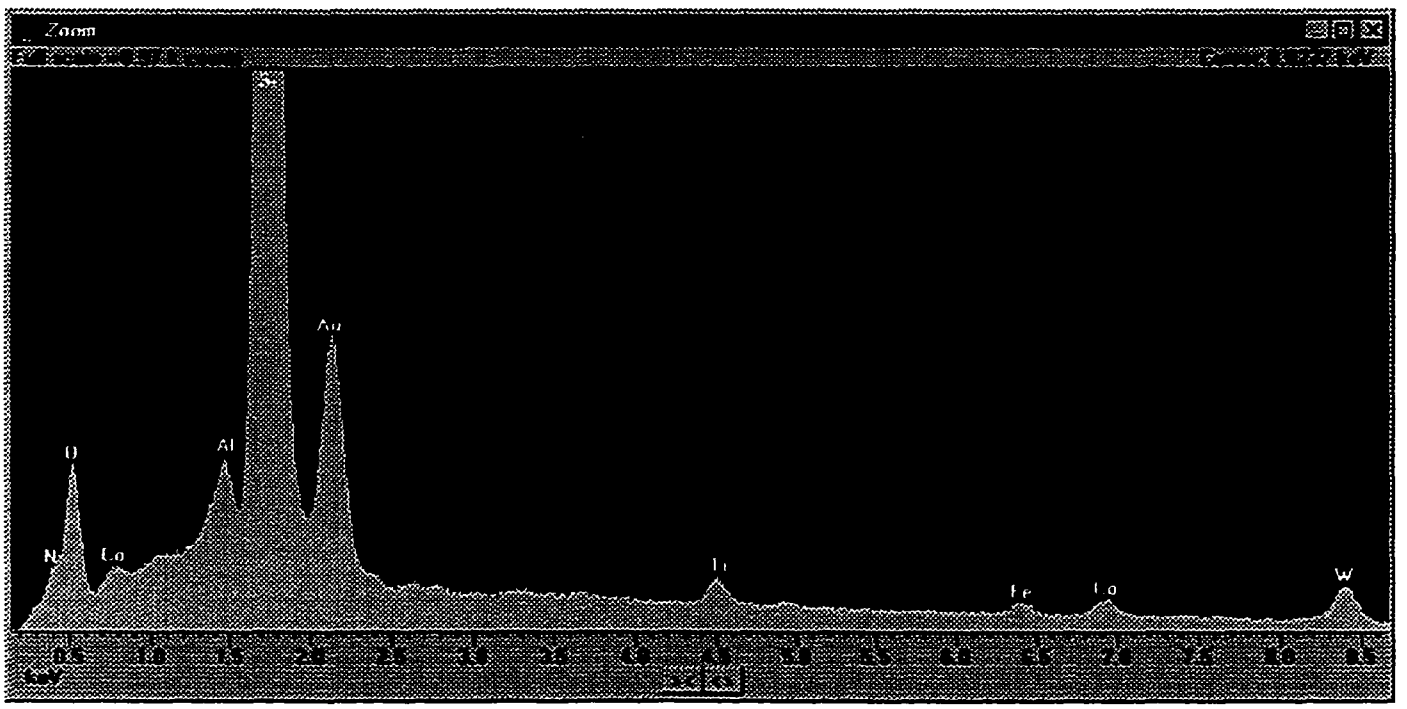

Figure 8.34 EDAX distribution of zone 5.

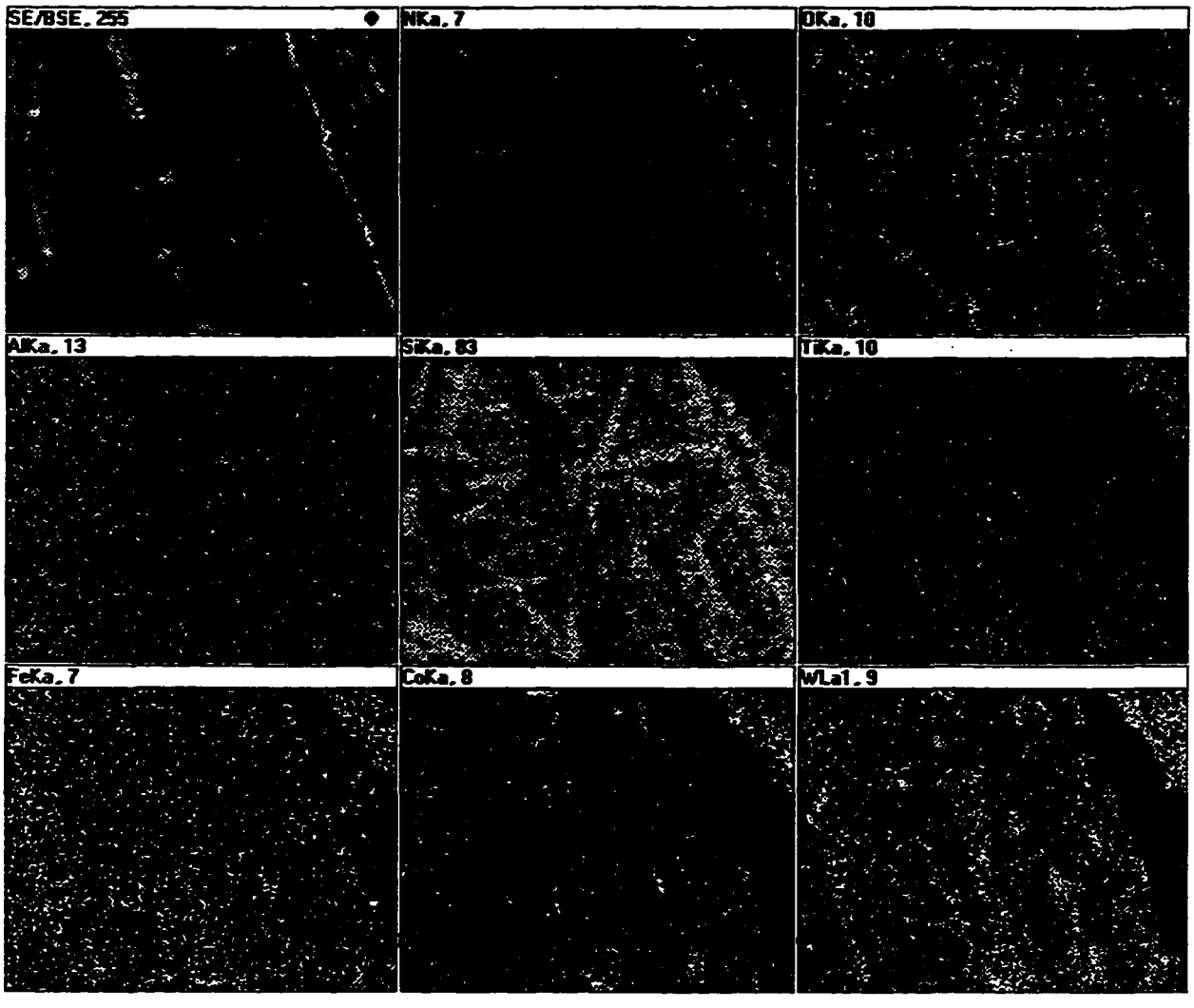

Figure 8.35 Elemental mapping of zone 5.

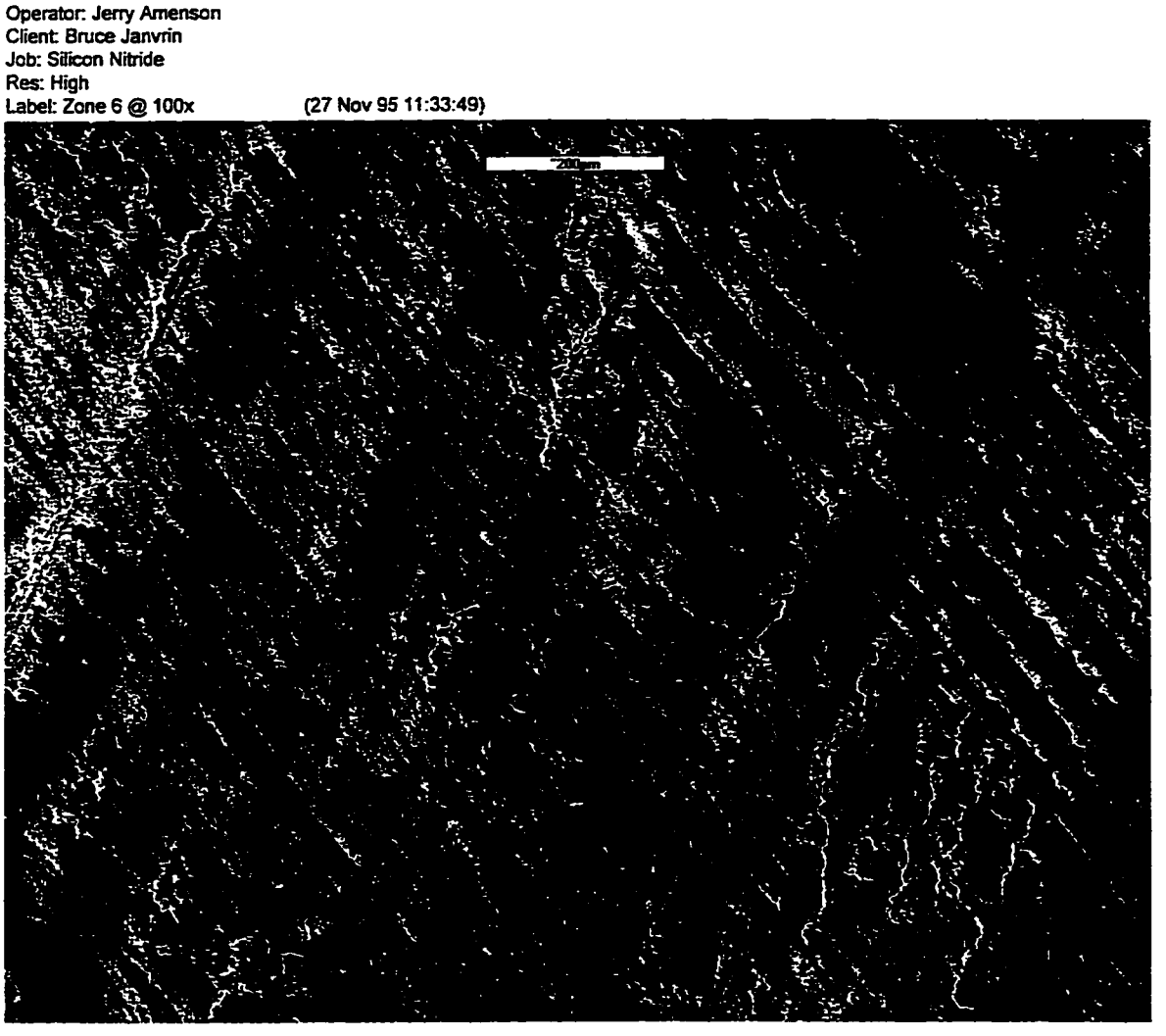

Figure 8.36 Scanning electron micrograph of laser-assisted turned zone 6 (100x)

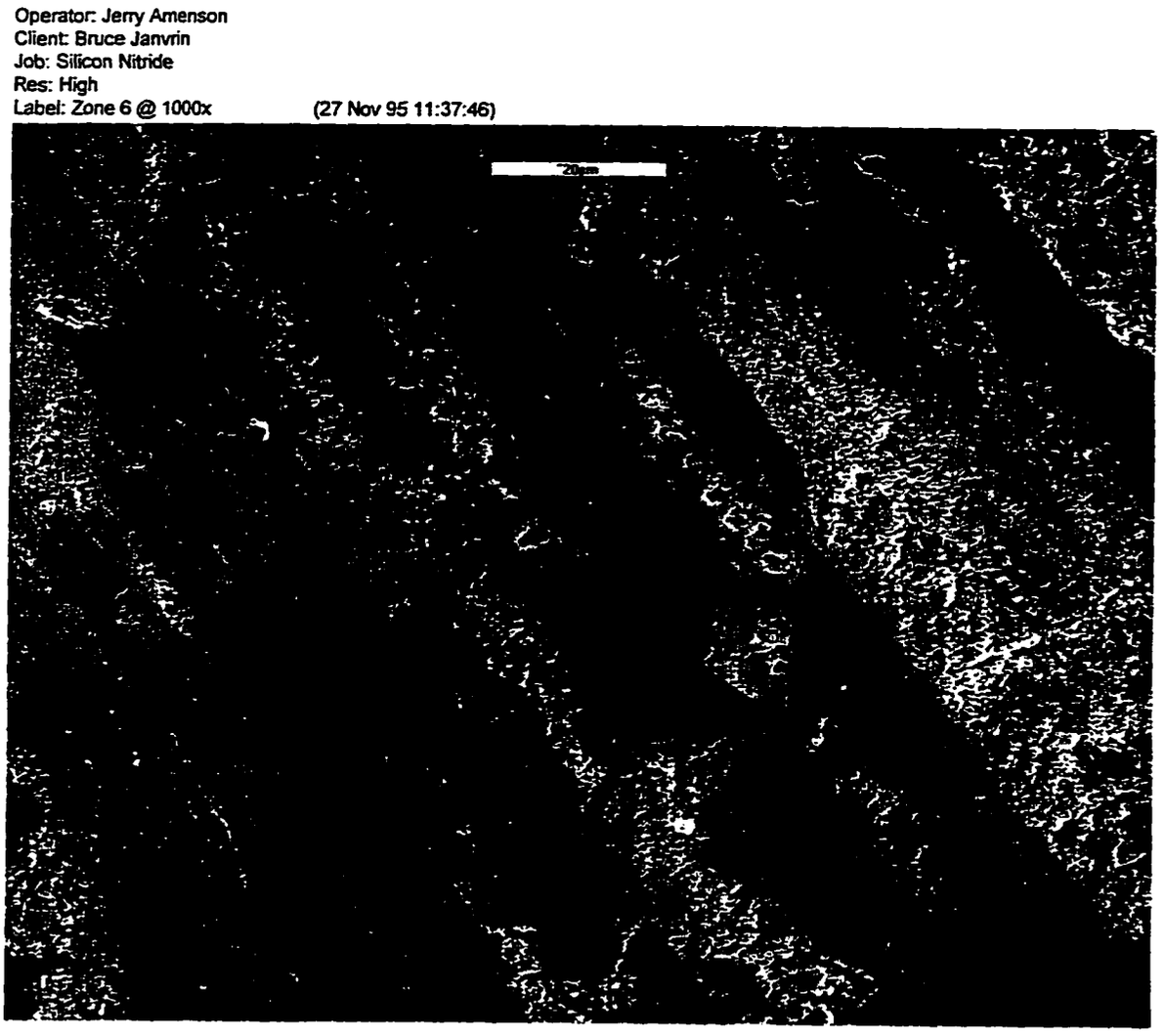

Figure 8.37 Scanning electron micrograph of laser-assisted turned zone 6 (1000x)

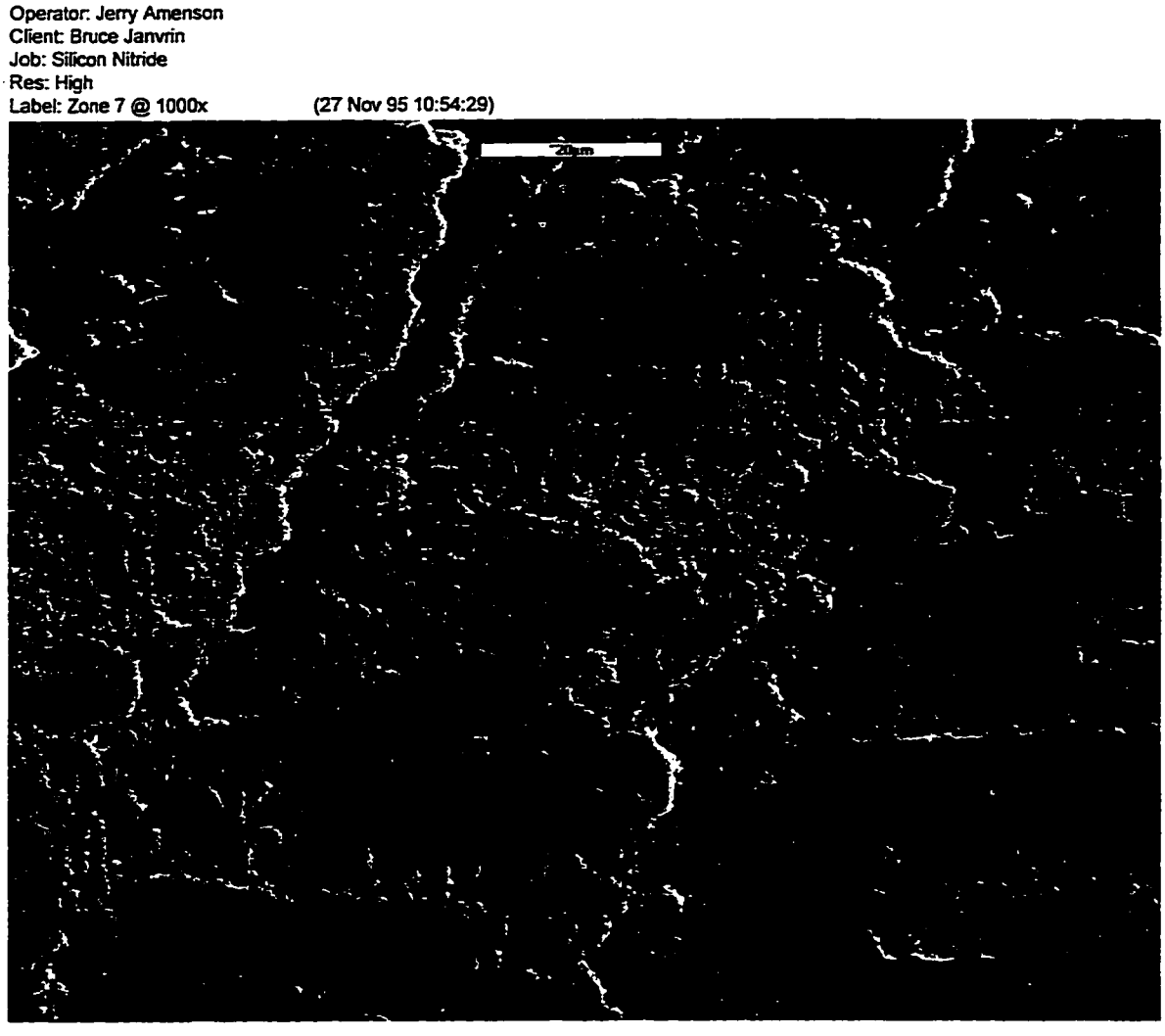

Figure 8.38 Scanning electron micrograph of laser-assisted turned zone 7 (1000x)

9 THERMAL MODELING OF LASER ASSISTED HEATING

The thermal model of the system has the following assumptions:

1. The intensity distribution of the laser illumination is uniform rather than Guassian. The initial output distribution of a Nd:YAG laser may be Guassian; however, the beam path through an appreciable length optical fiber mixes the modes of the laser beam, creating an uniform distribution.

2. The laser and the cutting tool are indexed by the lathe revolution.

3. The conduction of the energy is one dimensional only.

4. The thermal conductivity of the silicon nitride is heated rapidly and attains the value for 1273 K.

5. No plasma formation occurs at the surface.

6. No actual material removal is performed by the laser. Material is removed by the cutting tool only.

7. Cooling of the surface by convection is neglected.

8. A boundary condition of an imposed temperature is assumed for heating.

9. The heat of deformation of the workpiece chip is removed with the chip.

Most analyses of the part heating assume that the material is removed through melting with or without an assist gas and without any mechanical action.

The heating is carried out by a spot focused immediately before the cutting tool. The spot preheats the material. Since the spot is six times the feed, an instantaneous heating occurs six times prior to the cutting action. The action is one of sharp heating followed by a short period of time at ambient temperature. This process is repeated three times followed lastly by the shearing action of the cutting tool. The integrated time of heating is the total amount

of heating time. The total energy absorbed is the energy flux times the integrated time of heating. The total time of intergration is thus the time period of three revolutions.

Several thermal analyses of material cutting, welding and heating have been performed in the past. These analyses assume a Guassian heat source which makes a single pass with material melting. The material has a conductivity, density and a specific heat independent of temperature. This is not the case here since the beam has an uniform energy density, the thermal conductivity varies by three orders of magnitude and the specific heat also varies with temperature [127].

Another set of assumptions models the instantaneous heating of a laser on a turning object as if it were a continuous ring type heat source. At high speeds with longer interaction times, this is a very good approximation [128].

9.1 Mathematical model

9.1.1 Nomenclature

T	Temperature, K
t	Time variable, t
r, θ, z	Axes in cylindrical coordinates
q	Heat input from laser beam, W/m^2
α	Thermal diffusivity, m^2/s
K	Thermal conductivity, $W/m - K$

9.1.2 Analysis

The exact mathematical treatment of laser machining involves the solution of the three dimensional heat conduction equation under very complex and imperfectly understood conditions. Therefore, it is necessary to make certain simplifying assumptions inorder to obtain a solution to the governing differential equation.

The heat conduction equation [129] in cylindrical coordinates is given by

$$\frac{\partial T}{\partial t} = \alpha \left(\frac{1}{r} \frac{\partial}{\partial r} \left(r \frac{\partial T}{\partial r} \right) + \frac{1}{r^2} \frac{\partial^2 T}{\partial \phi^2} + \frac{\partial^2 T}{\partial z^2} \right) \tag{9.1}$$

Assuming no temperature variations in the θ-direction, the above equation can be simplified. Further it has been observed that the temperature on the face of the workpiece where the laser beam is incident remains virtually constant, thus making the problem independent of variations in the r-direction. Incorporating these assumptions into the general heat conduction equation (1) the simplified equation is obtained as

$$\frac{\partial T}{\partial t} = \alpha \frac{\partial^2 T}{\partial z^2} \tag{9.2}$$

The Fourier heat conduction equation may be applied on the face of the workpiece to yield a boundary condition

$$-K \frac{\partial T}{\partial t} = q(r,t) \qquad z = 0 \tag{9.3}$$

The incident laser beam on the face of the workpiece may be considered as a ring heat source with constant temperature across the whole face of the workpiece. This temperature has been observed to be $2173K$, yielding

$$T = 2173 \qquad \text{at} \qquad z = 0 \tag{9.4}$$

The temperature of the workpiece is assumed to be equal to room temperature initially

$$T = 300 \qquad \text{at} \qquad t = 0 \tag{9.5}$$

Numerical methods provide the easiest means for solving 9.1 once the necessary simplifications have been made. An explicit finite difference scheme was used to solve 9.2 with the boundary conditions 9.4 and 9.5. The differential equation 9.2 can be represented in finite difference form as

$$\frac{T_i^{n+1} - T_i^n}{\Delta t} = \alpha \frac{T_{i-1}^n - 2T_i^n + T_{i+1}^n}{\Delta z^2} + O[\Delta t, \Delta z^s] \tag{9.6}$$

where

$$T(x,t) = T(i\Delta z, n\Delta t \equiv T_i^n \tag{9.7}$$

Equation 9.6 can be rearranged as

$$T_i^{n+1} = RT_{i-1}^n + (1-2R)T_i^n + RT_{i+1}^n \tag{9.8}$$

where the quantity R is defined as

$$R = \frac{\alpha \Delta t}{(\Delta x)^2}$$

$$n = 0, 1, 2, \ldots \qquad \text{and} \qquad i = 1, 2, \ldots$$

The stability criterion for this scheme is given by

$$R = \frac{\alpha \Delta t}{(\Delta x)^2} \leq \frac{1}{2} \tag{9.9}$$

9.2 Solution

A program was written in MATLAB (appendix 1) to solve the finite difference scheme 9.6. The depth to which the desired temperature penetrated was calculated for 3 different speeds of rotation of the workpiece - 800, 1000, and 1200. The results are presented in graphical form as the temperature distribution with respect to time for a particular distance from the face of the workpiece where the laser beam is incident. Figure 9.1 and Figure 9.2 show the temperature distribution for a particular depth at 800 rpm, Figure 9.3 and Figure 9.4 show the temperature profile for a given depth at 1000 rpm, while Figure 9.5 and Figure 9.6 show the temperature distribution for a given depth at 1200 rpm.

Table 1.1 shows the physical properties and constants used in solving the mathematical model.

Table 9.1 Physical Properties and Constants

absorptivity	0.7
laser beam diameter	$0.6mm$
laser power	$100W$
thermal conductivity	$0.03W/m-K$
thermal diffusivity	$3e-7m^2/s$

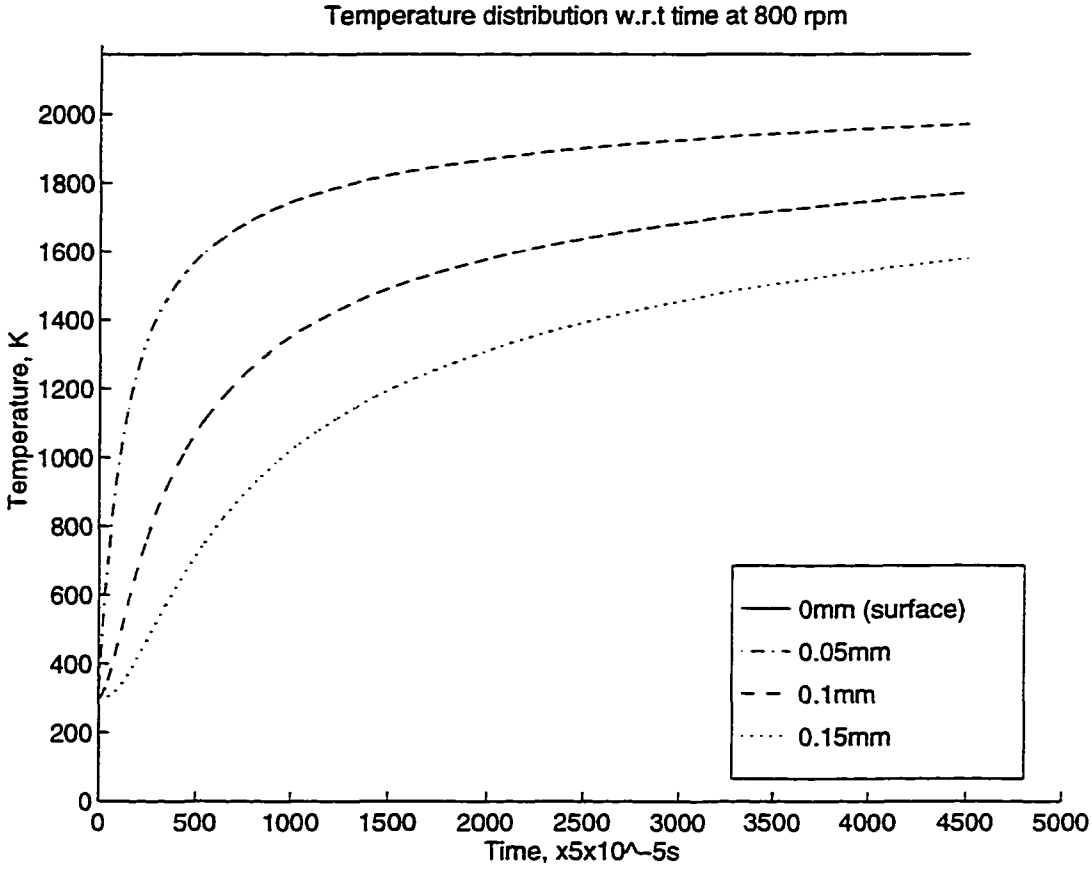

Figure 9.1 Temperature at 800 rpm for 0, 0.05, 0.1 and 0.15 mm from the face

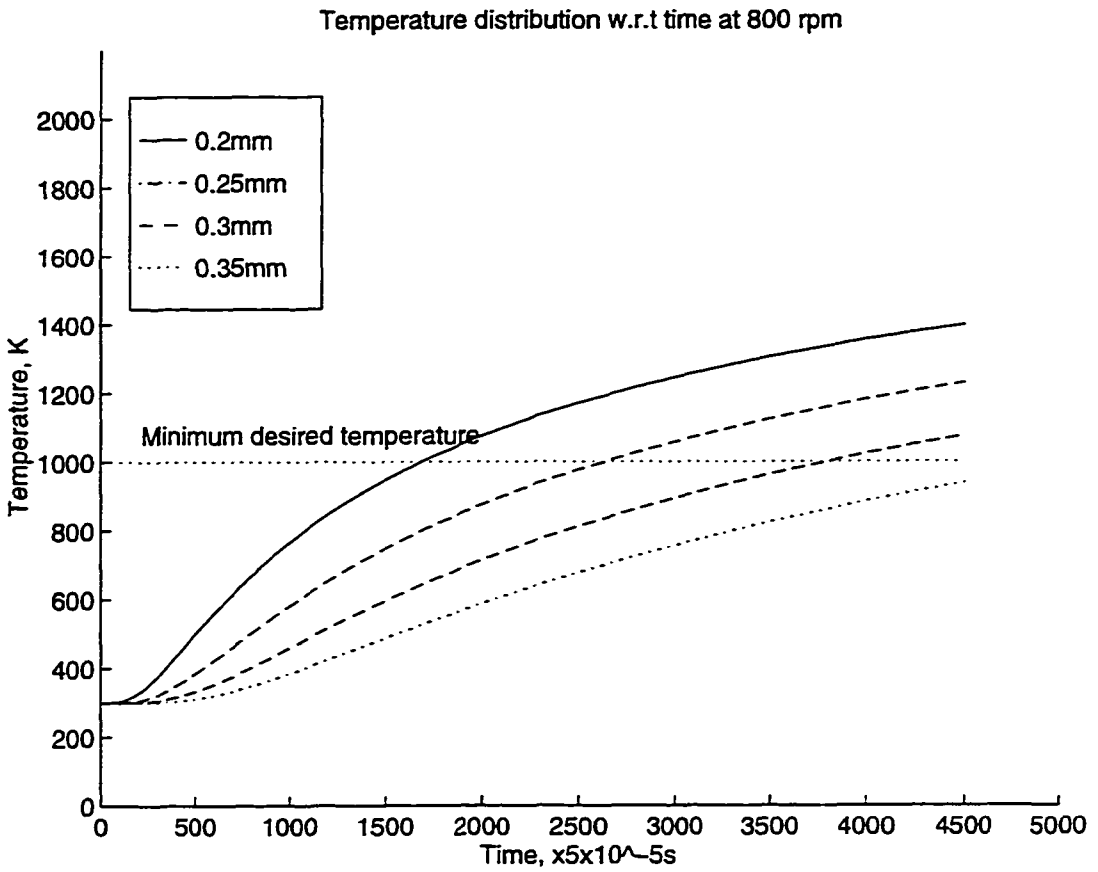

Figure 9.2 Temperature at 800 rpm for 0.2, 0.25, 0.3 and 0.35 mm from the face

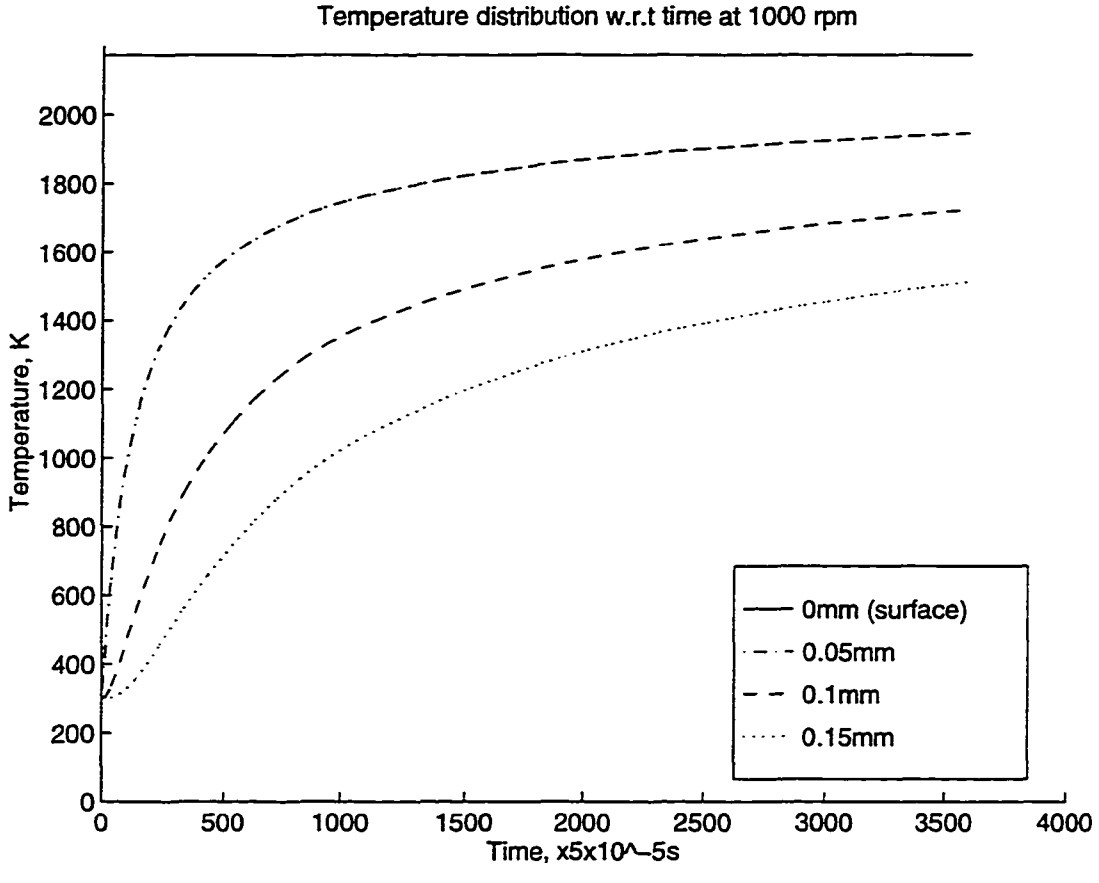

Figure 9.3 Temperature at 1000 rpm for 0, 0.05, 0.1 and 0.15 mm from the face

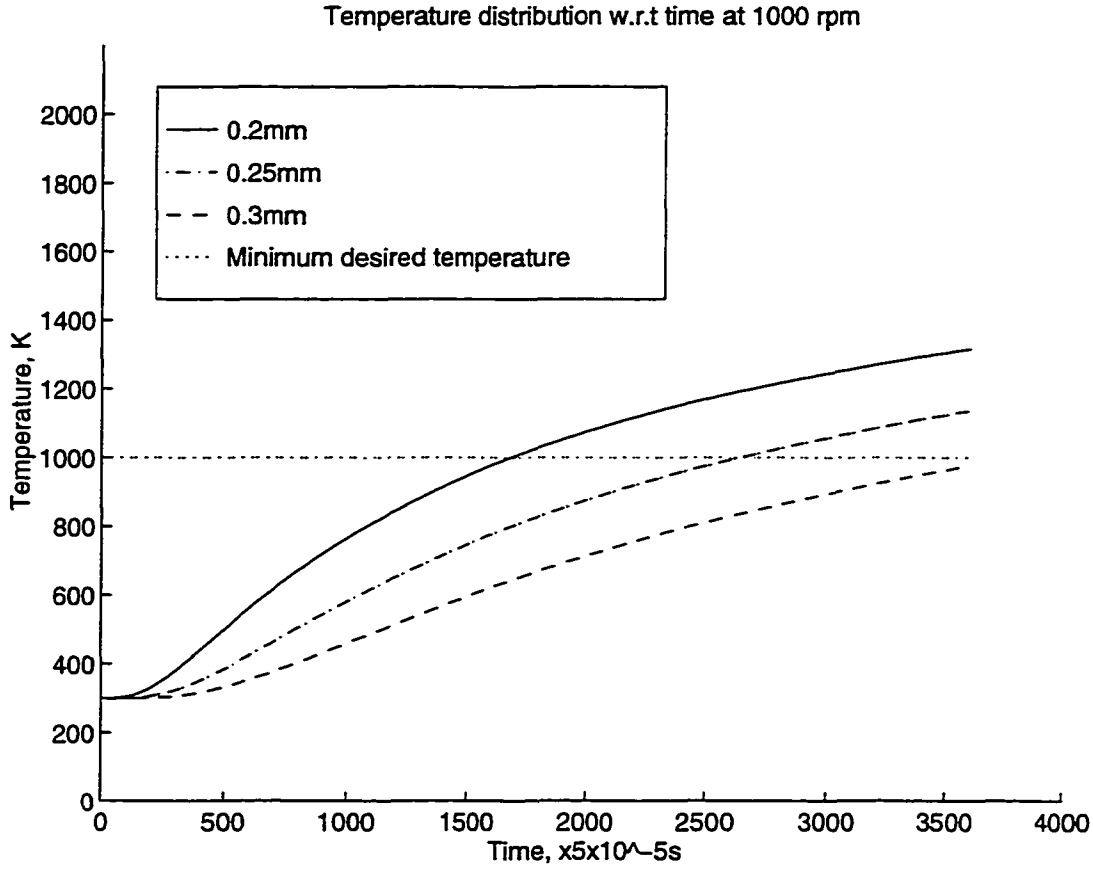

Figure 9.4 Temperature at 1000 rpm for 0.2, 0.25, and 0.3 from the face

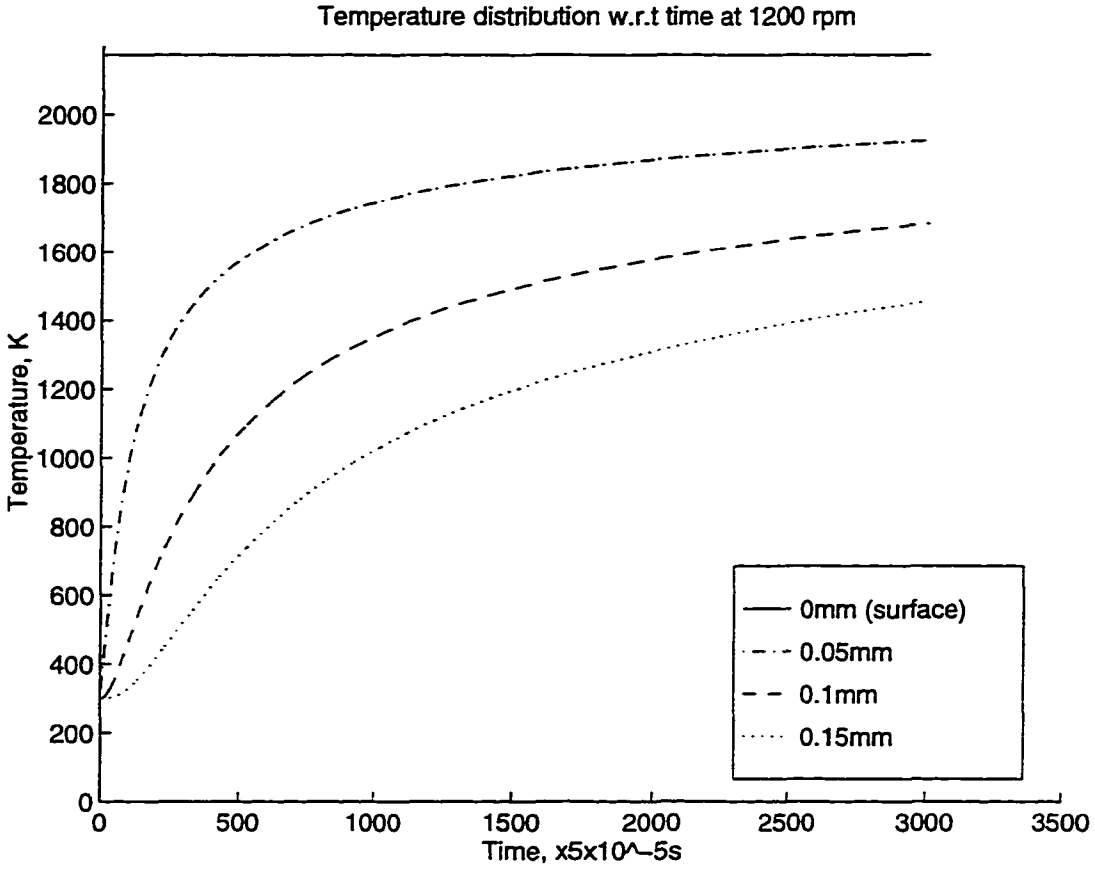

Figure 9.5 Temperature at 1200 rpm for 0, 0.05, 0.1 and 0.15 mm from the face

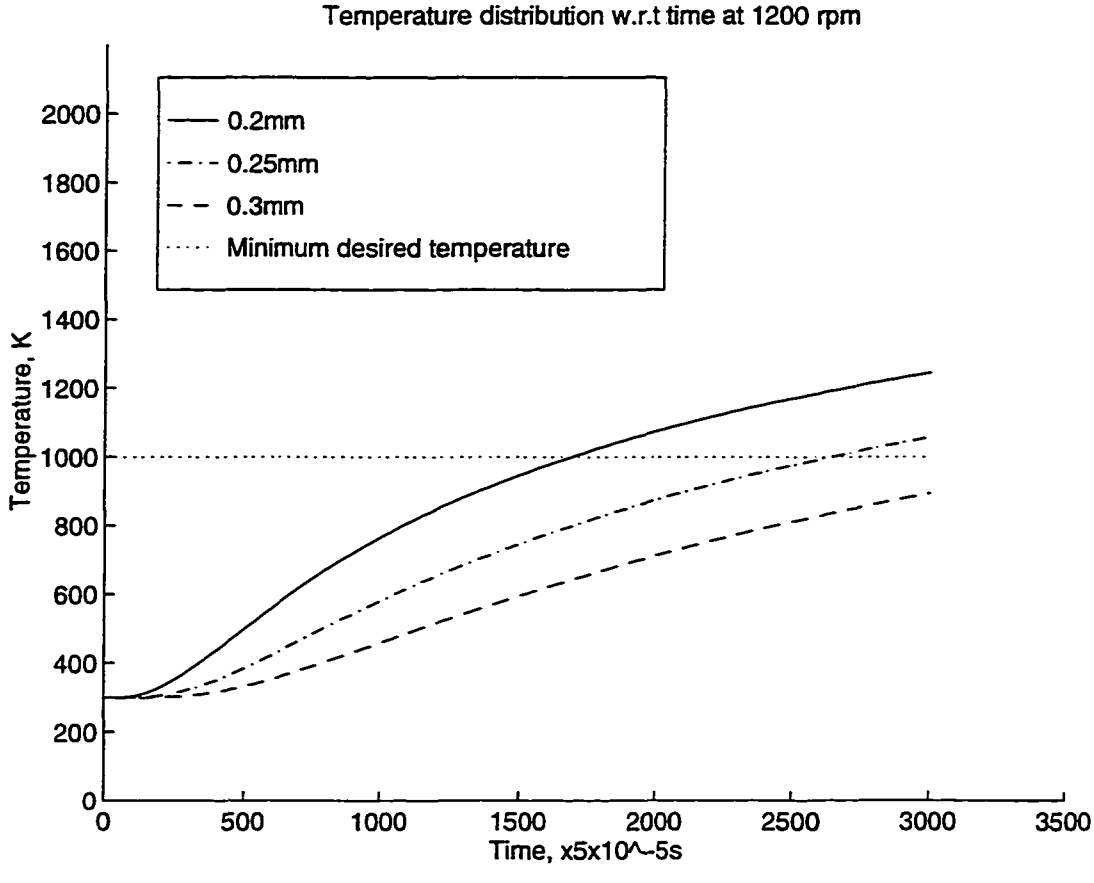

Figure 9.6 Temperature at 1000 rpm for 0.2, 0.25, and 0.3 from the face

10 CONCLUSIONS

1. Silicon nitride can be machined in the ductile region by use of Nd:YAG laser-assistance through a fiber optic focused into the shear area of cutting.

2. Coated carbide tools (TP 15, TP40,) provided the best machining of the silicon nitride. The thermal barrier of the coating improves the life of the cutting tools.

3. Heating of the intergranular oxide layer softened and resolidified over surface imperfections on the turned part.

4. Acceptable surface finishes equivalent to those commonly associated with lapping were obtained.

5. Use of the Nd:YAG laser-assisted turning of silicon nitride, especially with higher power continuous wave lasers coming available, can produce finished parts that are not obtainable through current grinding operations.

6. Thermal modeling can be used to analyze an optimal turning speed.

7. The absorption of 1064 nanometer irradiation heats the beta grains of hot isostatic presses silicon nitride without heating the intergranular silica and other oxides.

APPENDIX

1. Program for solving the mathematical model

```
clear
close all

% Program to predict depth of penetration of heated zone in
% laser preheating of a cylindrical metal rod before facing

K = 0.03; % Thermal conductivity in W/m-K
alpha = 3e-7; % Thermal diffusivity in m^2/s
absorptivity = 0.7;
beamdia = 0.6e-3; % Beam diameter in m
dt = 0.00005;
dz = 5e-5;
r = alpha*dt/dz^2;
rpm = 1200;
sizet = ((60/rpm)*1/dt) + 1;

T = zeros(sizet,3*sizet);
T1 = ones(sizet,sizet)*300;
T2 = ones(sizet,sizet)*300;
T3 = ones(sizet,sizet)*300;

q = ones(1,sizet)*(absorptivity*100/((pi/4)*beamdia^2));

T1(1,1) = 2173;

for t = 1:sizet-1

%   T1(1,t+1) = (1-2*r)*T1(1,t) + 2*r*(1-(dz*q(1,t)/K))*T1(2,t);
  T1(1,t+1) = 2173;


  for i = 2:sizet-1
```

```
    T1(i,t+1) = r*T1(i-1,t)+(1-2*r)*T1(i,t)+r*T1(i+1,t);

  end

  temp1 = (T1(sizet,t)-T1(sizet-1,t))+T1(sizet,t);
  T1(sizet,t+1) =  r*T1(sizet-1,t)+(1-2*r)*T1(sizet,t)+r*temp1;

end

T2(:,1) = T1(:,sizet);
T2(1,1) = 2173;

for t = 1:sizet-1

%   T2(1,t+1) = (1-2*r)*T2(1,t) + 2*r*(1-(dz*q(1,t)/K))*T2(2,t);
  T2(1,t+1) = 2173;

  for i = 2:sizet-1

    T2(i,t+1) = r*T2(i-1,t)+(1-2*r)*T2(i,t)+r*T2(i+1,t);

  end

  temp2 = (T2(sizet,t)-T2(sizet-1,t))+T2(sizet,t);
  T2(sizet,t+1) =  r*T2(sizet-1,t)+(1-2*r)*T2(sizet,t)+r*temp2;

end

T3(:,1) = T2(:,sizet);
T3(1,1) = 2173;

for t = 1:sizet-1

%   T3(1,t+1) = (1-2*r)*T3(1,t) + 2*r*(1-(dz*q(1,t)/K))*T3(2,t);
  T3(1,t+1) = 2173;

  for i = 2:sizet-1

    T3(i,t+1) = r*T3(i-1,t)+(1-2*r)*T3(i,t)+r*T3(i+1,t);

  end

  temp3 = (T3(sizet,t)-T3(sizet-1,t))+T3(sizet,t);
  T3(sizet,t+1) =  r*T3(sizet-1,t)+(1-2*r)*T3(sizet,t)+r*temp3;
```

```
end

T(:,1:sizet) = T1;
T(:,sizet+1:2*sizet) = T2;
T(:,2*sizet+1:3*sizet) = T3;

[figure1, figure2] = Figure(T,sizet);
```

A-1 Subroutine for plotting the results

```
function [figure1, figure2] = Figure(T,sizet)

hold
axis([0 3500 0 2200])
plot(T(1,:))
plot(T(2,:),'-.')
plot(T(3,:),'--')
plot(T(4,:),':')
xlabel('Time, x5x10^-5s')
ylabel('Temperature, K')
title('Temperature distribution w.r.t time at 1200 rpm')
legend('0mm (surface)','0.05mm','0.1mm','0.15mm')
hold

figure
hold
axis([0 3500 0 2200])
plot(T(5,:))
plot(T(6,:),'-.')
plot(T(7,:),'--')
a= 1000*ones(1,sizet*3);
plot(a,':')
xlabel('Time, x5x10^-5s')
ylabel('Temperature, K')
title('Temperature distribution w.r.t time at 1200 rpm')
legend('0.2mm','0.25mm','0.3mm','Minimum desired temperature')
hold
```

BIBLIOGRAPHY

[1] Konig, W. and A. Wageman. "Fine machining of advanced ceramics." *Ceramics Today - Tomorrow's Ceramics* (1991): 2769-2783.

[2] Bhattacharyya, A. *Metal Cutting: Theory and Practice* (Books and Allied Private Limited: Calcutta, India 1984).

[3] *Tool and Manufacturing Engineers Handbook Volume 1 Machining* (Society of Manufacturing Engineers: Dearborn MI 1982): 4-3 & 8-75.

[4] *Metals Handbook —Volume 16 Machining — Ninth Edition* (American Society of Metals International: Metals Park OH 1989).

[5] Trent, E. M. *Metal Cutting* (Butterworths: London 1977).

[6] Kirchner H. P., and E. D. Issacson. Residual stresses in hot pressed silicon nitride by single point grinding. *Journal of the American Ceramic Society* (1982): vol 65 no 1, 55-60.

[7] Mendiratta, M. G., and J. J. Petrovic. "Slow crack growth from controlled surface flaws in hot—pressed Si_3N_4." *Journal of American Ceramic Society* (May—June 1978): vol 61 no 5-6, 226-230.

[8] Petrovic, J. J. Mixed mode fracture of hot-pressed Si_3N_4." *Journal of American Ceramic Society* (May—June 1978): vol 68 no 6, 348-55.

[9] Krabacher, E. and M. Merchant. "Basic factors in hot machining." *Transactions of the ASME* (August 1951): 761-776.

[10] Green, D. J. "Compressive surface strengthening of brittle materials by a residual stress distribution." *Journal of the American Ceramic Society* (November 1983): vol 66 no 11, 807-810.

[11] Konig, W. and A. Wageman. "Machining of ceramic components: process—technological potentials." *Machining of Advanced Materials — NIST Special Publication 847* (July 1993): 3-17.

[12] Sheppard, L. "Machining of advanced ceramics." *Advanced Materials and Processes Including Metal Progress* (December 1987): 40-48.

[13] Rice, R. W. "Effects of ceramic microstructural character on machining direction — strength anisotropy." *Machining of Advanced Materials - NIST Special Publication 847* (July 1993): 185-204.

[14] Ives, L. K., C. J. Evans, S. Jahanmir, R. S. Polvani, T. J. Strakna and M. L. McGlauflin. "Effect of ductile-regime grinding on the strength of hot—isostatically—pressed silicon nitride." *Machining of Advanced Materials — NIST Special Publication 847* (July 1993): 341-352.

[15] Ito, S., M. Nakamura and W. Kanematsu. "Machining of high performance ceramics." *Bulletin Japan Society of Precision Engineering* (September 1987): vol 21 no 3, 167-172.

[16] Jahanmir, S., T. J. Strakna, G. D. Quinn and H. Liang. "Effect of grinding on strength and surface integrity of silicon nitride: part I and II." *Machining of Advanced Materials — NIST Special Publication 847* (July 1993): 263-294.

[17] Lin, C. J., M.G. Jenkins and M.K. Ferber. Evaluation of tensile static, dynamic, and cyclic fatique behavior for a HIPed silicon nitride at elevated temperatures. *Silicon Nitride Ceramics* edited by I. W. Chen (1993): 455-460.

[18] Anderson, C. A. and R. J. Bratten. "Effect of surface finish on the strength of hot pressed silicon nitride." *Science of Ceramic Machining and Surface Finishing II* (U.S. National Bureau of Standards: October 1979): 463-476.

[19] Becher, Paul. "Ceramic machining and surface finishing." *Treatise on Materials Science & Technology, Volume 9, Ceramic Fabrication Processes* (Academic Press: 1976): 217-226.

[20] Shore, P. and P. Leadbeater. "Advances in ductile mode machining." *Ceramic Bulletin* (1991): vol 70 no 10, 1608-1611.

[21] Hebbar, R., S. Chandrasekar and T. Farris. "Ceramic Grinding Temperatures." *Journal of American Ceramics Society* (1992): vol 75 no 10, 2742-2748.

[22] Mayeer, J. E. Jr. and G. P. Fang. "Diamond grinding of silicon nitride ceramic." *Machining of Advanced Materials — NIST Special Publication 847* (July 1993): 205-222.

[23] Malkin S. and Ritter J. E. Grinding mechanism and strength degradation for ceramics. *Journal of Engineering for Industry* (1989): vol 111, 167-174.

[24] Allor, R. L., T. J. Whalen and J. R. Baer. "Machining of silicon nitride: experimental determination of process/property relationships." *Machining of Advanced Materials — NIST Special Publication 847* (July 1993): 223-234.

[25] Konig, W., D. F. Dauw, G. Levy and U. Panten. "EDM—future steps towards the machining of ceramics." *Annals of the CIRP* (1988): vol 37 no 2, 623-631.

[26] Fate W. A. "Density dependence of shear modulus of Si_3N_4." *Journal of the American Ceramic Society* (1974): vol 57 no 8, 372.

[27] Firestone, R. F. "Abrassionless Machining Methods for Ceramics." *Science of Ceramic and Surface Finishing* edited by B. J. Hockey and R. W. Rice (National Bureau of Standards: 1979): 261-282.

[28] Hsu, R. K. C. and S.M. Copley. Producing three—dimensional shapes by laser milling. *Journal of Engineering for Industry* (1990): vol 112, 375-379.

[29] Wallace, R. and S. Copley. "Shaping silicon nitride with a carbon dioxide laser by overlapping multiple grooves." *Journal of Engineering for Industry* (November 1989): vol 111, 315-321.

[30] Wallace, R., M. Bass, and S. Copley. "Curvature of laser—machined grooves in Si_3N_4." *Journal of Applied Physics* 15 (May 1986): vol 59 no 10, 3555-3560.

[31] Wallace, R. and S. Copley. "Laser machining of silicon nitride: energetics." *Advanced Ceramic Materials* (1986): vol 1 no 3, 277-283.

[32] Wallace, R., M. Bass, and S. Copley. "Shaping ceramics with a continuous wave carbon dioxide laser." *Physical Processes in Laser—Materials Interactions* edited by M. Bertolotti (Plenum Press: New York 1983): 301-322.

[33] Farnum, G. "Reinventing the lathe." *Machining Source Book* (ASM International: Metals Park, OH 1988): 384-387.

[34] Solomah A. G. "Laser machining of silicon nitride." *Ceramics* (1991): 543-546.

[35] Tao H.Y., W. Chang, S. M. Copley, and J. A. Todd. "Effect of surface treatment on the strength of laser machined silicon nitride." *Laser Materials Processing III* (The Materials Society: Metals Park OH 1989).

[36] Chryssolouris, G., J. Bredt, S. Kordas and E. Wilson. "Theoretical aspects of a laser machine tool." *Journal of Engineering for Industry* (February 1988): vol 110, 65-70.

[37] McGeough, J. A. *Advanced Methods of Machining* (Chapman & Hall: London 1988).

[38] Nikumb, S. K., M. U. Islam and G. R. Campbell. "Precision material removal of structural ceramics and steels using Nd:YAG laser." *Proceedings of ICALEO 93* (October 1993).

[39] Monita, N., T. Watanabe and Y. Yoshida. "Crack—free processing of hot—pressed silicon nitride ceramics using pulsed YAG laser." *JSME International Journal Series III* (1991): vol 34 no 1, 149-153.

[40] Meiners, E., M. Wiedmaier, F. Dausinger, K. Krastel, I. Masek and A. Kessier. "Micro machining of ceramics by pulsed Nd:YAG laser." *Proceedings of ICALEO 91* (October 1991): 327-336.

[41] Ogata K., N. Miyanagi, K. Suzuki, and Y. Shimoura. Ceramic cutting with pulsed Nd:YAG laser. *ICALEO 90* (Laser Institute of America: Orlando FL 1990): 261-270.

[42] Hugel, H. "Integration of laser materials processing in metal cutting machine tools." *Proceedings of LAMP 92* (June 1992): 565-570.

[43] Yoshioka, S., and T. Miyazaki. "Blackening of zirconia ceramics in groove—making by Q—switched YAG laser." *Bulletin Japan Society of Precision Engineering* (December 1990): vol 24 no 4, 258-262.

[44] Blake, P., T. Bifano, T. Dow and R. Scattergood. "Precision machining of ceramic materials." *Ceramic Bulletin* (1988): vol 67 no 6, 1038-1044.

[45] Nakasuji, T., S. Kodera, S. Hara, H. Matsunaga, N. Ikawa, and S. Shimada. "Diamond turning of brittle materials for optical components." *Annals of CIRP* (1990): 89-92.

[46] Kitagawa, T. and K. Maekawa. "Plasma hot machining for new engineering materials." *Wear* (1990): vol 139, 251-267.

[47] Tour, S. and L. Fletcher. "Hot spot machining." *Iron Age* 21 (July 1949): 78-89.

[48] Schmidt, A. "Hot milling." *Iron Age* 28 (April 1949): 66-70.

[49] Pentland, W., C. Mehl and J. Wennberg. "Hot machining." *American Machinist/Metalworking Manufacturing* 11 (July 1960): no 492, 117-132.

[50] Moore, A. "Hot machining for single point turning." *Tooling and Production* (November 1977): 70-72.

[51] Smith, P.D. and B. F. Boult. "The hot—machining of austenitic manganese steel." *Production Technology* (1974): 306-320.

[52] Ready, J. *Industrial Applications of Lasers* (Academic Press: Boston 1978).

[53] Rajagopal, S. "Laser—assisted machining of tough materials." *Laser Focus* (March 1982): 49-54.

[54] Komanduri, R., D. Flom and M. Lee. "Highlights of the DARPA advanced machining research program." *Journal of Engineering for Industry* (November 1985): vol 107, 325-334.

[55] Copley, S. "Laser applications." *Handbook of High Speed Machining Technology* edited by R. King (Chapman Hall: New York NY 1985): 387- 416.

[56] Tipnis, V.J., G .I. Ravigagani, and S.J. Mantel Sr. Economic Feasibility of laser—assisted machining (LAM). *Proceedings of NAMRAC* (SME: Dearborn, MI 1981): 547-552.

[57] Tipnis, V.J., S.J. Mantel Sr. , and G .I. Ravigagani. Sensitivity analysis for macroeconomic and microeconomic models of new manufacturing analysis. *Annals of CIRP* (1981): vol 30 no 1, 401-404.

[58] Osveenko, A. et al (sic). "Temperature and state of surface layer of high alloy cast irons when machining with reheating." *Soviet Engineering Research* (1983): vol 3 no 3, 45-47.

[59] Jau, B., S. Copley and M. Bass. "Laser—assisted machining." *Proceedings of NAMRC 81* (SME: Dearborn, MI 1981): 12-15.

[60] Copley, S., M. Bass, B. Jau and R. Wallace. "Shaping materials with lasers." *Laser Material Processing* edited by M. Bass (North Holland: New York 1983): 299-336.

[61] Reznikov, A. N., and N. D. Berenov. "Optimum characteristics of cutting tools for plasma-arc machining." *Soviet Engineering Research* (1985): vol 5 no 10, 66-67.

[62] Poduraev, V., N. Sokolov and N. Berenov. "Plasma—assisted machining of large components made of difficult—to—machine materials." *Soviet Engineering Research* (1989): vol 9 no 9, 53-58.

[63] Uehara, K. "On the mechanism of temperature rise and the choice of tool material in electric hot machining." *Annals of the CIRP* (1977): vol 16, 85-91.

[64] Kitagawa, T. and K. Maekawa. "Plasma arc aided machining for difficult—to—cut materials." *Bulletin of the Japan Society of Precision Engineers* (December 1984): vol 18 no 4, 349-350.

[65] Akasawa, T., H. Takeshita, and K. Uehara. "Hot machining with cooled cutting tools." *Annals of CIRP* (1987): 37-40.

[66] Kitagawa, T., K. Maekawa and A. Kubo. "Plasma hot machining for high hardness metals." *Bulletin of the Japan Society of Precision Engineers* (June 1988): vol 22 no 2, 145-151.

[67] Schwartz, M., editor. *Handbook of Structural Ceramics* (McGraw Hill: New York 1992).

[68] Hirsch P. B. "Fundamentals of the brittle to ductile transition." *Materials Transactions* (Japanese Institute of Materials: 1989): vol 30 no 11, 841-855.

[69] Lewis, M.H. Crystallization of grain boundary phases in silicon nitride and sialon ceramics. *Key Engineering Materials* (TransTech Publications, Switzerland 1994): vol 89-91, 333—337.

[70] Konig, W., and Zaboklicki, A. K. "Laser–assisted hot machining of ceramics and composite materials." *Machining of Advanced Materials — NIST Special Publication 847* (July 1993): 455-463.

[71] Luxon, J. T., and D. E. Parker. *Industrial Lasers and Their Applications* (Prentice-Hall: Englewood Cliffs NJ 1992).

[72] Bass, M. "Laser heating of solids." *Physical Processes in Laser—Materials Interactions* (Plenum Press: New York 1983): 77-116.

[73] Copley, S. and M. Bass. "Shaping material with a continuous wave carbon dioxide laser." *Applications of Lasers Material Processing* edited by E. Metzbower (ASM International: Metals Park, OH 1979): 121-134.

[74] Dobbins W. P. and H. von Arb. The slab laser : productivity and processing applications in industrial applications. *ICALEO 90* (Laser Institute of America: Orlando FL 1990): 225-234.

[75] Belforte D. *Industrial Laser Review* (Penn Well Publications: Tulsa OK 1993). May p11-12

[76] Matsui, M. Status of research and development on materials for ceramic gas turbine components. *Material Research Society Symposium Proceedings - Vol 287* (Material Research Society: Pittsburgh PA 1993): 173-188.

[77] Hampshire, S. *Non-Oxide Technical and Engineering Ceramics* (Elsevier Applied Science: New York 1986).

[78] Ziegler, G., J. Heinrich and G. Wotting. "Relationships between processing, microstructure and properties of dense and reaction—bonded silicon nitride." *Journal of Materials Science* (1987): vol 22, 3041-3086.

[79] Zeng, J., O. Yamada, I. Tanaka and Y. Miyamoto. "Hot isostatic pressing and high—temperature strength of silicon nitride—silica ceramics." *Journal of American Ceramics Society* (1990): vol 73 no 4, 1095-1097.

[80] Thompson, D.P. New grain-boundary phases for silicon nitride *Silicon Nitride Ceramics: Scientific and Technological advances* 1993 Materials Research Society, Pittsburg PA Symposium Proceedings Vol 287 p79- 92

[81] McColm, I.J., and N. J. Clark. *Forming, Shaping and Working with High — Performance Ceramics* (Blackie: Glasgow & London 1988).

[82] Mitomo, M. "Thermodynamics, phase relations, and sintering aids of silicon nitride." *Silicon Nitride - 1: Ceramic Research and Development in Japan* edited by S. Somiya, M. Mitomo and M. Yoshimura (Elsevier Applied Science: London 1990): 1-12.

[83] Shimada, M., M. Koizumi, A. Tanaka and T. Yamada. "Temperature dependence of K_ic for high—pressed Si_3N_4 without additives." *Communications of the American Ceramic Society* (April 1982): C48.

[84] Tsuge, A., K. Nishida and M. Komatsu. "Effect of crystallizing the grain—boundary glass phase on the high—temperature strength of hot—pressed Si_3N_4 containing Y_2O_3." *Journal of American Ceramics Society* (1975): 323.

[85] Edington, J. W., D. J. Rowcliffe and J. L. Henshall. "The mechanical properties of silicon nitride and silicon carbide part I: materials and strength." *Powder Metallurgy International* (1975): vol 7 no 2, 82-96.

[86] Konig W. and M. Popp. High precision machining of advanced ceramic. *Ceramic Materials and Components for Engines* (1993): 1159-1169.

[87] Carslaw H. S. and J. C. Jaeger. *Conduction of Heat in Solids - Second Edition* (Cleardon Press: Oxford England 1959).

[88] Muncheryan, H. *Laser and optoelectronic engineering* (Hemisphere Publishing Corporation: New York 1991).

[89] Dawes, C. *Laser Welding* (McGraw-Hill: New York 1992).

[90] Svelto, O. *Principles of Lasers: Third Edition* (Plenum Press: New York 1989).

[91] Halliday, R. and D. Resnick. *Physics* (Prentice Hall: New York 1978).

[92] Loh, R. L., C. Rossington and A. G. Evans. "Laser technique for evaluating spall resistance of brittle coatings." *Journal of American Ceramic Society* (1986): vol 69 no 2, 139-142.

[93] Jellison J. L., D. M. Keicher and P. W. Fuerschbach. Performance of three-crystal 1800 watt CW Nd:YAG laser. *ICALEO 90* (Laser Institute of America: Orlando FL 1990): 123-131.

[94] von Allmen, Martin. "Coupling of laser radiation to metals and semiconductors." *Physical Processes in Laser—Materials Interactions* edited by M. Bertolotti (Plenum Press: New York 1983): 49-76.

[95] Maruo, H., I. Miyamoto and T. Ooie. "Processing mechanism of ceramics with high power density lasers." *Proceedings of LAMP '92* (June 1992): 293-298.

[96] Veltri R. and F Galasso "Effect of continuous wave high intensity laser radiation on the strength of silicon nitride and silicon carbide." *Communications of the American Ceramic Society* (April 1982): C53-54.

[97] Wu, C., and K. R. McKinney. "The effect of surface finishing on the strength of commercial hot pressed silicon nitride." *The Science of Ceramic Machining and Surface Finishing II* (U.S. National Bureau of Standards: October 1979): 477-482.

[98] Nonhof, C. J. *Material Processing with Nd-Lasers* (Electrochemical Publications Limited: Ayr, Scotland 1988).

[99] Greskovich, C. and S. Prochazka. "Stability of Si_3N_4 and liquid phase(s) during sintering." *Communications of the American Ceramic Society* (July 1981): C96-97.

[100] Klocek, P and G Sigel, Jr. *Infrared Fiber Optics* (SPIE Society of Optical Engineers: Bellingham WA 1989).

[101] Sahba, N. and T. J. Rockett. Infrared absorption coefficients of silica glasses. *Journal American Ceramic Society* (1992): vol 75 no 1, 209-212.

[102] Brendow B. and Mitra S. S. . *Fiber Optics* (Plenum Press, New York NY 1978).

[103] Blicblau, A.S. "Fabrication of Silicon Nitride Ceramics." *Key Engineering Materials* (TransTech Publications, Switzerland 1991): vol 53-55, 597-585.

[104] Clarke, D. R., N. J. Zaluzec and R. W. Carpenter. "The intergranular phase in hot—pressed silicon nitride I: elemental composition." *Journal of American Ceramic Society* (October 1981): vol 64 no 10, 601-607.

[105] Clarke, D. R., N. J. Zaluzec and R. W. Carpenter. "The intergranular phase in hot—pressed silicon nitride II: evidence for phase separation and crystallization." *Journal of American Ceramic Society* (October 1981): vol 64 no 10, 608-611.

[106] Glandus, J. C., and P. Boch. "Elastic and inelastic properties of nitrogen ceramics." *Nitrogen Ceramics* edited by R. L. Riley (Noordhoff: Leyden 1977): 515-520.

[107] Ekstrom, T. Transient liquid phase sintering of silicon nitride. *Key Engineering Materials* (TransTech Publications, Switzerland 1991): vol 53-55, 586-591.

[108] Ekstrom, T. "Sialon ceramics sintered with yttria and rare earth oxides." *Material Research Society Symposium Proceedings - Vol 287* (Material Research Society 1993).

[109] Rouxel, T., J. Besson and P. Goursat. "Improvement of creep resistance of sintered silicon nitride by hot isostatic exudation of intergranular glass." *Journal of American Ceramic Society* (1993): vol 76 no 11, 2790-2794.

[110] Kleebe, H. J., M.K. Cinibulk, I. Tanaka,J. Bruley, J.S. Vetrano, and M. Ruhle High-resolution electron microscopy observations of grain- boundary films in silicon nitride ceramics. *Tailoring of the mechanical properties of Si_3N_4 Ceramic* ed by Hoffman and Petzow 1994 Kluwer Acedemic Publishers Dordrecht Netherlands (1993): 259-274

[111] Messier, D. R. and F. L. Riley. "The α/β silicon nitride phase transformation." *Nitrogen Ceramics* (Noordhoff: Leyden, England 1977): 141-149.

[112] Ramanathan, S. and M. F. Modest. "Measurement of temperature and absorptance for laser processing applications." *Journal of Laser Applications* (1994): vol 6, 23-31.

[113] Takahashi, T., M. Isomura, Y. Endoh, and Y. Furuse SiO_2 doped Si_3N_4 ceramics *Key Engineering Materials* (TransTech Publications, Switzerland 1994): vol 89-91, 225-228.

[114] Jha, A. and S. J. Yoon. Aspects of stability of amorphous grain boundary phase in silicon nitride ceramics. *Key Engineering Materials* (TransTech Publications, Switzerland 1994): vol 89-91, 361-364.

[115] Kleebe, H. J., et al (sic). Statistical analysis of the intergranular film thickness in silicon nitride ceramics. *Journal of American Ceramics* (1993): vol 76 no 8, 1966- 1977.

[116] Kleebe, H. J. High-resolution electron microscopy observations of grain- boundary films in silicon nitride ceramics. *Silicon Nitride Ceramics* (1993): Materials Research Society Pittsburg PA vol 287 p65-78

[117] Clarke, D. R. and N. J. Zaluzec. "The intergranular phase in hot—pressed silicon nitride III: a refinement of the elemental composition." *Journal of American Ceramic Society* (August 1982): C132-133.

[118] Tandon, R. and D. R. Clarke. "Grain boundary fracture resistance of silicon nitride." *Key Engineering Materials* (TransTech Publications: Switzerland 1994): vol 89-91, 509-516.

[119] Lewis, C.. Silicon nitride: the rock-solid performer *Mechanical Engineering* (May 1989): 30:33

[120] Subramanian, K., P. Readington and S. Ramanath. "A systems approach for grinding of ceramics." *Machining of Advanced Materials — NIST Special Publication 847* (July 1993): 43-54.

[121] DeSalvo, G. "Hydrodynamic behavior at a tool—chip interface." Carnegie—Mellon University dissertion, 1968.

[122] DeSalvo, G., and M. Shaw. "Hydrodynamic action at a chip—tool interface." *Advanced in Machine Tool Design and Research* (Pergamon Press: Oxford & New York 1969): 961-971.

[123] Kuhne, A. and R. Oberacker, and G. Grathwohl Role of sintering parameters on microstrtucture development and mechanical properties of sinter/hip silicon nitride *Silicon Nitride Ceramics: Scientific and Technological advances* 1993 Materials Research Society, Pittsburg PA Symposium Proceedings Vol 287 p417-422

[124] Chadwick, M. M., R. S. Jupp, and D. S. Wilkerson. Creep behavior of a sintered silicon nitride. *Journal of American Ceramic Society* (November 1993): vol 76 no 2, 385-396.

[125] Lange, F.F. High-temperature strength behavior of hot-pressed Si_3N_4: evidence for subcritical crack growth *Journal of The American Ceramic Society* 1974 Vol 57 No 2 p84-87

[126] Arons R.M., J. K. Tien, and E. M. Lenoe "Observations of the viscoelastic strain recovery in hot—pressed silicon nitride." *Journal of the American Ceramic Society* (April 1979): vol 62 no 3-4, 216-217.

[127] Morrell, R. *Handbook of Properties of Technical and Engineering Ceramics - Part 1: Introduction for Engineers and Designers* (Her Majesty Stationary Office: London 1985): 92-183.

[128] Osisik, M. N. *Heat Conduction* (John Willey and Sons,New York 1993): p373-391

[129] Taniguchi, N *Energy Beam Processing of Materials* (Clarendon Press, Oxford 1989): p 276-293